Master Thesis in Geosciences

Cornice accretion, cracking and failure along with their meteorological controls at Gruvefjellet, Central Svalbard

Stephan Vogel

UNIVERSITY OF OSLO

FACULTY OF MATHEMATICS AND NATURAL SCIENCES

Cornice accretion, cracking and failure along with their meteorological controls at Gruvefjellet, Central Svalbard

Stephan Vogel

Master Thesis in Geosciences

Discipline: Physical Geography

Department of Geosciences

Faculty of Mathematics and Natural Sciences

UNIVERSITY OF OSLO

29 November 2010

Tutor: Hanne H. Christiansen (UiO) and (UNIS)

This work is published digitally through DUO – Digitale Utgivelser ved UiO

http://www.duo.uio.no

It is also catalogued in BIBSYS (http://www.bibsys.no/english)

TABLE OF CONTENT

ABSTRACT

The cornice development, accretion, cracking and eventual failure of cornices along the ridgeline of the Gruvefjellet plateau mountain and their controlling meteorological factors was studied in the two consecutive snow seasons 2008/2009 and 2009/2010. Three automatic time lapse cameras have been used and 45 field trips were carried out up to the Gruvefjellet plateau to investigate the ongoing process dynamics. These natural processes endanger infrastructure and inhabitants of Nybyen which is part of Longyearbyen, Svalbard's main settlement located at 78° N in the High Arctic.

Cornice accretion occurs as a direct response to the first snow falls in late September and October and proceeds throughout the entire snow season under a wide range of temperature conditions. Cornice accretion is controlled by distinct storm events which indicate significantly higher wind speeds than the overall snow seasons average. Particular high wind speeds lead to cornice scouring and reduce the cornice vertical as well as horizontal extent. Induced by pronounced temperature fluctuations, cornices crack and tilt around a fixed pivotal point. For the first time cornice tension crack openings were measured which showed a linear development. The particular breakover point of the cornice determines the duration from initial cracking to eventual failure. Throughout the two investigated snow season 180 cornice failures were recorded and collected in a cornice database. 70 failures were categorized as "D2 R3" avalanches and larger and displayed distinctive cornice fall avalanches.

The geomorphological impact of cornices is considerable in this High Arctic setting. During the process of cornice cracking considerable amounts of debris rip off from the headwall, accumulate in the opening crack and are eventually released by cornice fall avalanches. Thus cornices display active transport agents of debris from the plateau edge to the basal slope and contribute to the formation of talus cones.

In addition an extensive literature review on cornice development is given.

1. INTRODUCTION

Cornices are broadly defined as a wedge-like projection of snow formed by wind deposition to the lee of a ridgeline or slope inflection (Montagne et al. 1968, Latham and Montagne 1970). Cornices form annually along the ridgeline of the Gruvefjellet plateau mountain which borders the valley Longyeardalen on its eastern side. Longyearbyen, Svalbard's main settlement is located in that valley at 78° N in the High Arctic. The Gruvefjellet plateau source area in combination with a prevailing winter wind direction from the SE and the pronounced slope inflection leads to the yearly build up of these large cornices along the ridgeline. Cornices crack and eventually fail as cornice fall avalanches which display a natural hazard for residents and infrastructure of Nybyen located at the foot of the slope. Larger cornice failures and cornice triggered slab avalanches are observed in every snow season. Therefore I studied the cornice development – accretion, cracking and eventual failure - along the ridgeline of the Gruvefjellet plateau mountain and their controlling meteorological factors for the two consecutive snow seasons 2008/2009 and 2009/2010.

Cornices and their peculiar nature have attracted the curiosity and concern of both scientists and mountaineers in the past (Latham and Montagne 1970) due to their particular shapes and their ability to trigger avalanches when breaking off (Paulcke and Welzenbach 1928, McCarty et al. 1986, Kobayashi et al. 1988, McClung and Schaerer 2006, Eckerstorfer et al. 2008, Eckerstorfer et al. 2009). However, there has been surprisingly little research carried out on cornices.

2. SVALBARD

2.1. Location and general Climate

The Svalbard archipelago is located in the Atlantic sector of the High Arctic between 74° - 81° N and 10° - 35° E (Figure 1). The climate in Svalbard is categorized as a High Arctic climate according to French (2007) due to its periglacial environment with extreme winter temperatures and thus the occurrence of continuous permafrost. Temperatures above freezing occur only 2-3 months annually. According to the Koeppen-Geiger climate classification, Svalbard's climate is additionally characterized as a polar tundra climate (Kottek et al. 2006).

Svalbard is situated in a pathway of heat and moisture transported to the Arctic thus the climate is warmer and more moist than generally expected in that latitude (Førland et al. 1997). Furthermore the warm Norwegian Current, which flows partly along the west coast of Svalbard leads to mainly winter sea ice-free conditions (Førland et al. 1997). Svalbards climate is influenced by frequent low pressure passages over the Norwegian Sea and the interaction of the Icelandic low with a high pressure over Greenland (Hanssen-Bauer et al. 1990, Førland et al. 1997). Svalbard's main island is Spitsbergen with the study area located in the central part of the region Nordenskiöld Land at 78° N (Figure 1). Here mean annual air temperature (MAAT) at sea level was -5.3°C at Longyearbyen Airport for the period of 1980 – 2010. For 2009 the MAAT at sea level was significantly warmer with -3.7°C (*www.eklima.no*). Interannual variations are more pronounced for the winter season and vary between 3-6°C, while variations between 0.2-0.6°C are accounted for in the summer season (Humlum 2002). At Longyearbyen airport the measured precipitation amounts are relatively low with about 190 mm water equivalent, which represents the driest parts of Svalbard (Førland et al. 1997). For the normal period between 1980 and 2010, 196 mm water equivalent of precipitation are accounted for. In 2009 153 mm water equivalent of precipitation was recorded at Longyearbyen airport (*www.eklima.no*). Though, a significant horizontal precipitation gradient exists (Humlum 2002). Humlum (2002) modelled a 100% correction factor for measured precipitation values to overcome underestimation due to wind action.

Even though large interannual variations occur, snow fall displays the dominant form of precipitation and may fall at any altitude throughout the entire year (Humlum 2002). On average an increase in the snow accumulation of 97 mm water equivalent per 100 m increase in elevation was found (Winther et al. 2003). In particular at the eastern and western coasts glaciation is widespread and extensive. Permafrost is largely continuous with increasing thickness from coastal areas to the highlands. Thereby topography is of special importance as it relates both to differences in altitude and aspect (Humlum et al. 2003).

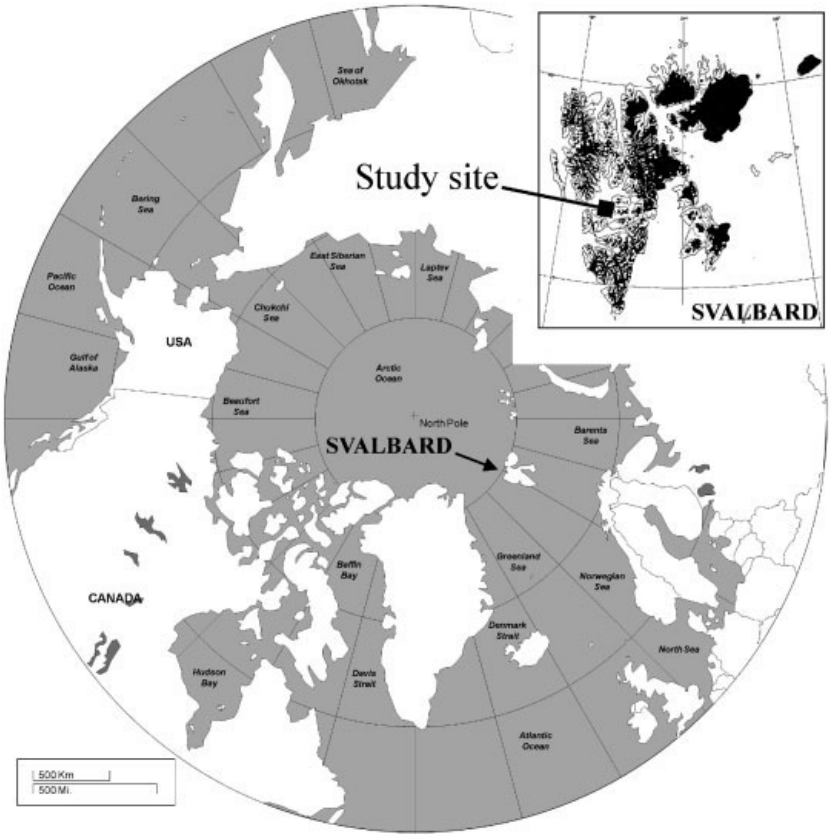

Figure 1 Location map of Svalbard (from Humlum et al. (2007))

The study area located in Nordenskiöld Land displays E – W and NE – SW extending valleys that intersect mountain massifs > 1000 m a.s.l. of a plateau-shaped form as well as the dominating alpine topography (Major et al. 2001, Humlum 2002) (Figure 3). The average altitude of Nordenskiöld Land is considered about 420 m a.s.l. (Humlum 2002).

Under the influence of wind, the snowpack is very unevenly distributed with snow free areas on wind exposed slopes and mountaintops and the accumulation of thick snowdrifts on lee slopes (Jaedicke and Gauer 2005). The wind strength in combination with the absence of any high vegetation leads to these significant redistributions of snow. During the winter time the dominant wind direction is from the SE, though the topography leads to local channelling effects (Humlum 2002).

2.2. Field location Gruvefjellet

Longyearbyen, Svalbard's main settlement in the High Arctic is located in the valley Longyeardalen at 78° N. This NE-SW extending valley is delimited by the two plateau shaped mountains Platåberget and Gruvefjellet to the W and E respectively (Figure 3). Their distinct plateau shape results from the near-horizontal bedding of the Tertiary-age sandstone layers (Major et al. 2001). The plateau mountain Gruvefjellet rises to a maximum altitude of 525 m a.s.l. and its west facing crest to about 460 m a.s.l. The plateau extends NW – SE for more than 2 km which displays a large source area, where considerable amounts of snow are accumulated and consequently redistributed.

The nearly 335 m high Gruvefjellet slope displays a free face with distinct talus cones below on which debris flow tracks are preserved. Most of the debris flows found in the valley Longyeardalen occurred as a result of heavy rain in July 1972 (Larsson 1984). The Gruvefjellet slope displays an example of the free-face model described in French (2007). The talus cones are subdivided by rock noses right at the plateau edge and a second level of outcrops at the upper slope section of the Firkanten formation, a harder sandstone layer (Major et al. 2001). Thus five major gullies are divided in the studied Gruvefjellet slope section which split up into several starting zones at the ridgeline (Figure 2). The slope section beneath the plateau edge has a slope inclination of 50° to 60°. No perennial snow patches develop on the Gruvefjellet slope.

In Nybyen, a part of Longyearbyen and situated at 125 m a.s.l., 17 houses are built on old avalanche deposits underneath the Gruvefjellet slope (Figure 10). During both winter and spring, more than 200 students and tourists live in these houses. Cornice fall avalanches represent a recurring natural hazard for the inhabitants and infrastructure of Nybyen.

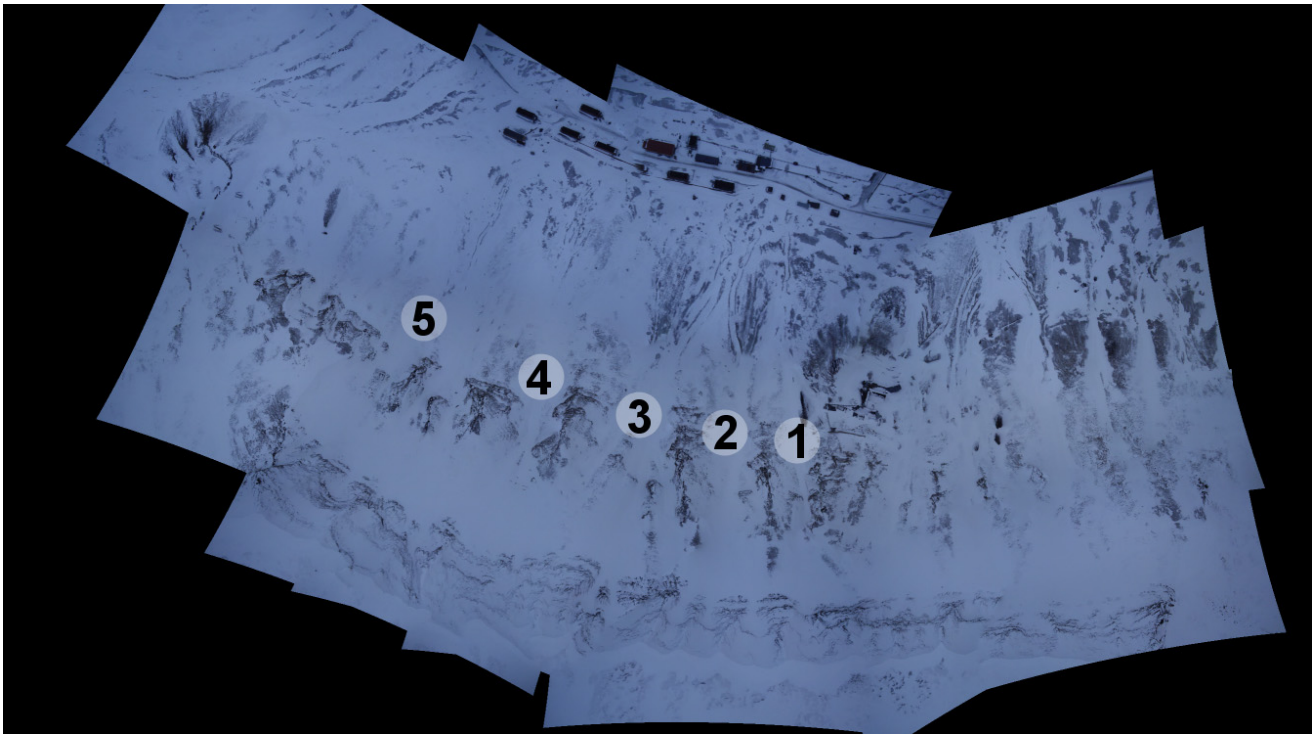

Figure 2 Aerial mosaic of 120 images taken 680 m above the valley bottom on 5 April 2010. The Gruvefjellet ridgeline is in the lowermost part and the houses of Nybyen in the upper part of the picture. The vertical height difference is about 335 m. Numbers indicate the five major gullies from Gruvefjellet. From North towards South, 1- Einbahnstraße, 2- Triple Y, 3- S, 4- Wrong Step, 5- Willy Sagnol. © KOLIBRI GEO SERVICES

2.3. Avalanches in Svalbard / CRYOSLOPE

Only little research has been done on snow avalanches in Svalbard. André (1990b) investigated the geomorphologic effect of spring avalanches and frequencies of debris flows and slush avalanches (André 1990a). Safety aspects in the Longyearbyen area were evaluated and avalanche zoning was carried out by the NGI, the Norwegian Geotechnical Institute (e.g. Hestnes 1996b, 1996a, 1999).

Hestnes (2000) described past avalanche events and identified meteorological factors which cause avalanches. Humlum (2002) modelled wind and precipitation in relation to topography in the area around Longyearbyen. Ellehauge (2003) carried out the first winter-spring avalanche observation in the Longyearbyen area. Humlum et al. (2007) linked snow avalanches to rock glacier development.

More systematic avalanche observations in Svalbard started in 2007 with the initiation of the CRYOSLOPE Svalbard project (2007-2009) coordinated by the University Centre in Svalbard. Its main scientific goal was to study the effects of modelled climate change on cold mountain slope processes in the high arctic Svalbard landscape by using the existing landforms as archives of past activity. These paleo-archives were combined with observations on modern active slope processes and meteorology in the slope area. Thereby year around avalanche observation constituted a major part. An avalanche database was established for the area surrounding Longyearbyen (*www.skred-svalbard.no*) (Figure 3). This master thesis is part of the outcome of the CRYOSLOPE project and all major cornice fall avalanches of my study have additionally been included in the CRYOSLOPE database for further studies. Eckerstorfer et al. (2008) and Eckerstorfer et al. (2009) described the monitoring programme and a major cornice triggered slab avalanche on an adjacent slope of the Gruvefjellet study area (Eckerstorfer et al. 2009). Eckerstorfer and Christiansen (2010) investigated an extreme slush and slab avalanche event around Longyearbyen between 14 and 19 January 2010.

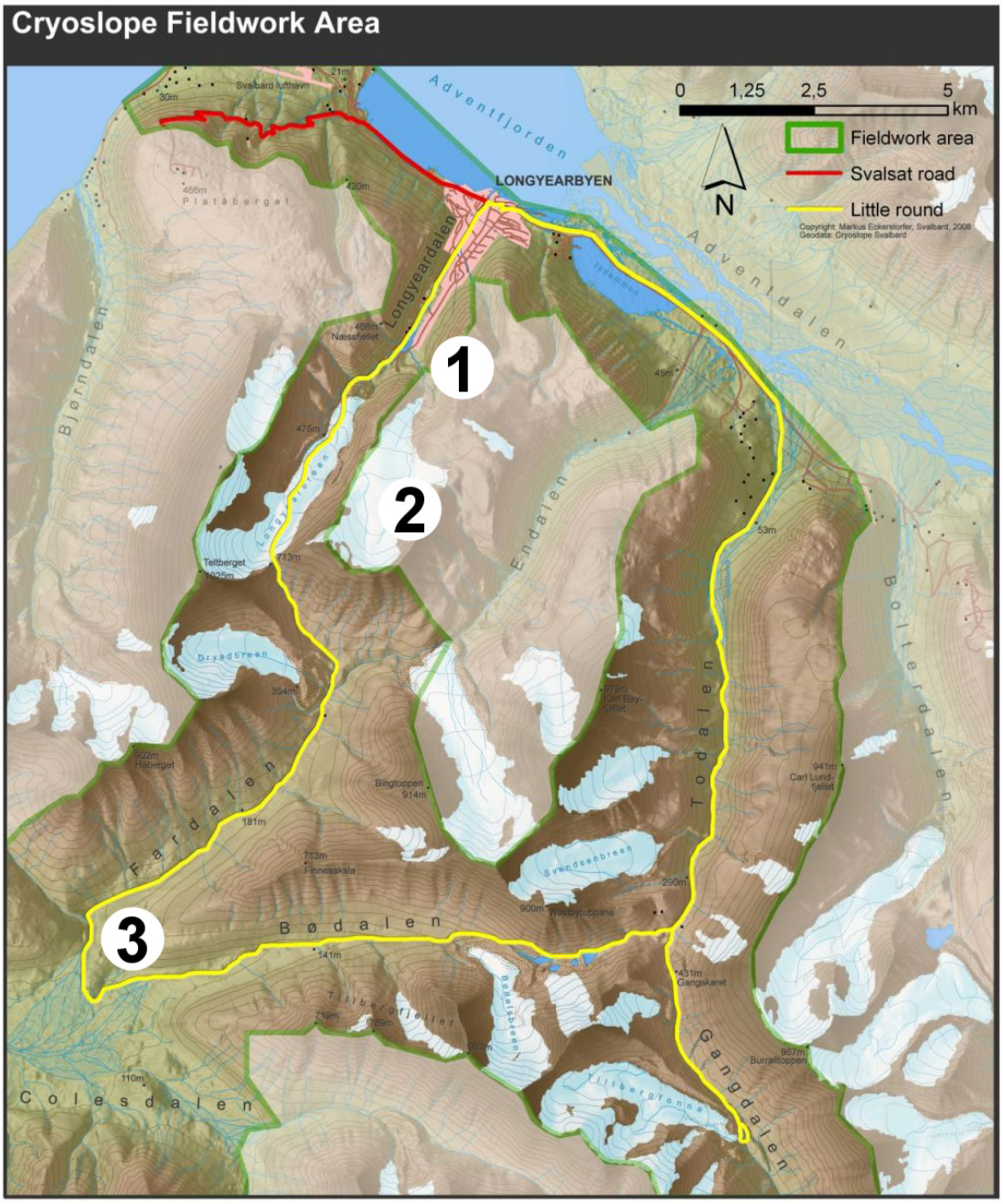

Figure 3 Topographic map of the CRYOLOPE field area around Longyearbyen (from *www.skred-svalbard.no*). Numbers indicate the three locations investigated in this master study, 1- Gruvefjellet cornice site, 2- adjacent site above the glacier Larsbreen, 3- Cornice accretion experiment site in lower Fardalen

2.4. Snow climate of Svalbard

Avalanche formation depends on the primary weather and atmospheric factors like precipitation patterns and intensity, wind direction and wind speed, sensible heat and radiation heating or cooling on snow (McClung and Schaerer 2006). Snow pack characteristics are determined by the snow climate type which in a broad, general sense, is divided into a 'continental' or either 'maritime' one. For snow climates in between, the term 'transitional' was suggested (McClung and Schaerer 2006). Tremper (2008) used the term 'intermountain', for mountains with an intermediate influence of Oceans. Though, the author stressed that considerable overlap exists and that – depending on time – each climate may occur anywhere, as they just represent a particular setting.

For central Svalbard a 'High arctic maritime snow climate' was proposed by Eckersdorfer and Christiansen (accepted) in particular for the area surrounding Longyearbyen (Figure 3). The snow climate is maritime and characterised by a thin, cold snow pack consisting of a persistent cold depth hoar base with ice layers and wind slabs above. These ice layers form due to a seesaw pattern of cyclonic activity bringing warm air to Svalbard. A multiplicity of avalanches occurs as a direct response to these cyclonic snow storms. Cornice fall avalanches occur as well as a direct response to cyclones and represent over 50% of all observed avalanches (Eckerstorfer et al. 2008, Eckerstorfer and Christiansen accepted).

3. CORNICE THEORY

Cornices are broadly defined as a wedge-like projection of snow formed by wind deposition to the lee of a ridge-line or slope inflection (Montagne et al. 1968, Latham and Montagne 1970) (Figure 4). Kobayashi et al. (1988) found that the windblown snow deposits on an unsupported, cantilever slab notwithstanding the behaviour of eddies on the lee-ward of a mountain ridge.

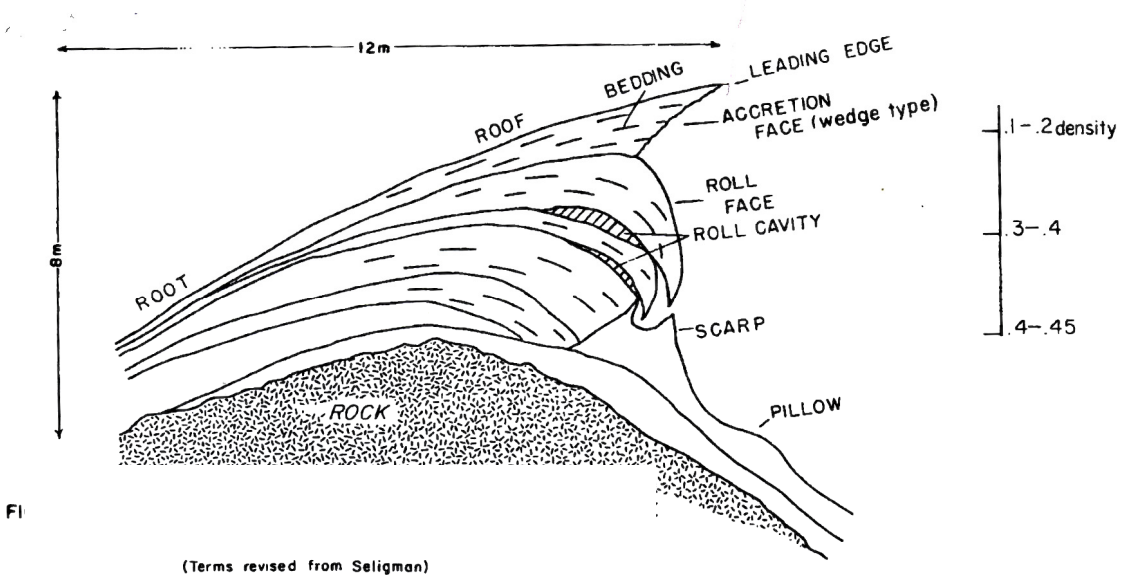

Figure 4 Schematic cross section of a typical mature cornice (from Montagne et al. (1968))

Paulcke and Welzenbach (1928) distinguished cornices along ridges and plateaus as well as winter and permanent cornices. Seligman (1936) defined different cornice sections. The author described the cornice root as the union between the deposit forming the cornice and the snow of the ridge or mountain side. Subsequently the cornice roof displays the snow surface between the root and the face. This front part of the cornice was subdivided by Montagne et al. (1968) into the leading edge, the furthest extension of the roof, the accretion face and roll face (Figure 4). The steep-fronted snow drift below the lower part of the roll face was named ‘scarp’ by Seligman (1936), though it is a translation of the German term ‘Gegenböschung’, used by Paulcke and Welzenbach (1928).

Montagne et al. (1968) retained ‘Snow cushion’ or ‘pillow’ referring to the low drift that connects the scarp with the undisturbed snow of the lee slope below the cornice (Figure 4).

3.1. Cornice formation

3.1.1. Accretion processes

A number of different processes may contribute to cornice formation and growth (Figure 5). Downwind accretion of snow particles in successive outward as well as upward extending layers represents the most common type. This accretion is called wedge type growth since a wedge shaped mass is formed along the leading edge with an accretion face showing an approximate initial angel of 50° to 70° inclined inwards. Under conditions of a copious supply of stellar snow flakes in combination with effective grain to grain adhesion, a horizontal sheet may extend as much as 10 cm into space, having a thickness of just a few cm. Due to their own weight, these features might sluff off, collapse or just curl downwards in a plastically behaviour under the influence of gravity. If stiffen the sheet may form the base for succeeding layers of the wedge or a vertical type. The latter one builds rather upwards without further horizontal extension; thereby the accretion face remains approximately vertical (Montagne et al. 1968) (Figure 5).

Under a wide range of temperatures, wind and humidity, wedge accretion most commonly takes place due to the mechanical clinging of either rimed or unrimed new stellar snow flakes. Consecutive sintering proceeds along the leading edge and hardens the mass. Density measurements in the forming cornice revealed a range from 0.1 g/cm³ for the clinging stellar snow types to 0.25 g/cm³ for the already sintered granular type.

In addition it was found that wedge accretion is not restricted to the abundance of stellar snow flakes; granular snow has also been observed to account for cornice growth under conditions of high relative humidity, slightly below freezing temperatures, and moderate surface wind speeds of from 7 to 15 m/sec. Montagne et al. (1968) described furthermore a very rapidly, nearly instantaneous, sintering process of rounded saltating grains which extend particle by particle outward and up the leading edge.

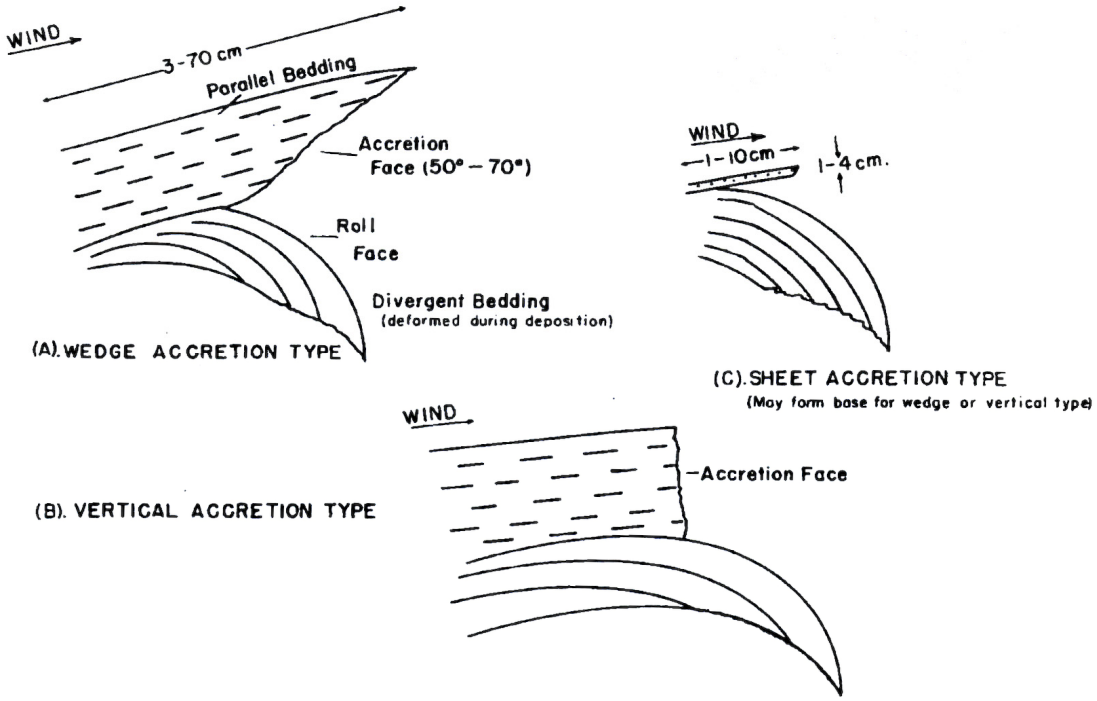

Figure 5 Details of snow cornice accretion types (from Montagne et al. (1968))

Naruse et al. (1985) compared mean grain diameter, bulk density and hardness of the surface layer (0.05-0.15 m) along the cornice root and roof as well as the scarp (Figure 4). These were found to be larger at the cornice root and roof as a result of sorting of snow particles in the deposition-erosion process. Smaller particles are more likely to be transported over the face by wind or collide with falling particles and redeposit at the scarp, while the larges ones remained along the cornice root and roof. Furthermore the scarp displays lower wind speeds and therefore lower falling velocities of the snow particles, which in turn leads to less effective compaction (Naruse et al. 1985).

3.1.2. Snow adhesion processes

Latham and Montagne (1970) stated that under momentary calm conditions or intervals snow grains have been observed to halt randomly near or at the leading edge. Though this method cannot be applied for steady wind conditions nor does it account for the horizontal projection of particles from the lee edge. The authors suggested additional explanations for the rapid adhesion of smooth, granular crystals.

For example the refreezing of a liquid water layer produced by frictional contact of the grains may explain the rapid bonding. At temperatures close to 0°C pressure melting may be of importance. Still the authors claimed that this is limited to the case when pressure melting, frictional heating and the time of contact of a saltating crystal with the snow surface has exceeded the time required for the liquid film to refreeze. Furthermore the possible influence of electrical forces in the adhesion progress has been investigated, as the exposed position of cornices may represent an electrical field at their surface, which is much greater than that of the adjacent environment. This might be the case particularly during a snow-storm where the extreme fields may reach sufficient magnitude to promote or support cornice development (Latham and Montagne 1970).

Measurements by Latham and Montagne (1970) along three cornices at Bridger Ridge, south-western Montana, revealed that the vertical electrical field strength increased rapidly with increased distance from the summit. Though the maximum achieved value was still two orders of magnitude below the minimum required to produce a significant increase in the degree of aggregation.

Based on crude calculations, Latham and Montagne (1970) indicated that pressure melting is unlikely to be important in the development of cornices formed from granular snow crystals. Furthermore frictional heating is believed unlikely to produce permanent bonding at temperatures warmer than about -8°C. The authors emphasised however that the latter mechanism might be of importance at lower temperatures. Since the velocity of snow crystals is unlikely to be as great as the wind speed as adopted in the calculation, the threshold temperature might even be somewhat lower. The rough calculations indicated that electrostatic forces will be of no significance at high velocities, but may be of importance at velocities below about 0.3 m/s (Latham and Montagne 1970).

These more favourable conditions may occur below and at the lee side of the leading edge (Montagne et al. 1968, Latham and Montagne 1970). Latham and Montagne (1970) stated that this finding is consistent with observations that snow crystal collection occurs on the sheltered accretion face of a cornice during its development. These observations were confirmed by McCarty et al. (1986). Previously Montagne et al. (1968) had stated that the accretion of snow crystals to the face might not be significant amounts unless blown by eddy currents which flow through gaps in the cornices.

Moreover Latham and Montagne (1970) gave two approaches on how electrostatic forces might promote growth at the leading edge of cornices, as wind velocities are considered to exceed the calculated threshold of 0.3 m/s: Windshear might provide more suitable conditions for electrostatic bounding and snow-particle velocities may be considerably less than the wind speed (Latham and Montagne 1970). Kobayashi et al. (1988) agreed in the latter approach and stated that windblown snow particles are approximately one thousand times heavier then air and therefore their motion might differ from that of air. Montagne et al. (1968) found that the wind speed was reduced several percent towards the leading edge of a cornice, which was slightly tilted due to deformation.

Montagne et al. (1968) emphasised that wedge growth (Figure 5) by accretion of granular snow particles has been observed both on clear days as well as on days when riming was occurring. To conclude, Latham and Montagne (1970) summarized that all three suggested mechanisms may contribute to the development of snow cornices to a certain extent.

3.1.3. Topographical and meteorological restrictions

McClung and Schaerer (2006) found that snow drift development changes significantly at a minimum change-of-slope angle of about 10° (Figure 6). Thereby sharp breaks of slope cause more turbulence in the over-passing air than in a comparable gradual slope change since pressure changes are greater. The airflow might separate from the ground on the lee side and even cause a reversal of flow direction along the snow surface with vertical eddies (McClung and Schaerer 2006).

This particular type of flow is described as the snow cornice flow or cusp effect (e.g. Heskestad 1965). Hereby the wind expands smoothly over the windward side of a ridge onto the lee side under the influence of a vortex situated in the cavity behind the cusp-like edge (termed 'leading edge' in Montagne et al. (1968)) of the cornice.

Figure 6 Cornice along the Gruvefjellet ridgeline during snow drifting conditions 31.3.2010. Stake in upper left corner of the picture is about 0.5 m high. Photograph towards S

Cornice formation might take place under relatively low wind speeds of about 7 m/s if humidity, temperature and snow conditions are favourable (Figure 6). The latter one includes a source for the snow supply which is in some cases the cornice root itself. Under these circumstances the cornice root tends to scour as the leading edge extends. If the wind speed exceeds about 27 m/s the entire cornice surface is scoured leading to an abrupt reduction of its weight (Montagne et al. 1968). McClung and Schaerer (2006) stated that the threshold wind speed for cornice formation is very comparable to the threshold wind speed for transport over loose, cold snow (5 to 10 m/s). Since the incorporated snow of a cornice is usually hard and dense (up to 500 kg/m^3) the threshold wind speed for scouring might be even greater than 25 m/s (McClung and Schaerer 2006).

3.2. Cornice characteristics

3.2.1. Cornice shape in relation to slope

Independent of the particular mechanism leading to cornice development and growth, the local slope morphology controls shape, size as well as extent of the cornice. In particular the declivity of the lee slope delimits the outwards projection. If the inclination exceeds 35°, the horizontal component of the developing cornice is limited due to the narrowed support along the lee slope line. On the Bridger Range, in southwestern Montana, lee slopes average about 35° and maximum vertical thicknesses of cornices measure about 10 m in late winter. From the ridgeline these cornices extend as much as 15 m outward and upward (Montagne et al. 1968).

Investigations in the northern and central parts of Hokkaido Island revealed that the cornice direction distribution were almost perpendicular to the ridge direction. Thereby Kobayashi et al. (1988) distinguished between upper layer and surface wind direction. Longitudinal stripes formed on the cornice roof along the surface wind were used to determine the cornice direction. The authors suggested that these surface winds flow up along the mountain slope and over the ridge by choosing the shortest course, which is perpendicular to the ridge direction (Kobayashi et al. 1988).

3.2.2. Cornice development

In order to analyse the formation processes of snow cornices, Kobayashi et al. (1988) dug a trench (10 m in length, 1.6-1.8 m in width and 0.6-0.8 m in depth) perpendicular to the prevailing wind direction. Coloured water was sprayed into the trench from a windward position during snow drifting to achieve a temporal resolution. The authors found that a tiny cornice was forming at the windward edge of the trench with windblown snow particles depositing on top of the projection (Figure 7). With adding particles and due to plastic deformation the snow slab hung down, though the cornice roof was always horizontal during snow drifting. No windblown snow attached on to the lower surface as the spayed on snow was not covered successively (Kobayashi et al. 1988).

Lateral view pictures indicated that the windblown snow only plunged into the trench. Their findings are in contrast to the approaches of Latham and Montagne (1970) in relation to the importance of electrical forces in cornice development. Although the trench was just a rather small scale experiment, the collection coefficient of windblown snow particles was unexpectedly large ranging from 25% to 50%. The authors explained these large values with the main snow mass being transported by saltation very near to the cornice surface. Furthermore the saltation motion of the snow particles might facilitate the deposition even on slightly sagging snow cornices (Kobayashi et al. 1988).

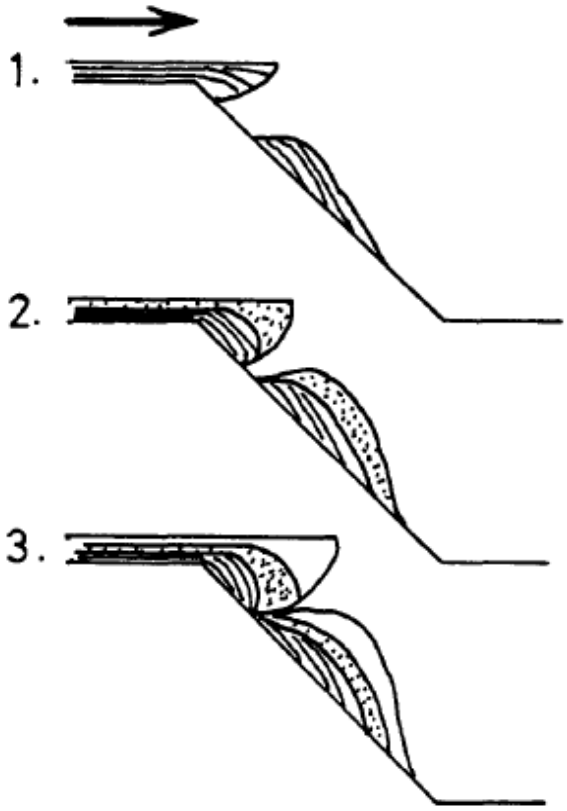

Figure 7 Schematic diagram of the formation process of a snow cornice

(from Kabayashi et al. (1988))

Comparable with the trench observation, the authors found that growing cornices at the Teshio Range in the northern part of Hokkaido Island also maintained a horizontal roof. Cross sections revealed that the cornice gradually hung down by creep, while windblown snow deposited on the cornice roof at the same time. Collection coefficients of windblown snow particles deviated a bit from the small scale trench experiment with values of 2 % in January but about 50 % in March. Kobayashi et al. (1988) suggested that in the early stage of cornice growth the deposition area was rather limited, while later in the season in March this area was about 2 m in length along the wind direction.

3.2.3. Cornice deformation

Montagne et al. (1968) divided cornice deformation into several sub-processes which may take place within the cornice mass. Under near freezing conditions snow behaves more plastically and therefore the deformation of the growing edge is accelerated. Though, the authors emphasised that in all cases gravity is the primary force.

One critical aspect in cornice deformation is the enclosure of an air space due to downward folding of the accretion wedge forming a curved tongue. The authors suggested the term 'roll cavity' for this zone of weakness that may be several feet (1 ft = 0.3 m) in both height and width (Figure 8). The size of the roll cavity is dependent upon the geometry of the original wedge and the quality of downward folding. In compressed form the roll cavity represents a persistent zone of weakness within the cornice mass where future fractures might localize. Slightly below freezing temperatures, contemporaneous deformation and cornice growth might occur in a way that the bedding layers in the accretion wedge tend to diverge toward the upper and outer edge. In contrast during relatively cold conditions these processes are limited and divergent bedding does not form during accretion. Therefore Montagne et al. (1968) suggested it might be possible to estimate the temperature conditions under which the cornice wedge formed by analysing the nature of its bedding

Creep and glide processes operate in the entire cornice mass continuously (Montagne et al. 1968) (Figure 8) which is comparable with alpine snow; ongoing metamorphism and high porosity are the reason for this (McClung and Schaerer 2006). Creep rates in snow increase exponentially with the reciprocal of the temperature. It is estimated that in seasonal snow about 90% of the creep, which is responsible for densification, is attributed to the rearrangement of grains, while only 10 % or less are due to mechanical effects which include deformation of ice grains (McClung and Schaerer 2006).

As creep processes proceed, tension fractures tend to open and are located between the cornice mass and the ridgeline bedrock (Figure 17). Bits of bedrock might be incorporated into the icy wall of the cornice and prove that formerly the cornice was in solid contact with the rock. This was observed at Bridger Ridge with tension fracture widths of 1 m near the surface (Montagne et al. 1968).

Cornice deformation processes have been investigated by Montagne et al. (1968) using time-lapse photography and the installation of vertical rods placed in the cornice roof behind the leading edge. Comparable to snow creep, the rods were tilted as much as 30° from the vertical within 9 days. The same pattern was found in marked strata. The authors emphasised that independently from the more rapid deformation of the unsupported accretion wedge, the entire solid cornice mass tends to roll downward in time (Figure 8).

Figure 8 Cornice cross section in lower Fardalen showing distinct bended layers due to ongoing snow creep. Total height of the trenched cornice was more than 3 m. Note the two enclosed roll cavities. Photograph taken 12 May 2009

3.2.4. Cornice strength and failure

In order to investigate cornice response to its meteorological environment, McCarty et al. (1986) monitored a particular cornice during a one month period and conducted density, strength, temperature, and physical properties profiles. Irrespective the short period of observation, the study demonstrated the quick response of the cornice to changes in meteorological conditions.

Strength profiles using a ram penetrometer were conducted at, respectively, 1 m windward of the apex, the apex, and 1 m leeward of the apex throughout the observation period (Figure 9). It was found that the cornice root on the windward side of the cornice never reached the thickness of the apex since it is subject to strong scour and periods of strong solar insolation. The profiles revealed that the cornice was heavily stratified which mirrored the harsh and often variable conditions during development. Throughout the observation period the lee side showed the fastest as well as most pronounced response to the changing meteorological conditions. The exposed contact surface of the lee side is the greatest of the three sections, since it is subjected to warming or cooling from three surfaces (top, right end, and bottom). By the end of the observation the lee side had essentially turned isothermal and the general strength of the entire mass had been reduced to a small fraction of its former reading. Overall temperature gradient metamorphism might play a crucial role in the variation of the mechanical and physical properties of a cornice. Nevertheless the authors stated that the strength of cornices may often be unpredictable and under some circumstances might even withstand the influence of explosives. On the other hand at some stages a small disturbance might already cause failure (McCarty et al. 1986).

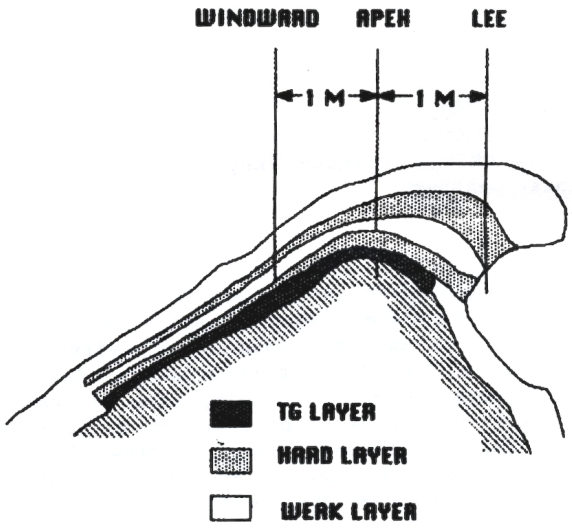

Figure 9 General cornice stratigraphy (from McCarty (1986))

Mosimann (2009) added that cornices can be very stable structures since they are able to endure their dead load. Spontaneous failures might occur already during the cornice development or later in the season when the snow gets softer with the onset of melt. Burrows and McClung (2006) distinguished three meteorologically-related triggers of cornice failure: (1) Loading of the cornice roof by new fallen or windblown snow during storm and wind events at a rate that exceeds the strength/fracture toughness of the cornice. The authors suggested that within this type of failure creep fracture is the primary crucial factor. (2) Distinct temperature changes of the roof surface due to abrupt air temperature changes, rain-on-snow events or heating by solar radiation. (3) Seasonal warming/prolonged midwinter warm periods (Burrows and McClung 2006).

Rain on snow events are known to increase the creep rate in the surface layer of a dry snow slab and thereby decrease slab stability (Conway 1998). The author found that the alterations by rain only affect the surface: Only the surface snow had warmed up to 0°C; even though liquid water was confined to the upper 0.15 m of the snow pack, the failure layer of many slabs was in about 0.55 m of depth. Avalanche activity increased significantly on all slopes after the onset of the rain event. Burrows and McClung (2006) suggested that this mechanism might similarly influence cornice stability. The same may account for the delayed time effects of increased loading by rainfall with further weakening due to longer-term warming.

Eckerstorfer et al. (2008) reported from Svalbard that cornice failures occur throughout the entire snow season, though are most common after significant temperature rises in combination with strong winds, as well as during the melting period. Additionally the authors found that the largest observed avalanches were cornice falls, which triggered both slabs and loose snow avalanches (Eckerstorfer et al. 2008, Eckerstorfer et al. 2009) (Figure 35). More generally McCarty et al. (1986) stated that in most cases of failure solely the overhanging portion of the cornice breaks off, though, the fracture might extend in some cases into the windward side of the apex. Based on accident reports form Switzerland, Mosimann (2009) suggested that cornices in high mountains might be more ‘breaking resistant’ during summer time when the snow is heavily compacted. The better visibility of tension factures might also lead to the low accident numbers during summer time as mountaineers therefore might be more aware of a safe travel route.

4. METHODS

The cornice development was studied in the two consecutive snow seasons 2008/2009 and 2009/2010, each lasting from the beginning of October until the end of July. The first distinctive snow observed on Gruvefjellet represents the start of the snow seasons, while the melt of the last cornice remnants along the ridge line represents the end. Within both snow seasons, fieldwork was conducted between January and July. Two automatic time lapse cameras were used throughout the entire two years to observe the cornice development and eventual failure. One was photographing from the valley bottom, while the other was operating parallel to the ridgeline (Figure 10). Furthermore the automatic camera photographs were used to record and quantify cornice failures, achieve daily snow depth data and to investigate the development of cornice cracks. Meteorological data were collected from the automatic weather station 'Gruvefjellet', situated in the central part of the Gruvefjellet plateau source area.

Figure 10 The valley Longyeardalen 21 January 2010 looking NE. The plateau shaped mountains Platåberget and Gruvefjellet with the study area are seen to the left and right of this photograph, respectively. The houses of Nybyen are seen on the right side and Longyearbyen in the background.

4.1. Fieldwork

Fieldwork was carried out in both snow seasons between January and July, due to the polar night in combination with the rather slow onset of the snow season and corresponding to the end of the snow season, respectively. 45 field trips were carried out up to the Gruvefjellet plateau, mostly by ski (Figure 11). For the majority of the field trips up the plateau, a route over the glacier Larsbreen was chosen. This route provided insight into the cornice development as well as observations on recent cornice failures along the adjacent part of Gruvefjellet above Larsbreen. In general, this gave a good overview and enabled comparison of the two areas. For the remaining field trips, the route through the valley of Vannledningsdalen was chosen, which provided quick access to the plateau area (Figure 3). The automatic camera and other equipment were transported through this valley. Countless brief field trips were carried out from Nybyen up the Gruvefjellet slope to investigate recent cornice fall avalanches. During the polar night period (October to February) long exposure photographs were taken regularly of the entire Gruvefjellet slope.

Figure 11 Fieldwork along the Gruvefjellet ridgeline 23 March 2010. During the installation of the cornice crack measuring set-up a belay rope was used. Longyearbyen is seen below

4.2. Meteorological station ‘Gruvefjellet’

The meteorological station ‘Gruvefjellet’ is part of a network of meteorology, permafrost and CTD stations run by the University Centre of Svalbard (UNIS). It is situated on the Gruvefjellet plateau at 464 m a.s.l. (Figure 3).

Air temperature (10 cm, 1 m and 3 m), wind speed (min, max, average) and wind direction are recorded continuously on an hourly basis and available online (http://www.unis.no/20_RESEARCH/2060_Online_Env_Data/weatherstations.htm).

Furthermore ground temperatures in intervals down to 5 m and relative humidity are measured. The station is located about 500 m from the cornice study site in the middle of the Gruvefjellet plateau (Figure 12).

Figure 12 The automatic weather station 'Gruvefjellet' 5 February 2010

4.3. Snow monitoring by automatic cameras

Three automatic time lapse cameras were used to monitor the cornice development, in the form of cornice accretion and scouring as well as eventual failure. Furthermore snow depth and snow distribution was determined by a snow stake in the camera's field of view. Christiansen (2001) described this inexpensive technique as an alternative to traditional snow monitoring by sonic sensors, snow pillows or manual measurements of snow depth. The author pointed out that the use of automatic cameras provides additionally aerial and general weather information useful for understanding the process dynamics studied. All three cameras were visited regularly to ensure the mode of operation.

Figure 13 The automatic time lapse camera set-up of 'Sverdrupbyen' installed in a weather proof box and mounted on a tripod. The time lapse controller is to the left of the digital camera and the 12V battery to the right. The solar panel is fixed on the weather proof box.

4.3.1. The Sverdrupbyen camera

The automatic camera ‘Sverdrupbyen’ became operational 5 December 2008. It stood on an artificial ridge on the western side of the valley Longyeardalen, which is blown free from snow throughout winter (Figure 3, Figure 10). The camera system was established on a tripod 1 m above the terrain surface and additionally secured by ropes and several boulders around its legs. A standard digital SLR camera (Pentax K110D) was used with an 18-55 mm lens. The digital photographs were stored as jpg-files on a 2 GB SD card. The camera was equipped with a Harbortronics DigiSnap 2000 time-lapse controller and connected to a 12V battery. The entire system was placed into a weatherproof box, with a clear plastic glass window in front of the camera and a solar panel on top of it (Figure 13). The camera photographed the entire Gruvefjellet slope above Nybyen with the mine ‘Nye Gruve II’ as the margin towards N (Figure 14).

Figure 14 Automatic time lapse photograph of the 'Sverdrupbyen' camera across the valley Longyeardalen from 2 June 2010. Large failures are visible in the gullies 'Wrong Step', 'Willy Sagnol' as well as remnants in 'Triple Y'. The houses of Nybyen are in the lower part of the photograph and the mine to the very left.

During the twilight periods and polar night, daily pictures were taken around noon to use the daylight as much as possible. After the return of the sun I enhanced the temporal resolution to two daily pictures from 20 April 2009 (4.00 h and 16.00 h) and six daily pictures from 20 May 2010 (3:30 h, 7.30 h, 11.30 h, 15.30 h, 19.30 h, and 23.30 h). These increase time resolutions were chosen to improve the event-time accuracy and to relate the failures to meteorological variations or direct sunshine on the slope. Furthermore an increased time resolution enables one to separate several rather small failures in one gully possible occurring on the same day. The horizontal distance to the Gruvefjellet cornice site was about 1100 m across the valley.

4.3.2. The Gruvefjellet camera

The automatic camera 'Gruvefjellet' was installed parallel to the Gruvefjellet plateau edge facing NNE 11 February 2009 (Figure 15). It was fitted into a 0.5 m high stone cairn. Following Christiansen (2001) the camera was installed almost perpendicular to the dominant winter wind direction to use the obtained photographs even during snowdrift periods. Additionally this position minimises the amount of snow in front of the used weatherproof box. I used a Kodiak Easyshare CX6200 digital camera equipped with a time-lapse controller. The use of a 12V battery in addition to a solar panel on top of the box was similar to the 'Sverdrupbyen' camera (Figure 13). The cameras field of view included parts of the valley bottom, the plateau edge and large parts of the plateau source area towards the 'Gruvefjellet' automatic weather station (Figure 15).

The aim of this camera setup was to monitor cornice accretion, erosion as well as cracking. Throughout both snow seasons two daily pictures were taken. However, no pictures were taken between 28 April – 16 May, 2 June – 9 June and 6 September – 1 November in 2009 due to recurrent error indications. In 2010 the period of 18 March – 6 May was not covered by automatic photographs due to a malfunction in the battery recharge function. As a consequence of recurrent camera malfunctions no persistent photograph time was achieved throughout the snow seasons.

Figure 15 Automatic time lapse photograph of the 'Gruvefjellet' camera looking NE from 15 February 2010. The snow depth measuring stake is about 0.5 m high and pronounced cornice cracks are seen along the ridgeline. This photograph indicates that even in the early part of the year and the absence of sunlight, automatic time lapse photography may gives valuable information

4.3.3. The Fardalen camera

The automatic camera 'Fardalen' was installed in the narrow river valley of lower Fardalen at the transition to Colesdalen (Figure 3). I used the same setup as was used for the 'Sverdrupbyen' camera (Figure 13), though the weatherproof box was fitted into a stone cairn. The camera was set up after a cornice failure in the narrow valley and was operational between 19 March and 20 May 2010. The aim was to observe cornice accretion and generally the rebuilding of the new cornice using time-lapse photography. Therefore a very high temporal resolution was used with six photographs a day (3.00 h, 7.00 h, 11.00 h, 15.00 h, 19.00 h, and 23.00 h) from a nearly frontal position (Figure 16).

Figure 16 Automatic time lapse photograph of the 'Fardalen' camera from 14 April 2010. Snow machine for scale

4.4. Snow depth distribution

Snow depth and its variability were recorded at one measuring stake at the crossover of the main plateau of Gruvefjellet to the cornice root in both snow seasons. I installed a wooden stake with coloured height indications in front of the automatic camera 'Gruvefjellet' 15 February 2009 (Figure 17). On 8 June 2009, close to the end of the first snow season, the stake tipped over and was reinstalled closer to the camera on 8 July 2009 for the following snow season. Under sufficient light conditions a daily snow depth value could be assessed with an accuracy of 5 cm in the snow season of 2008/2009 and 2 cm in 2009/2010 respectively. Additional stakes with height indicators were drilled in parallel to the plateau edge to achieve a general picture of the snow distribution and for better orientation during the fieldwork (Figure 18). Furthermore nine stakes were installed in a line on a prominent rock nose towards the cornice root, covering about 25 m, to determine the nature of deformation due to snow creep following Montagne et al. (1968). Reindeer and pronounced storm events destroyed three stakes in the first snow season and six stakes in the second one. Four stakes were additionally used as locations for manual photographs on each field trip.

No daily snow depth values could be assessed in periods of enhanced snowdrift that hindered visibility. Naturally in periods without automatic camera photographs no snow depth values could be obtained.

Figure 17 Automatic time lapse photograph of the 'Gruvefjellet' camera from 16 May 2010. The coloured height indicators on the snow depth measuring stake represent 10 cm. Note the opening cornice crack in the foreground on the left side

Figure 18 Row of snow stakes on a rock nose towards the cornice root and along the ridgeline towards the automatic camera 'Gruvefjellet' seen in the background. Photograph towards S (taken by Markus Eckerstorfer on 22 February 2009)

4.5. Cornice sizing

Cornice growth was determined by analysing the daily pictures of the automatic camera 'Gruvefjellet' (Figure 15). Particularly the horizontal growth was not possible to measure and quantify in a secure manner without cornice perturbation. Therefore merely periods of 'cornice accretion', 'pronounced cornice accretion' and 'cornice scouring' in terms of erosion under the influence of high wind speeds in excess of 25 m/s (Montagne et al. 1968, McClung and Schaerer 2006) were distinguished. 'Pronounced cornice accretion' represented storm events that visually led to significant cornice growth independent of the events duration. This determination was achieved relative to all selected storm events that led to cornice accretion of the two observed snow seasons. 'Cornice scouring' represented storm events that significantly reduced the cornice extent horizontally and vertically. Selected periods of 'cornice accretion', 'pronounced cornice accretion' and 'cornice scouring' were compared to the hourly recorded meteorological data of the 'Gruvefjellet' automatic weather station (Figure 12). This enabled to determine a time limitation for the particular events on an hourly resolution. Furthermore the selected events of cornice accretion and scouring could be coupled with the continuous snow depth values achieved in front of the camera (Figure 17). This displayed the particular event's effect on the snow cover at the transition of the main plateau to the cornice root.

Automatic photographs during the polar night provided only limited information, therefore merely the variation of the outward extension of the cornice, masking the illuminated Longyearbyen below, could be detected in good visibility. Periods without daily automatic camera pictures were not investigated. By using only fieldwork observations, cornice variations could not be detected in the applied accuracy and could not be coupled to the meteorological data and snow depth measurements.

4.6. Cornice crack measurements

Cornice crack measurements were conducted in both snow seasons along the Gruvefjellet plateau edge, once cornice tension cracks appeared at the surface. The setup consisted of two stakes. One was installed on the plateau and represented the reference point. The second stake was equipped with a thin line and inserted into the cracked cornice part, about 0.5 m away from the crack to avoid any interference with the exposed cornice fracture (Figure 19). The initial distance to the reference stake was indicated by a knot in the line. In the course of the snow season the relative distance of the knot to the reference stake was measured manually on a cm scale, on every fieldtrip. This enabled an elementary, and most notably a safe method to quantify the cornice crack opening. Furthermore this method did not cause further surface perturbation along the cornice root and roof once the set-up was installed.

Figure 19 Cornice crack measurement set-up 23 April 2010. The crack is about 0.5 m wide and refilled by drifted snow. Note the coloured height indicators on both stakes. (Photograph taken by Manuel Marienfeld)

In the snow season 2008/2009 12 measurements were conducted between 28 April and 14 June 2009 in the starting zone of the gully 'Wrong Step'. In snow season 2009/2010 two measuring setups were installed at the same cornice crack several meters apart starting 5 February 2010 in the starting zone between the gullies 'Wrong Step' and 'Willy Sagnol'. Only one measurement was taken at each spot on 10 February before a cornice failure destroyed both setups. Thereafter 15 measurements were carried out in the period between 24 March and 24 June at a remaining cornice in the starting zone of the gully 'Wrong Step'. In the latter period, the two stakes used were also equipped with coloured height indicators which enabled additional snow distribution data on a micro scale (Figure 19). These were used to investigate the snow accretion variability from the plateau towards the cornice root. Furthermore the general impact of snow depth variations on the measured cornice crack opening rate was studied.

4.7. Cornice failure monitoring and database

Using the automatic camera 'Sverdrupbyen' with intervals of up to six pictures a day the changes along the ridgeline of the Gruvefjellet plateau could be detected (Figure 14).
The high photograph resolution of the digital SLR camera was beneficial and enabled significant zooming into particular photographs to determine variations. Failures were observed and investigated in great detail and collected in a cornice database. The failures were assigned to one of the five major gullies (Figure 2) and the recorded picture time of the automatic camera was taken as event-timing if there was no eyewitness. The magnitude of each failure was determined by two values – the destructiveness ("D") and the size relative to the given slope ("R") following Greene et al. (2004). The "D" value describes the destructive potential of an avalanche from the mass of deposited snow. Each category displays the destructive force applied to an object (person, car, trees) located in the avalanche track or at the beginning of the runout zone. The "R" value estimates the size of an avalanche relative to the particular avalanche path where it occurred. Both values range from 1 to 5 (Greene et al. 2004).

Furthermore a graduation in relation to the entrained debris was done based on the visibility of debris on the snow surface after failure: DC1 (no entrained debris visible), DC2 (some entrained debris visible) and DC3 (high debris content) (Figure 21). This represented a simplified graduation of the sophisticated debris classification by André (1990b), dividing debris-free avalanches, and very slightly, slightly, moderately, highly and extremely dirty avalanches based on their apparent debris content.

The morphology of the avalanche deposits was differentiated between 'Tongue' and 'Fan' to investigate the interaction of slope angel and deposited avalanche mass. The split-up into several minor tongues was included into the intermediate category 'Tongue/Fan', to account for several rather small intervals of failures at the same starting zone forming one avalanche deposit.

In addition to the camera's continuous registration, direct observations and inspections were done on the Gruvefjellet slope particularly in the case of larger cornice fall avalanches (Figure 20). Special features such as the maximum debris size were noted and included into the cornice database as a comment. If possible the fracture at the plateau edge was visited during the following field trip (Figure 21).

Cornice fall avalanches recorded between 2006 and 2008 included in the CRYOSLOPE database (*www.skred-svalbard.no*) - prior to the continuous observation of the slope by automatic cameras in this thesis study - were included in the cornice database if the documentation and photographs showed sufficient details.

Figure 20 Inspection of a large cornice fall avalanche in the gully 'Triple Y' on 20 June 2009. Note red backpack for scale

Figure 21 Inspection of a cornice scar along the ridgeline 10 June 2010. The debris-rich runout is visible in the low inclined slope section

5. RESULTS

5.1. Meteorology

Both snow seasons 2008/2009 and 2009/2010 are comparable from a meteorological point of view. Though the average hourly temperature throughout the snow seasons (October until July) varied between -8.7°C in 2008/2009 and -6.8°C in 2009/2010, with maximum values of +11.3° C (27.07.2009) and +9.4°C (14.07.2010) respectively at Gruvefjellet (464 m a.s.l.). The lowest temperatures were -30°C (11.01.2009) and -28°C (23.02.2010). Both snow seasons showed pronounced mid-winter warm spells with sudden temperature rises of more then 20°C, reaching melting conditions, induced by low pressure systems reaching Svalbard. Average hourly mid-wind speeds were 4 m/s in 2008/2009 and 3.9 m/s in 2009/2010. Highest hourly mid-wind speeds were 16.3 m/s in 2008/2009 and 19.1 m/s in 2009/2010. Thereby hourly maximum values of 25.6 m/s (25.12.2008) and 32.4 m/s (07.03.2010) were measured at the 'Gruvefjellet' automatic weather station which corresponded with distinct air temperature rises due to low pressure systems coming in. Average hourly maximum wind speeds were in excess of 6 m/s in the investigated snow seasons – 6.2 m/s in 2008/2009 and 6.4 m/s in 2009/2010 (Diagram 1, Diagram 3).

The predominant winter wind direction was from the SE, though variation became more distinct towards the end of the snow season (Diagram 2, Diagram 4). The observed storms indicated an overall wind direction from the ESE.

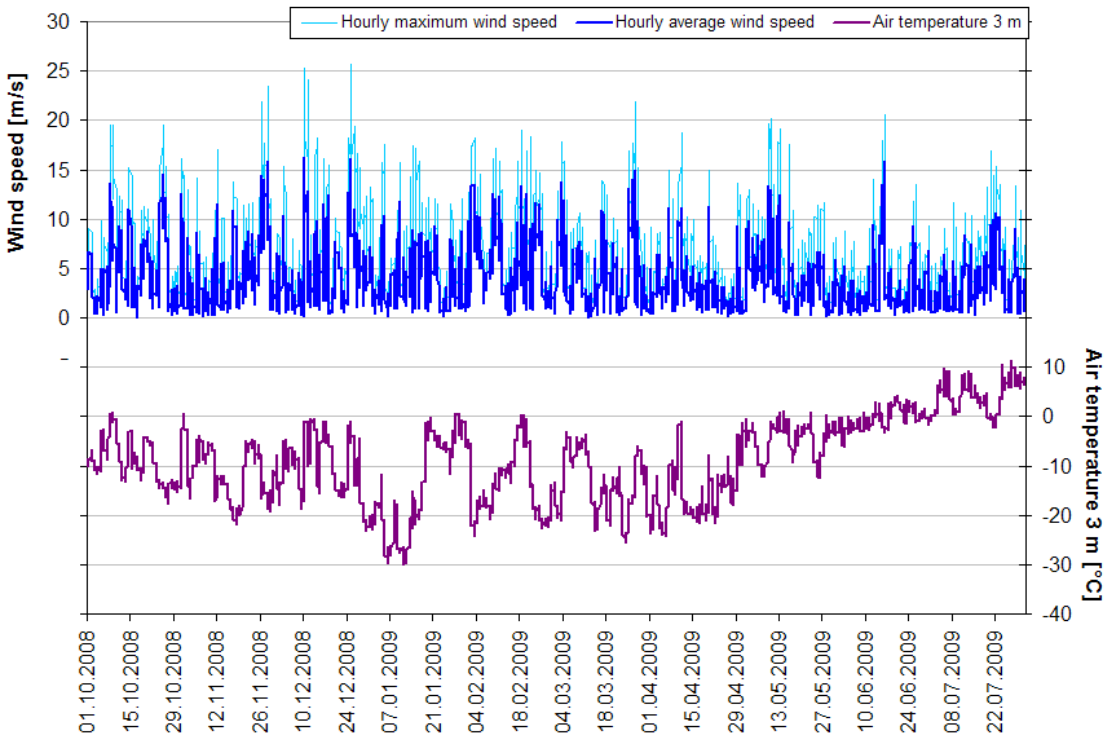

Diagram 1 Meteorology of the snow season 2008/2009

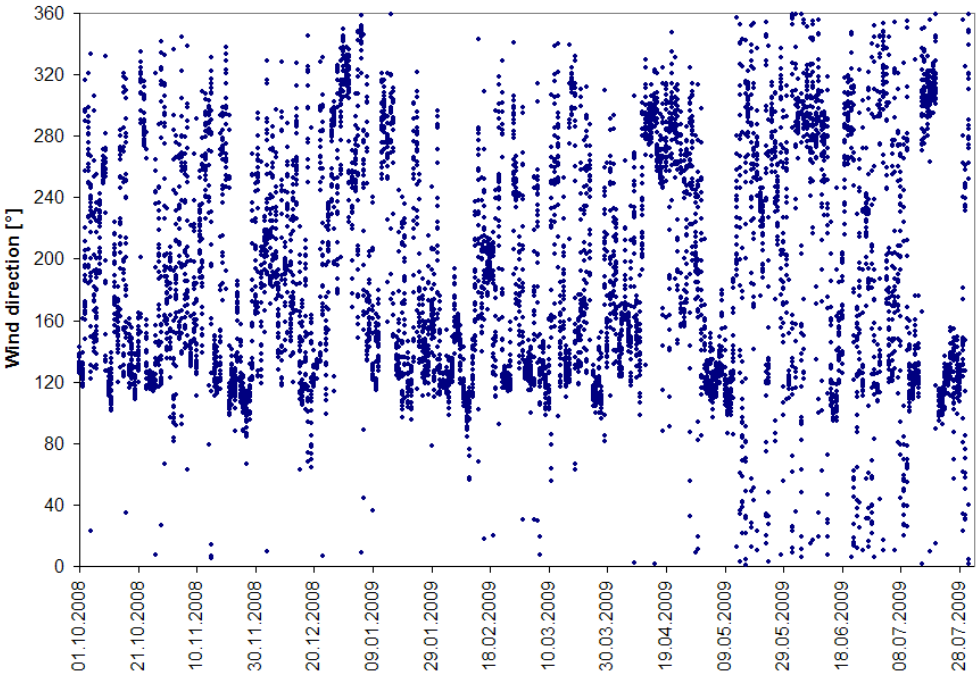

Diagram 2 Wind direction distribution of the snow season 2008/2009

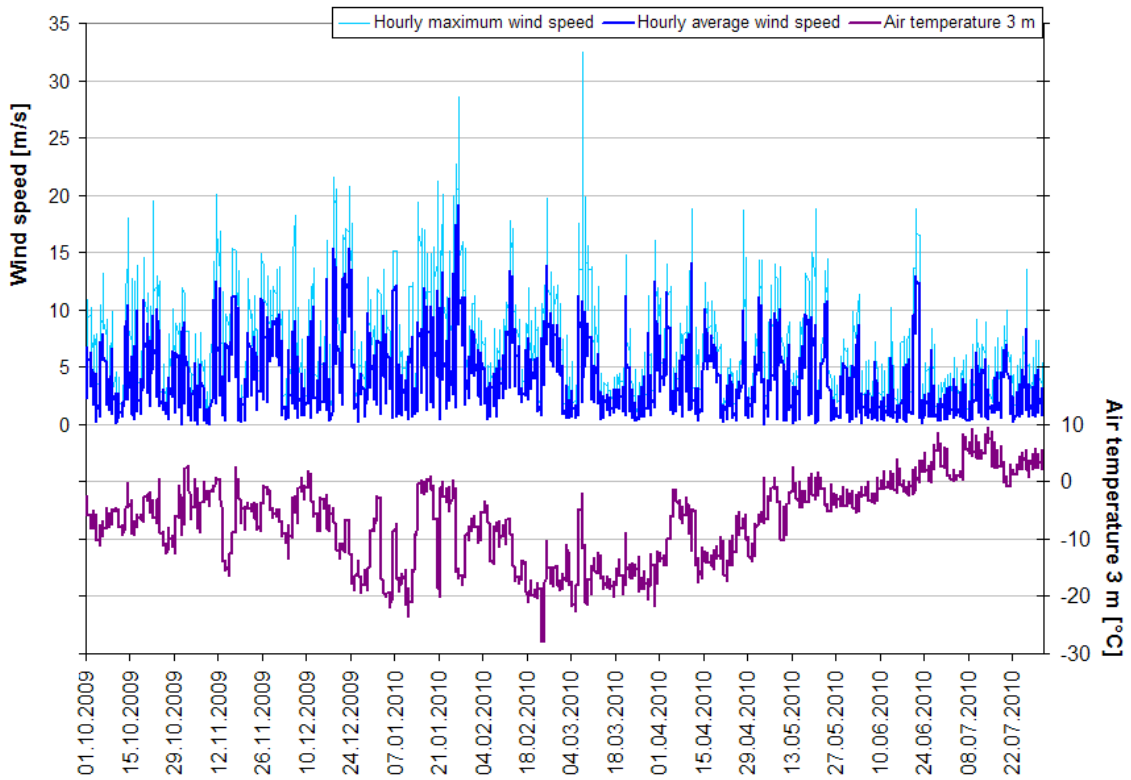

Diagram 3 Meteorology of the snow season 2009/2010

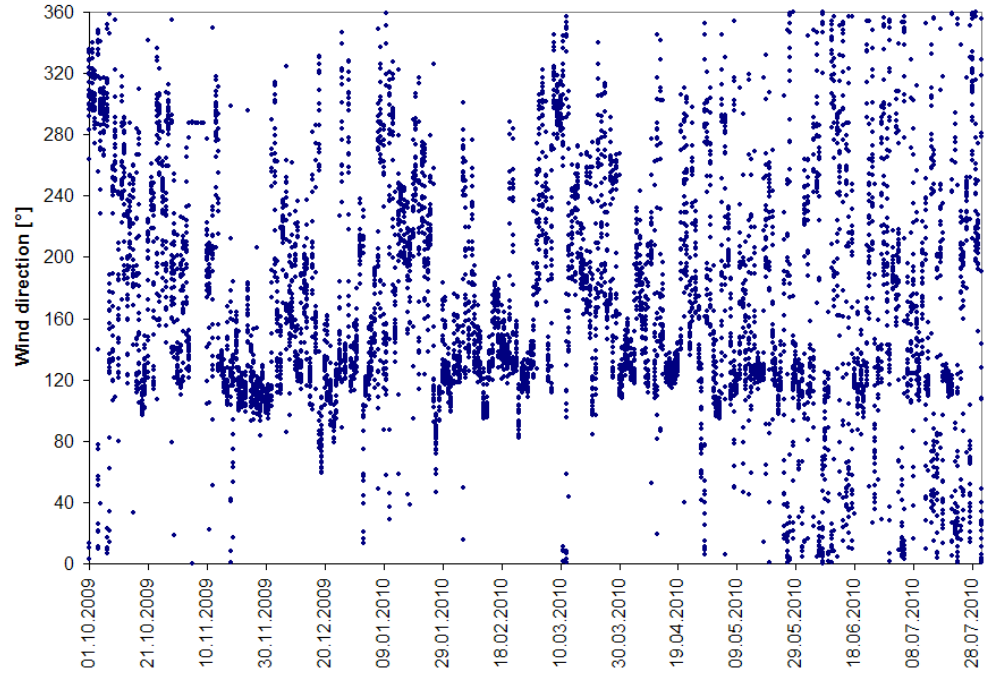

Diagram 4 Wind direction distribution of the snow season 2009/2010

5.2. Cornice accretion and scouring

5.2.1. Overview

The obtained automatic camera pictures and the fieldtrips up the plateau indicated that cornices grow to a relevant size within a short time after the first snowfall. Cornice accretion took place as a direct response to the first snow falls recorded 23 September 2008 and 13 September 2009 respectively. Though, the actual process of cornice accretion could not be investigated and remained elusive. Cornice accretion proceeded throughout both entire snow seasons. The Gruvefjellet plateau area around the snow depth measurement stake became snow free in the last week of June in both snow seasons. The last cornice remnants along the ridge line had melted away by the end of July in both snow seasons. No remnants survived the summer time, which makes the cornices along the ridgeline of Gruvefjellet an annual phenomenon.

5.2.2. Cornice accretion experiment

I carried out a cornice accretion experiment to quantify the cornice accretion which was unfeasible during the polar night. The cornice development was investigated in the small river valley of lower Fardalen (Figure 3). In contrast to the Gruvefjellet slope, this location provided access to the cornice scarp from below. After a significant cornice failure a 5 m wide and approximately 1.5 m deep trench was dug further into the remaining cornice bedding 19 March 2010. The automatic camera pictures and direct observations revealed the importance of pronounced storm events in relation to cornice accretion (Figure 16). The trench was completely filled up by 22 March 2010 and one wedge shaped layer had developed that already crept downwards after one significant storm event. This pronounced downward folding of the leading edge led to the formation of roll cavities which were seen developing following 12 wind drifting events (Figure 22).

Figure 22 Investigation of roll cavity formation on the experimental side in lower Fardalen on 3 February 2010. Person for scale

Their particular importance in relation to cornice failures was affirmed by a cornice triggered slab that occurred 17 April 2010 (Figure 23). Furthermore the location in Fardalen enabled the investigation of the cornice scarp. Wind slabs were deposited to the lee of the cornices during storms. This makes these areas below the cornices prone to slab avalanche releases, which are in particular triggered by cornice failures. Even though the Fardalen site represents a slope of about 10 m to 15 m in height, the observed cornice triggered slab avalanche was large in relation to the slope extent with cornice blocks up to 2 m in diameter in the runout zone (Figure 23). Additionally the inclination of the cornice scarp was found to increase with further deposition of drifted snow. This might be a crucial factor in relation to slab release below cornices. Though, no measurements were conducted here.

The experimental site in Fardalen has proven to be a useful location for comparison, and observations of the Gruvefjellet site could be studied in greater detail.

Figure 23 Cornice triggered slab with blocks up to 2 m in diameter in the runout observed by the automatic time lapse camera 'Fardalen' on 17 April 2010.

5.2.3. Snow depth measurements

Snow depth was measured at the crossover of the main Gruvefjellet plateau to the cornice root throughout both snow seasons (Figure 17). On the Gruvefjellet plateau source area considerable amounts of snow were accumulated, redistributed by wind and eventually redeposited along the ridgeline. The very beginning of both snow seasons were not covered by the automatic camera 'Gruvefjellet'. The automatic camera 'Sverdrupbyen' recorded the first snow within the Gruvefjellet slope section 23 September 2008 and 13 September 2009, respectively. The onset of the snow cover was very slow. The Gruvefjellet slope section displayed a more or less continuous snow cover not before late October. Though the snow cover on the main plateau was more pronounced during the second snow season 2009/2010. The plateau area became mostly snow free at the beginning of July within both snow seasons, as constant temperatures above freezing and 24 hours of incoming radiation presumably overcome the differences in snow depth. The snow depth measurements revealed some distinct variations within both investigated snow seasons. In the snow season 2008/2009 snow depth values varied between 15 cm and 20 cm for most of the time with the maximum value of 45 cm on 29 March 2009 (Diagram 5).

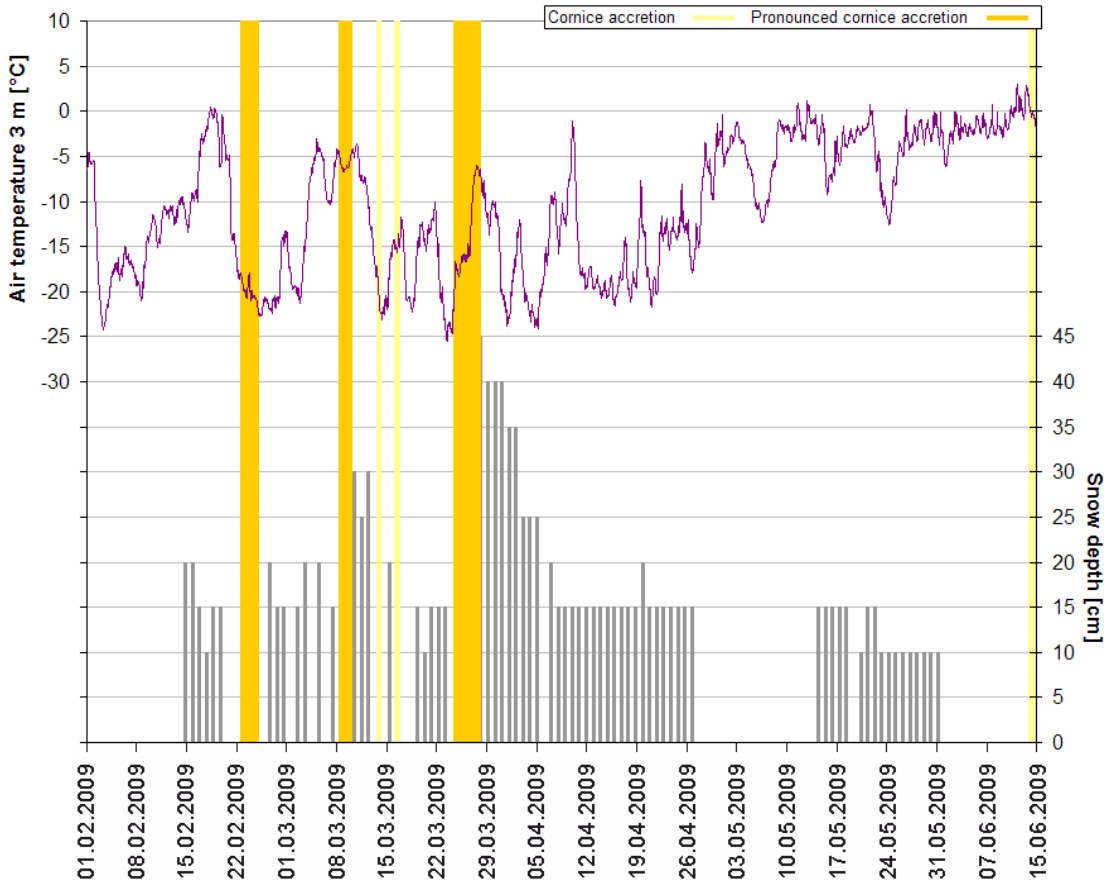

Diagram 5 Recorded snow depth close to the cornice root and controlling periods of cornice accretion of the snow season 2008/2009 after the installation of the 'Gruvefjellet' camera

The ground at the stakes initial position became snow free 25 June 2009. The snow depth values of the 2009/2010 snow season were in general somewhat higher. Values ranged around 25 cm for most of the time. The maximum value of 38 cm was recorded 03 March 2010 (Diagram 6). In contrast to the majority of snow depth variations, this increase was not caused by any storm event. The snow depth dropped significantly from 21 June to 25 June 2010 from 26 cm to 4 cm driven by temperatures constantly above freezing and 24 hours of incoming solar radiation. On 26 June 2010 the ground around the measurement stake became snow free.

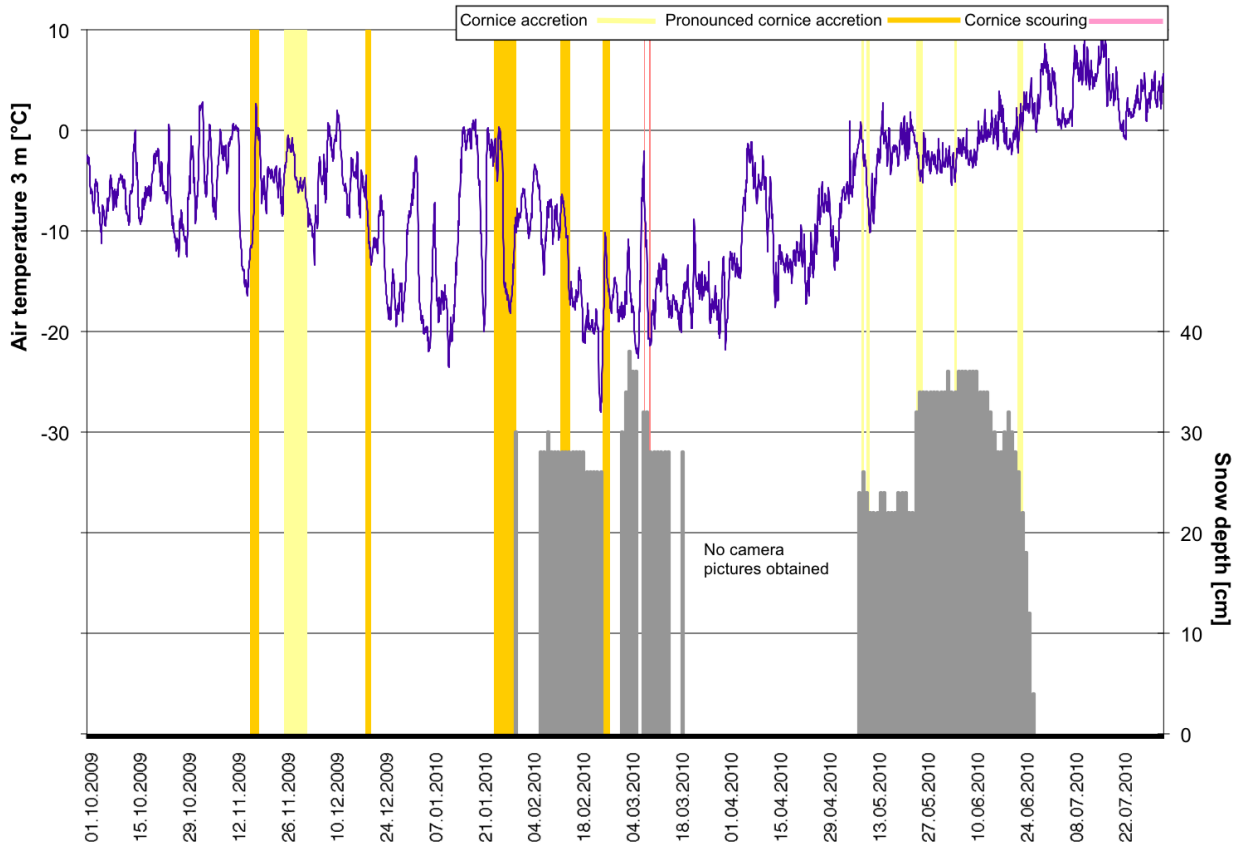

Diagram 6 Recorded snow depth close to the cornice root and controlling periods of cornice accretion and scouring of the snow season 2009/2010

The results revealed that measuring snow depth at or close to the cornice root is a valuable method to investigate and quantify periods of cornice accretion and scouring. Despite this, longer periods without measurements due to the malfunctioning of the automatic camera hindered analysis of the two snow seasons to some extent. Furthermore the stake with height indicator had to be reinstalled at the end of the first snow season. The micro topography of the Gruvefjellet plateau close to its edge is variable and therefore may have influenced the measurement conditions of the two snow seasons.

5.2.4. Meteorological influence on cornice accretion

During the second snow season 2009/2010 11 storms that contributed to cornice accretion could be identified, 5 storms led to considerable cornice growth (Diagram 8). Only 6 storms were identified in 2008/2009, of which 3 increased the cornice mass significantly (Diagram 7). In both snow seasons 10 events with increasing wind speeds were identified where no cornice accretion was visually observed by the automatic camera pictures. Though, these included the polar night as well as periods without camera observations. The duration of the storms decreased towards the end of the snow season 2009/2010. In 2008/2009 such a trend was not observed, though the duration of the storms varied between 93 hours (25 – 28 March 2009) and 13 hours (14 March). The length of period varied more significantly in the second snow season 2009/2010 between 151 hours (25 November – 1 December 2009) and 12 hours (2/3 June 2010). On average the storm duration was about 2 days – 46 hours in 2008/2009 and 54 hours in 2009/2010.

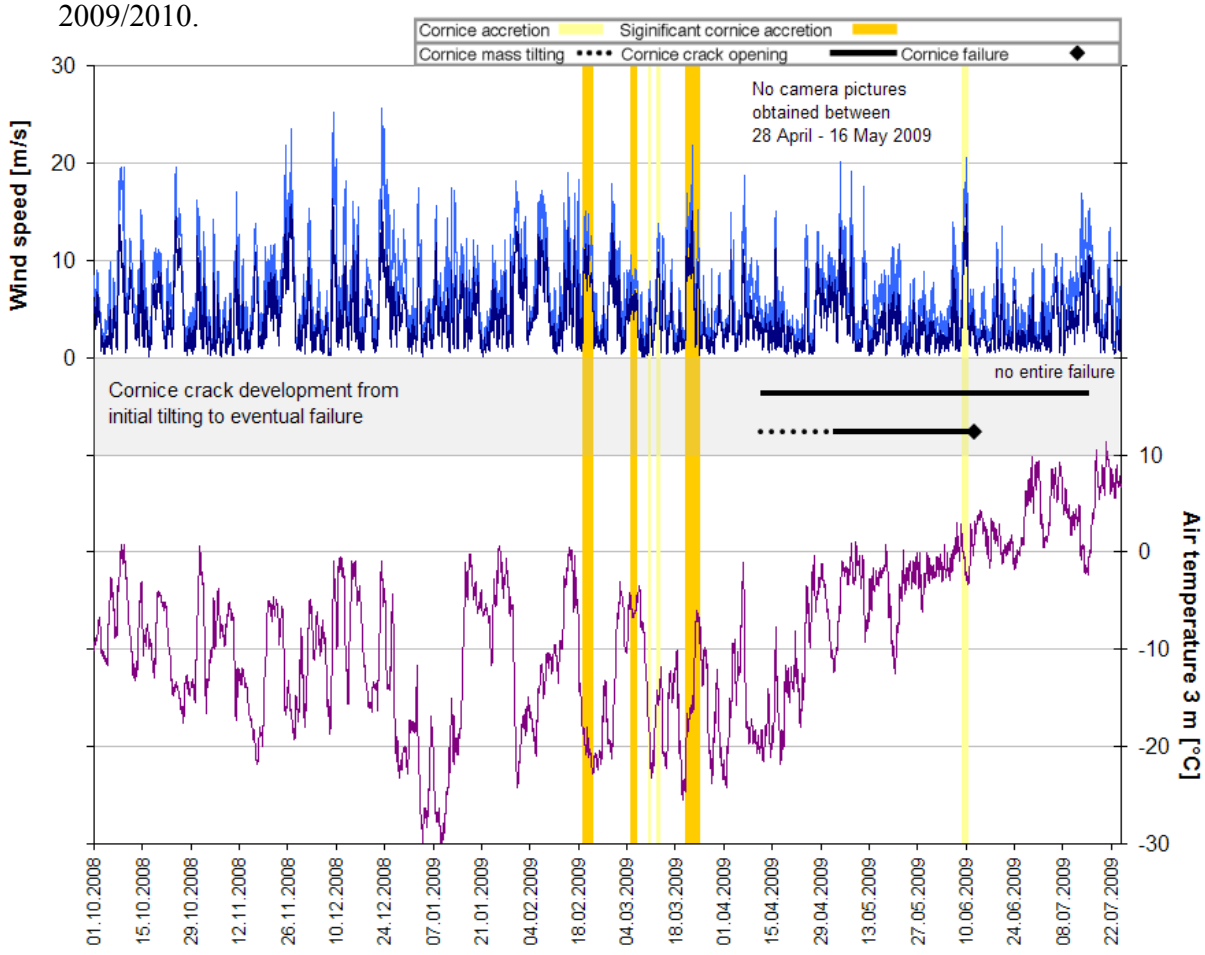

Diagram 7 Meteorology of the 2008/2009 snow season with periods of cornice accretion. The development of two cornice cracks is shown from initial tilting to eventual failure

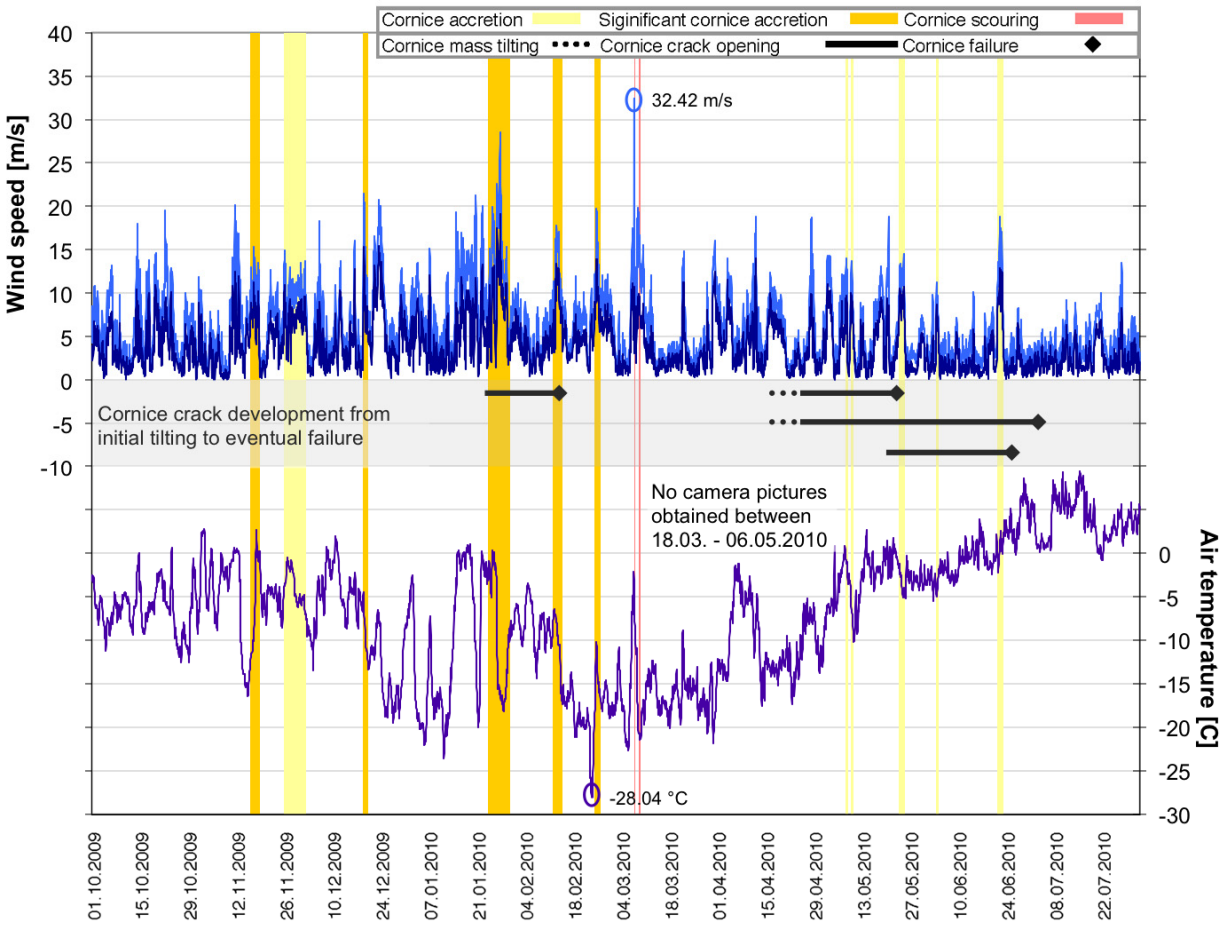

Diagram 8 Meteorology of the 2009/2010 snow season, periods of cornice accretion and scouring. The development of four cornice cracks is shown from initial tilting to eventual failure

The measured snow depths at the crossover of the main plateau to the cornice root were mainly controlled by the observed storm events. The vast majority of the significant variations in snow depth were directly caused by storm events that either led to cornice accretion or caused cornice scouring (Diagram 5, Diagram 6). The largest increase in snow depth occurred between 26 March and 29 March 2009, when values rose from 15 cm to 45 cm as a result of the 93 hour long storm event which led to pronounced cornice accretion. In the second snow season, the storm event 23/24 March 2010 was most distinctive with an increase of 12 cm to 34 cm measured snow depth.

Even towards the end of the snow season with air temperatures close or above 0° C and 24 hours of incoming solar radiation, cornice growth was observed in both years (Diagram 7, Diagram 8). These events occurred as a direct response to new snow fall. The snow pack was already isothermal at this stage and therefore the snow presumably too heavy to be redistributed.
The last storms that contributed to cornice accretion were on 14 – 16 June 2009 and 20 – 22 June 2010, respectively. The latter storm did not have any effect on the measured snow depth as probably melting due to average temperatures above freezing altered the net effect. However, even in the early part of the snow season the storm event between 11 February and 14 February 2010 did not cause variation in the recorded snow depth. Despite this, the storm led to considerable cornice accretion and did not vary from the average meteorological storm conditions. This might indicate that cornices can grow horizontally with only minor vertical increase at its root due to their wedge-like shape.

In both snow seasons, the selected storm events that led to cornice accretion showed an average hourly mid-wind speed of about 8 m/s. The storms average hourly maximum wind speed varied between 10.9 m/s in 2008/2009 and 12.1 m/s in 2009/2010
(Diagram 7, Diagram 8). The predominant storm direction was ESE, which is essentially across the main Gruvefjellet plateau towards the ridge line. No coherency of cornice accretion and air temperature development was found. Cornice growth was observed throughout the entire snow season during storms with average air temperatures between -20°C (22 – 25 February 2009 and 14 March 2009) and +0.2°C (22 – 22 June 2010). The influence of temperature on the particular accretion process could not be investigated.

These findings indicate that cornice accretion along the Gruvefjellet plateau edge is the result of very pronounced storm events from ESE that last up to several days and succeed throughout the entire snow season under a wide range of temperature conditions. Furthermore periods of cornice accretion and scouring could be identified by the snow depth measurements at the crossover of the main plateau to the cornice root (Diagram 5, Diagram 6). Not surprisingly a coherency of storm duration and the cornice accretion magnitude was observed.

However, three selected storms varied from the findings described above. Two storm events showed remarkable low wind speeds, just slightly above the snow seasons average hourly maximum of about 6 m/s. The 46 hour long storm of 8 March 2009 indicated an average hourly maximum wind speed of 7.9 m/s. During this storm the snow depth measurements recorded a significant increase of 15 cm to 30 cm total snow depth on 11 March 2009 (Diagram 5).

The following storm on 14 March 2009 showed even lower wind speeds throughout its 13 hour duration – 6.5 m/s average hourly maximum wind speed. No snow depth values could be recorded the following day, but the measurement of 16 March 2009 indicated a reduction of 10 cm in snow depth in comparison to the previous value of 13 March 2009 (30 cm) (Diagram 5). Regardless, a horizontal accretion of the cornices was also observed hereafter. One explanation for the reduction at or close to the cornice root during these comparable low wind speeds might be the observed variation in snow depth within the previous days. Therefore the time for the formation of bonds and therefore hardening of the snow cover was rather limited.

In the snow season of 2009/2010 one storm indicated a pronounced ENE direction. The storm started 18 December 2009 and lasted for 30 hours. Despite the unusual wind direction the storm led to a significant horizontal growth of the cornices. This was contemporaneous with a temperature drop from -4.9°C to -11.9°C. The measured storms average hourly maximum wind speed was 14.2 m/s and therefore did not show a deviation from the average storm wind speed recordings. No snow depth measurements were taken in this period due to the polar night.

These three events indicate that under particular conditions storm events of comparable low magnitude or with a deviation of the predominant winter wind direction lead to cornice accretion. Furthermore these affirm the necessity of observations by automatic camera and regular fieldtrips to determine cornice accretion.

5.2.5. Cornice development

Each of the observed storms that caused cornice accretion added a new layer onto the cornice mass. These wedge-like layers were bedded initially parallel to the plateau surface and therefore approximately horizontal. A very steep inclined accretion face was observed (Figure 6). Several times the cornice surface was partly rough and displayed sastrugis perpendicular to the plateau edge.

Gradually the leading edge and successionally the entire wedge crept downwards in particular under the load of following deposited cornice accretions. Towards the end of the snow season with rising temperatures, this process accelerated. The formation and development of roll cavities described by Paulcke and Welzenbach (1928) ("Hohlkehle") and Montagne et al. (1968) was observed as this downward folding proceeded. Roll cavities have been observed to be partly closed by further involution of proximate layers. In general, these zones remained weak spots within the cornice mass and many partial failures have been observed at this interface (Figure 8, Figure 24).

Figure 24 Formation of roll cavities observed along the Gruvefjellet plateau edge on 1 March 2010. Each tongue-like cornice layer represents a cornice accretion event. Photograph towards NE

5.2.6. Cornice scouring

Cornice scouring due to high wind speeds was found to be of minor importance along the ridgeline of Gruvefjellet. Besides scouring, settlement of the cornice mass and downward folding was observed to be responsible for visual horizontal and vertical shrinking. Only two distinctive events of cornice scouring could be identified, both occurred in the second observed snow season 2009/2010. On 7 March 2010 wind gusts up to 32 m/s were measured, which represented the highest value of the entire observation period (Diagram 9). The wind direction of this approximate 3 hour scouring event was from S to SW (186° - 230°). This was in contrast to the prevailing winter wind direction and displayed a significant angle towards the plateau edge and the developed cornice. Snow depth measurements indicated a distinct reduction by 4 cm within 24 hours to 32 cm total snow depth (Diagram 6).

The second event on 8/9 March 2010 showed only hourly maximum wind speeds between 15 m/s and 19 m/s from WNW and NW (298° - 319°) which is opposite of the prevailing winter wind direction (Diagram 9). The storm was most pronounced for about 7 hours. Snow depth measurements indicated a reduction of 4 cm within 24 hours to 28 cm total snow depth (Diagram 6). Both events reduced the cornice extent vertically as well as horizontally. On 8 March 2010 the partial erosion of the cornice scarps was observed from underneath. These two observed scouring events revealed a distinct effect on the measured snow depth. Though as only two scouring events could be observed, the general impact of cornice scouring on the snow cover along the cornice root and roof cannot be depicted more quantitatively. Similar to the cornice accretion conditions, the influence of temperature on cornice scouring conditions remained elusive. The two visually affirmed events occurred at average temperatures of -20°C (8 March 2010) and -5°C (7 March 2010). The closeness of the two observed events remained also unclear. Notably, both storms indicated a significant angle towards the plateau edge. However, in the first snow season 2008/2009 no cornice scouring was visually observed. Though, cornice scouring might have happened in the periods not covered by automatic camera pictures. On 25 December 2008 an hourly maximum value of 25.6 m/s was recorded by the Gruvefjellet automatic weather station (Diagram 7).

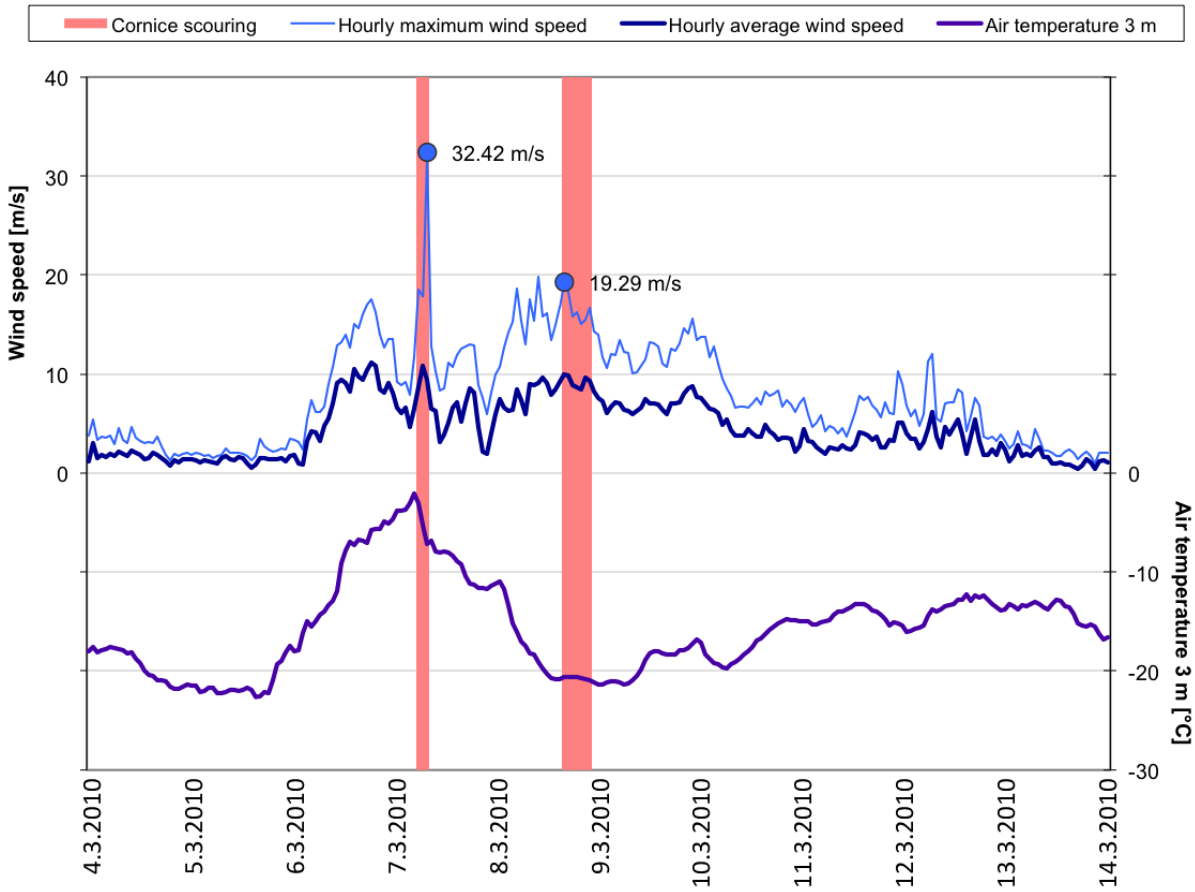

Diagram 9 Meteorological conditions of the two visually observed cornice scouring events along the ridgeline of Gruvefjellet

Apart from the visually affirmed scouring events a very pronounced storm started 24 January 2010 lasting for 133 hours. It reached hourly maximum wind speeds exceeding 25 m/s from an easterly direction for 5 successive hours. Thereby hourly mid-wind speeds between 14.1 m/s and 19.1 m/s were recorded. The overall 133 hour storm event was identified to cause cornice accretion (Diagram 8).

Though, the time resolution of the 'Gruvefjellet' automatic camera was too low to analyse if those particular five hours of increased wind speed caused cornice scouring. Additionally the light condition during polar night was not sufficient to identify marginal developments.

Only those storm events were selected where cornice variations were visually determined by the 'Gruvefjellet' automatic camera pictures. Additional storm events that caused cornice accretion and scouring respectively may have occurred during the polar night where photograph resolution was very limited. The same accounts for periods that have not been covered by automatic camera photographs due to malfunctions of the camera. The varying number of scouring as well as accretion events between the snow season 2008/2009 and 2009/2010 may reflect the duration of visual observation by automatic camera pictures to some extent. Though it has to be taken into account that the second observed snow season however showed slightly higher wind speeds in general. The position of the automatic weather station 'Gruvefjellet' on the central part of plateau source area – about 500 m away from the edge – has to be considered also. In particular the wind conditions at the plateau edge may vary to some extent from those measured in the central part of the plateau. This in turn displays the dependency on automatic camera photographs.

5.3. Cornice cracking

5.3.1. Overview

Cornice tensions cracks opened between the cornice mass and the Gruvefjellet plateau edge. The development of six cornice cracks was observed in the studied slope section during both snow seasons. Numerous cornice cracks outside the field site were additionally inspected. The first cracks along the Gruvefjellet ridgeline were observed on 17 April 2009. The location was outside the cameras field of view, therefore the actual crack opening was not observed. Cornice measurements started 28 April 2009 and lasted until 14 June 2009, 12 cornice crack opening values could be obtained. On 18 June 2009 the upper rim of the measured cornice collapsed into the developing crack and ended the first series of measurements. A second cornice crack developed between 6 May and 16 May 2009. Though, a slight depression at the cornice root was already observed in mid-April, just at the location were the crack opened later in May. The upper part of the cornice collapsed into the opening crack 14 June 2009.

The central part of the cornice eventually failed 20 June 2009 into ‘Willy Sagnol’ followed by a number of minor failures of the lateral unsupported remnants.
In contrast to the first snow season, in 2009/2010 distinct cornice cracks were already observed in the early part of the snow season on 23 January 2010 (Figure 25). Measurements started 5 February 2010. After two measurements large parts of the cracked cornice failed into ‘Wrong Step’ and ‘Willy Sagnol’ on 14 February 2010. The cornice crack measurement installations were destroyed. Some major parts of this cornice remained cracked and stayed in place. The third series of measurements was carried out at the biggest of those on 24 March 2010. The series of 15 measurements lasted until the end of June when melting affected the measurement stakes and led to tilting. No actual cornice fall avalanche occurred.
The development of a cracked cornice was also observed within the camera’s field of view (Figure 17). Direct observation suggested that the cornice body was already slightly tilted by 16 April 2010, though no cracks were apparent on the surface. The crack eventually opened 23 April 2010. The main part of the cornice failed into ‘Willy Sagnol’ on 25 May 2010. This cornice fall again was followed by a number of minor failures of the lateral unsupported remnants until mid-June. Outside the camera’s field of view another two cornice developments were observed and visited regularly. One crack opened as well on 23 April 2010, after minor tilting was observed on previous field trips. It avalanched into ‘Wrong Step’ on 1 June 2010. The second cornice was observed cracked on 18 May 2010 and failed into ‘S’ 24 June 2010.

These data indicate that the period between crack development and eventual failure can be variable. The observed periods averaged between four to five weeks. Three times a tilting of the cornice mass or a slight depression in the cornice root were observed prior to the appearance of the crack at the surface. Certainly the obtained data are limited and periods prior to the appearance of the crack at the surface vary between one week and four weeks. Though this initial progress was observed as well several times outside the investigated area. Determining an actual date for the beginning of this initial process proved to be very challenging. Additionally it was found that the formation of cornice cracks does not necessary lead to cornice failure and vice versa.

5.3.2. Control on initial cornice cracking

Prior to all crack openings, distinct temperature variations were detected. A significant warming to a maximum temperature of -1°C was recorded on 11 April 2009, when temperatures rose about 20°C within less than a week. This warming presumably caused the development of the first cracks observed 17 April 2009 and led to the slight depression indicating the forming second crack. The latter one eventually opened between 6 May and 16 May 2009 following another pronounced warming. Temperatures around 0°C were momentarily reached on 2 May and 13 May, interrupted by a significant temperature drop to -12°C on 8 May 2009 (Diagram 7).

A very pronounced mid-winter warm spell in combination with large amounts of rain occurred between 14 January and 19 January 2010. Following this, temperatures dropped back to nearly -20°C on 21 January 2010 and open cracks were observed 23 January 2010 (Figure 25). A similar pattern reoccurred when temperatures reached -2°C on 6 April 2010 after an increase of about 20°C within a week. This was followed again by a significant temperature drop to -17°C on 13 April 2010. Two cornice cracks were found open 23 April 2010, while already signs of cornice tilting were observed about a week earlier on 16 April 2010. The last observed cornice crack along the Gruvefjellet plateau edge appeared open on 18 May 2010. No signs of previous tilting were noticed. Again, broad temperature variations were found previous to this date. Temperatures rose nearly 15°C within a week and reached 0°C on 7 May 2010. This was followed by a temperature drop to -10°C on 10 May 2010 and a successive increase back to 0°C on 18 May 2010 (Diagram 8).

These results display the very close relationship between the opening of cornice tension cracks in connection with initial tilting of the cornice mass and very pronounced temperature variations. Even though only six cornice crack developments have been investigated in the studied area, all indicated a very similar meteorological pattern.

Figure 25 Extensive cornice cracks observed 15 February 2010 which opened as a direct response to the mid-winter warm spell between 14 and 19 January 2010 with large amounts of rain. Photograph towards S

5.3.3. Control on cornice crack development

The crack development from initial cracking to eventual failure showed a continuous opening. The observed cracks developed within the automatic camera's field of view proved this especially. Measured air temperature seemed to represent a minor influence on the further development of the crack, once it appeared open at the surface. This is in stark contrast to the initial cracking process. The observations suggested that the entire cornice mass - once cracked – hinged around a fixed pivotal point. This process led to the curling of the entire cornice mass reaching a position above the plateau edge. The pivotal point may be around the second sedimentary step observed below the plateau edge (Figure 29). Here the temperature conditions presumably remain steady despite the large air temperature variations measured throughout the crack development. Therefore constant snow creep apparently accounted for the linear crack opening development under the action of gravity and metamorphism.

Temperature variation may influence the snow creep of the upper cornice part to some extent, though the observed cornice movement was cohesive within its entire mass. Excluded from this were the very ends of the snow seasons, when the upper cornice layers were water saturated due to melting conditions.

5.3.4. Cornice crack development

The observed cornice cracks showed a very similar development (Figure 26). A slight depression in connection with a bulge in the cornice root was observed in many cases followed by a tilting of the entire cornice mass and presumably represented a necessary progress within the formation of cornice cracks. However, this was not observed in all cornice crack developments.

The initial cracking occurred parallel to the plateau edge. With further opening of the crack, lateral tension cracks developed at an obtuse angle to the initial cracking, forming a pronounced C-shape. This was contemporaneous with an up folding of the central cornice body. Tilting and opening of the crack proceeded until the cornice mass displayed a very steep, close to vertical position. Thereby parts of the cornice might be above its initial position at the plateau edge. The former leading edge and roll face got progressively rounded by small failures. Roll cavities indicated a particular weak area within the cornice mass and the majority of these small failures occurred along these (Figure 24). The numerous small failures in turn also affected the cornice scarp and pillow by successively eroding these (Figure 28). The central cornice mass may detach from the ridgeline as much as 2 to 3 meters. Eventually failures of the outermost central cornice part occurred (Figure 21), while the lowermost cornice section remained sitting on the second sedimentary step observed. The unsupported lateral remnants successively avalanched in rather small events over a period of time (Figure 31).

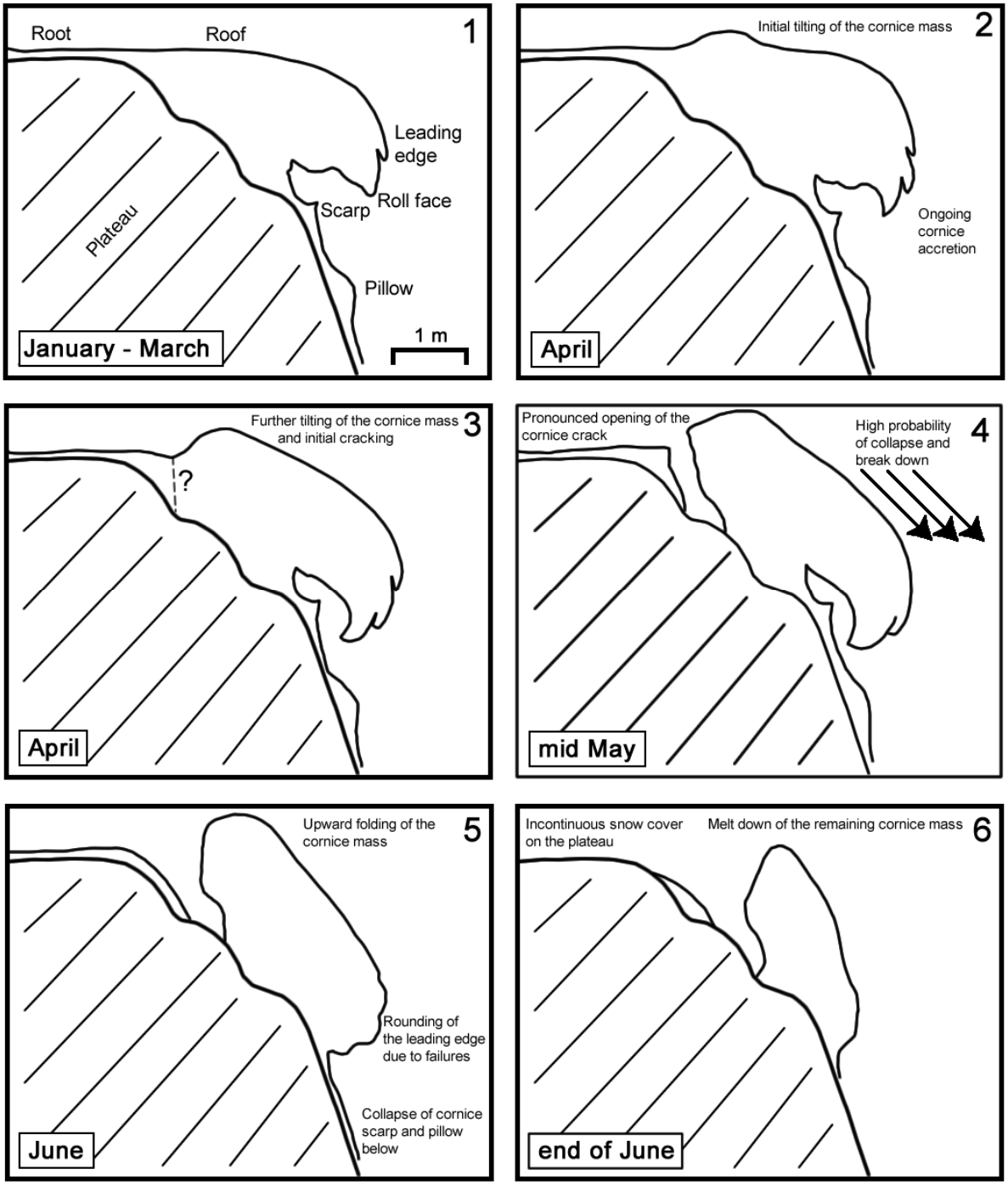

Figure 26 Pictogram of the cornice crack development from initial tilting to eventual failure throughout the snow season

5.3.5. Cornice crack measurements

The results of the two long lasting cornice crack measurements affirmed the continuous cornice crack development observed by the 'Gruvefjellet' automatic camera. The measured opening distances displayed a steady increase. Though decrease in the opening rate occurred in both of the snow seasons towards the end of the snow seasons with temperatures just around 0°C. Especially in the 2009/2010 snow season this was very pronounced and led to stagnation. The two long lasting series of measurements were conducted under similar overall air temperature conditions. Average air temperatures varied between -4.5°C (28 April - 06 June 2009) (Diagram 1) and -5.5°C (16 April – 6 June 2010) (Diagram 3) with similar minimum values of -18.0°C and -17.3°C and maximum air temperatures of 1.1°C and 2.7°C. Using the same time span in 2009 resulted in an average air temperature of -7.2°C (16 April – 6 June 2009), which goes along with the general somewhat lower average air temperature of the 2008/2009 snow season. The short lasting series of measurements indicated an average air temperature of -8.8°C for the period between 5 February and 10 February 2010.

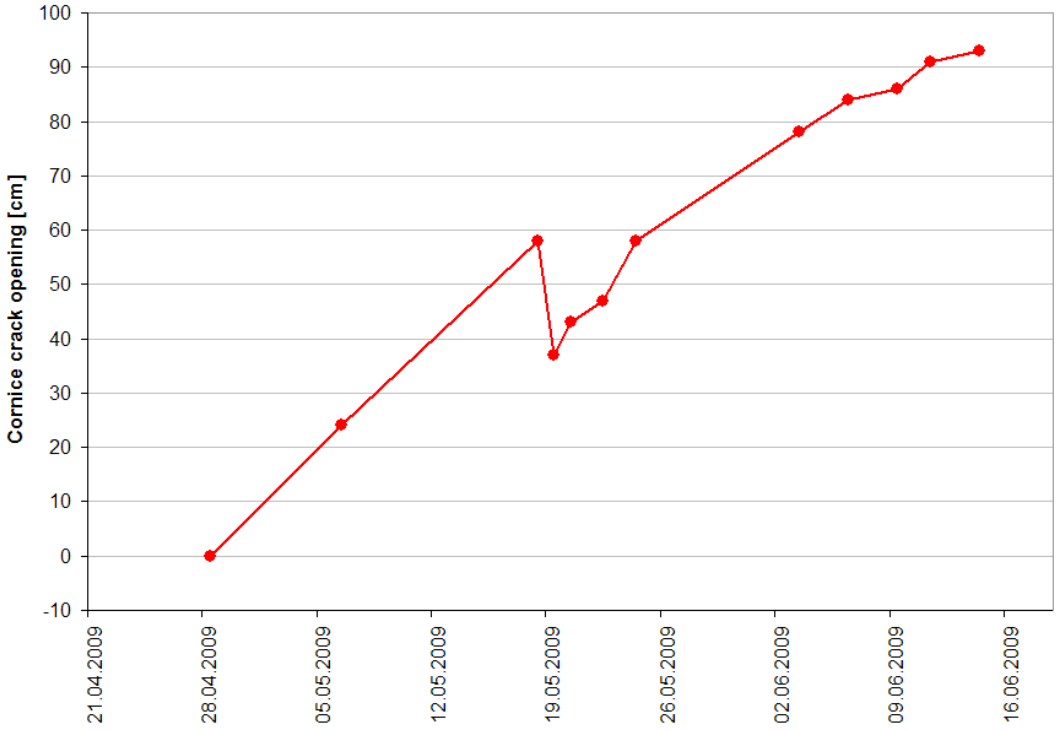

Diagram 10 Cornice crack opening measurements of the first snow season 2008/2009

In the 2008/2009 snow season, the measured crack opened a relative distance of 93 cm between 28 April and 14 June 2009 (Diagram 10). On 19 May 2009 a reduction of 21 cm to the previous day was measured. This was caused by a surface perturbation, where the upper most layer of the tilted cornice part crept slightly towards the plateau. The protruding measurement stake was affected by this. As the stake illustrated a distance to the pivotal point it enhanced the magnitude of this surface perturbation additionally. The ensuing measurements indicated the same opening rate as prior to the perturbation. This revealed the correctness of the measurements, capturing the development of the entire cornice mass.

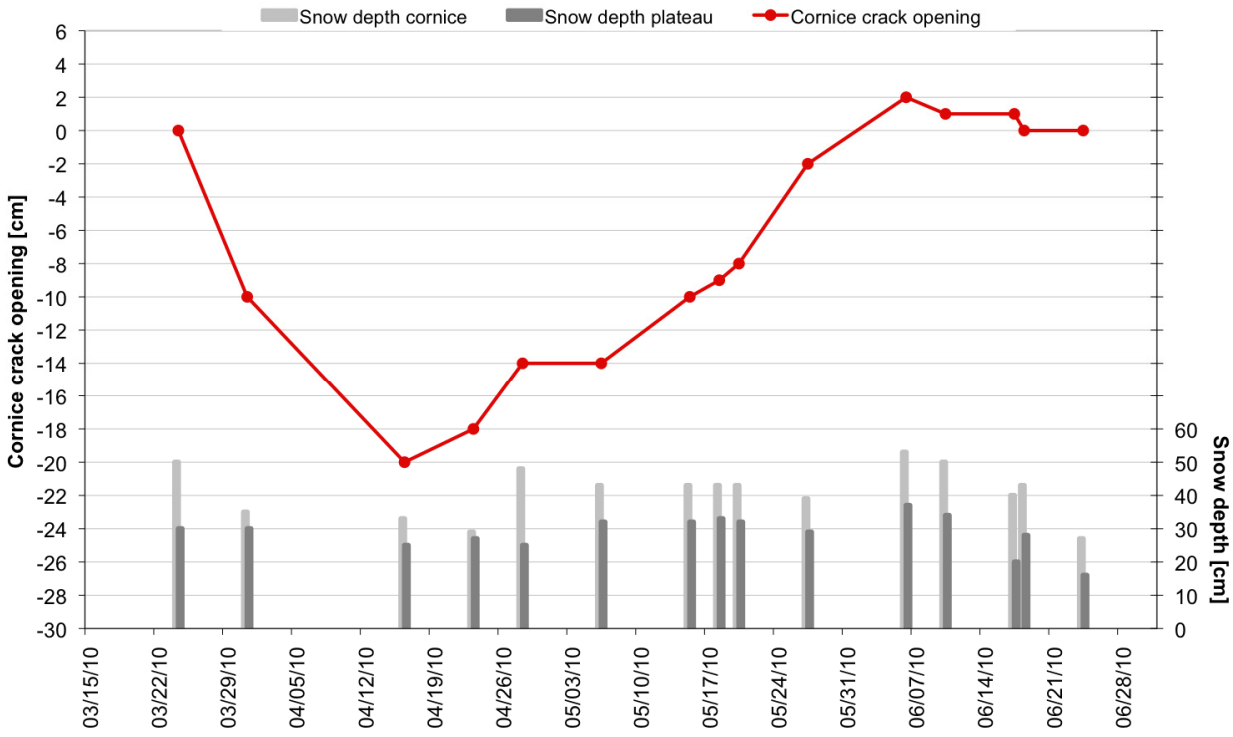

Diagram 11 Cornice crack opening measurements and on-site snow depth recordings of the 2009/2010 snow season

The measurements of 2009/2010 showed a similar continuous development in the main part (Diagram 11). The first two measurements indicated, however, a reduction of the crack opening of 20 cm between 24 March and 16 April 2010. Though an actually closure of the crack was not observed.

A slight tilting of the cracked cornice part towards the plateau may have caused this measured reduction in cornice crack opening. Similar to the 2008/2009 measurements, between 16 April and 6 June 2010 a continuous opening movement was measured. Within this period, the crack opened a relative distance of 22 cm. The following readings indicated stagnation and a slight decrease in the measured crack opening until 24 June 2010.

The two series of measurements showed a very similar pattern towards the end of the snow season with air temperature conditions close to 0°C. Probably the readings underestimate the cornice crack opening to some extent. The measurement stakes were affected by melting, especially the one which was installed into the cracked cornice. In particular this was the case in the second series of measurements when a metal stake was used. Additionally proceeding measurements and thereby slightly tightening the attached line progressively tilted the measurement stake towards the plateau und thereby reduced the effective distance. This was noted several times during fieldwork (Figure 19).
Even though the measured crack opening was continuous in the main part of the two series of measurements, the actual opening rates of the observed cornice cracks varied considerably. In the two divided periods in 2009, prior and after the decrease due to surface perturbation, cornice crack opening rates were notably similar. Between 28 April and 18 May 2009, the crack opened a relative distance 58 cm and constituted an opening rate of 2.9 cm/d. After the decrease, between 19 May and 06 June 2009, the crack opened a relative distance of 47 cm and indicated an opening rate of 2.6 cm/d. Excluding the decrease on 19 May 2009, the cornice crack displayed an overall relative opening of 105 cm within 38 days and therefore an average cornice crack opening rate of 2.76 cm/d. Thereby the last three readings between 6 June and 14 June 2009 were excluded as well, as an underestimate of the actual cornice crack opening was assumed (Diagram 10).
The same accounts for the period at the end of the second series of measurements between 6 June and 24 June 2010. The two initial readings indicate a distinctive reduction of the cornice opening, however this was not observed. Therefore these were considered false measurements and thus excluded from the series of measurements.

A period of 51 days between 16 April and 6 June 2010 remained. Within this time span, the cornice crack opened a relative distance of 22 cm and constituted a cornice crack opening rate of 0.43 cm/d (Diagram 11).

The two very short lasting series of measurements between 5 February and 10 February indicated the highest cornice opening rate recorded. Within this period, the cornice crack opened a relative distance of 7 cm and 43 cm, resulting in an opening rate of 1.4 cm/d and 8.6 cm/d, respectively. Even though the two readings were conducted at the same cornice crack, the difference in the resulting opening rate is notable. After the installation only one reading was taken at each spot before failure occurred and destroyed the setup on 13 February 2010. This was in contrast to the both long lasting series of measurements where no failure brought the series to an end. It remains elusive if the cornice crack opening rate essentially increases just prior to eventual failure. Though the two cornice crack developments observed by automatic camera did not indicate a varying opening movement before failure occurred.

The great variations in the averaged daily opening rates display the influence of other factors in addition to snow creep. One delicate factor which may influence the cornice crack opening rate is the actual size and therefore the volume of the cracked cornice. Thereby the dimensions of the cracked cornice parts, their horizontal and vertical extent are of special interest. This is associated with the distance between the prominent rock noses which confine the horizontal cornice extent at the Gruvefjellet plateau edge (Figure 2). Additionally the micro-topography of the plateau edge differs to some extent and may therefore give varying support to the cornices along the edge from beneath. The topography apparently determines the particular breakover point of the cornices. However, the cornice cracks measured within the two snow seasons were conducted at differing spots, which prohibited further comparison.

Furthermore it revealed the influence of several factors in the process of cornice crack development. Though the short observation period of two consecutive snow seasons has to be taken into account. However, these factors discussed are very complex and hard to quantify in the way they influence the cornice crack development.

5.3.6. Relationship of cornice crack opening and snow depth variation

During the two series of crack measurements snow depth values were recorded at the crack location in the 2009/2010 snow season. The measurements close to the cornice root during the short lasting series of cornice crack measurements (5 – 10 February 2010) did not indicate any variation in snow depth. Within this period the regular snow depth measurements in front of the camera showed only a slight increase of 2 cm at the crossover of the main Gruvefjellet plateau to the cornice root on 8 February 2010 (Diagram 6).

Simultaneously with the long lasting cornice crack measurements, snow depth values were achieved at the cracked cornice part as well as on the plateau side close to the crack (Figure 19). Both measurements showed the same variations in the main part, though these were more pronounced at the stake on the cracked cornice part. Thereby only the relative variations in snow depth could be observed (Diagram 11).

The highest cornice crack opening rate of this series was measured between 23 April and 28 April 2010 and went along with a pronounced increase in snow depth on the cracked cornice of 19 cm. However, the plateau side measurement indicated a decrease in snow depth of 2 cm. Another slight increase in the cornice crack opening rate was found between 20 May and 27 May 2010. Though both snow depth measurements indicated a decrease in snow depth in this period. Stagnation in the cornice crack opening was recorded between 28 April and 6 May 2010. At the same time the snow depth measurement on the cracked cornice indicated a decrease of 5 cm. In spite of this, an increase of 7 cm in snow depth was measured on the plateau side. This again indicated the high variability of snow depth of the cornices towards the leading edge. The two series of snow depth measurements clearly display the impact of snow melt towards the end of the snow season where an underestimate of the cornice crack opening was assumed. On 6 June 2010 both measurements constituted the highest reading of the series. Until 24 June 2010, snow depth was reduced due to melt by 26 cm on the cracked cornice part and 21 cm on the plateau side (Diagram 11).

The varying snow depths were found to influence the cornice crack development to some extent. Though these variations can be ruled out as a main driving force, since the opening of the cornice crack proceeded throughout May 2010, when hardly any variation in snow depth was recorded. Indeed, considerable increase in snow depth presumably enhances the cornice crack opening rate due to rising stress exerted onto the tilting cornice part.

5.4. Failure monitoring

5.4.1. Overview and classification

Between January 2009 and July 2010 180 cornice failures have been recorded along the Gruvefjellet plateau edge and rated according to the classification of Greene et al. (2004). Observations were based on the automatic camera 'Sverdrupbyen' which represented a continuous record of the two investigated snow seasons (Figure 14). For better classification of the observed failures the destructive force value "D2.5" was applied (Diagram 12). This category describes the destructive force of an avalanche as the ability to kill a person and damage a car in the track or at the beginning of the runout zone. Typical path lengths are in excess of 100 m. The largest cornice fall avalanches observed in the Gruvefjellet slope section were classified as "D3 R4".

In the new North American public danger scale avalanches are more broadly described with respect to their destructive force as "small" if their destructive force is < "D2", "large" for avalanches between "D2-D3" and "very large" for avalanches categorized as >"D3" (Stratham et al. 2010). In the following mainly "D2 R3" and larger failures are described, as those represent essentially cornice fall avalanches. Furthermore the release area of those could be detected more accurately.

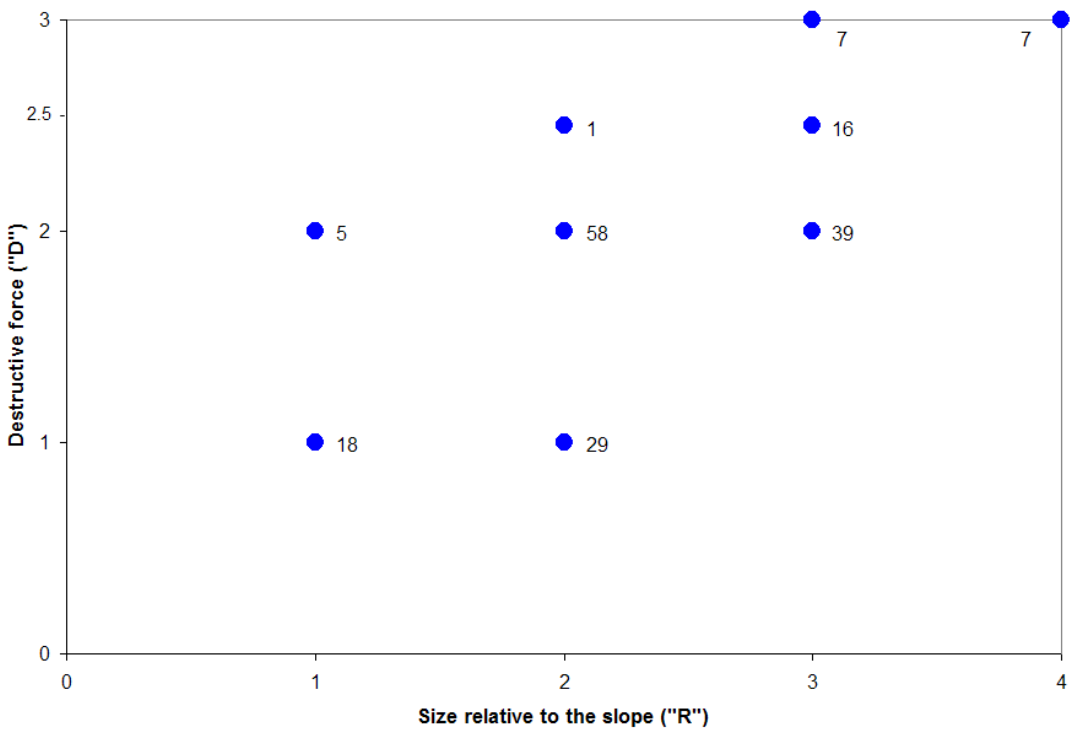

Diagram 12 Distribution of 180 cornice failures with regards to their destructive force "D" and size relative to the slope "R" of the two investigated snow seasons 2008/2009 and 2009/2010

5.4.2. Size distribution

The avalanche sizes relative to the path according to Greene et al. (2004) were adjusted to the conditions of the Gruvefjellet slope. “R1” and “R2” avalanches were small failures that ran out just below the free face and between the rock noses, respectively. These were mostly due to collapse of the cornice scarp and pillow or minor failures of the accretion face. “R3” avalanches ran out beneath the rock noses which subdivide the entire Gruvefjellet slope. “R4” avalanches represented large cornice fall avalanches that fanned out and essentially reached low inclined terrain (Figure 2). Major avalanches classified as “R5” in Greene et al. (2004) did not occur within the two observed snow seasons.

About 30% (52 failures) of the observed cornice failures were categorizes as “D2 R1” and smaller. The class of “D2 R2” and “D2 R3” failures was most abundant with 58 and 39 observed failures, respectively. These constituted about 55% of all recorded failures.

70 failures were categorized as “D2 R3” and larger, which displayed distinctive cornice fall avalanches. 14 cornice fall avalanches (approx. 8%) were categorized as “D3”, which constituted the highest destructive force observed. Thereof seven were graded as “D3 R4” cornice fall avalanches (Diagram 13). These largest classified failures covered the talus cones.

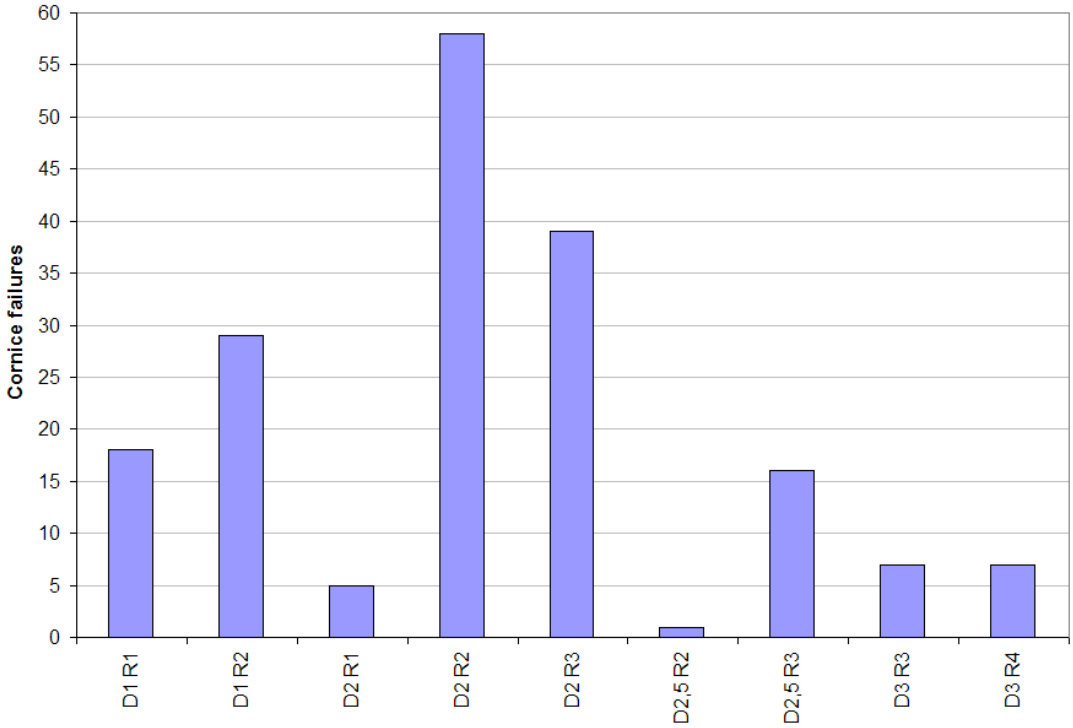

Diagram 13 Size distribution of 180 cornice failures recorded in the two snow seasons 2008/2009 and 2009/2010

5.4.3. Time distribution

The time distribution of the 70 recorded cornice fall avalanches classified as “D2 R3” and larger indicated a pronounced predominance of cornice failures towards the very end of the snow season. About 80% (57 failures) of the recorded failures occurred in June 2009 and 2010 (Diagram 15). Therefore a clear relationship of cornice fall avalanches and rising temperatures above freezing in connection with 24 hours of direct solar radiation appeared.

Furthermore a major part of previously cracked cornices eventually failed in June after being progressively tilting for a period of time. In the case of these entire cornice falls the rising temperatures were less important than the duration since crack initiation.

Cornice failures were recorded from December throughout the entire snow season (Diagram 15). This reveals that several factors interact in relation to cornice failure. The cornice crack development described above indicate that even in the early part of the snow season warm spells led to the formation of cornice cracks and eventual cornice failure. The meteorological data showed that in both snow seasons these warm spells were most pronounced in the early part of the snow season, due to the overall lower average air temperatures (Diagram 1, Diagram 3). Afterwards temperature conditions remained steadier with less pronounced variations which might reflect the scarcity of cornice fall avalanches recorded in March (1) and April (2). Despite rising temperatures, temporary above freezing, only four cornice fall avalanches were recorded in May during both snow seasons.

Cornice fall avalanches were observed to occur under varying meteorological conditions throughout the entire snow season within the Gruvefjellet slope section and the adjacent areas. The interaction of several factors in relation to cornice failure is revealed by the comparison between the two snow seasons in relation to their avalanche classes (Diagram 14). This comparison depicts large variation in the occurrence of particular avalanche classes between the two snow seasons. The disparities were more pronounced in the low magnitude classes as well as in the high magnitude classes. Cornice fall avalanches categorized as “D2.5 R2” and “D2.5 R3” combined did not show annual variations in the total numbers. No “D3 R3” avalanches were recorded in the 2008/2009 snow season, whereas seven “D3 R3” as well as four “D3 R4” cornice fall avalanches occurred in 2009/2010. In contrast to this, only three avalanches were categorized as “D3 R4” in the 2008/2009 snow season. In particular these large magnitude failures display a distinct uneven distribution in the two observed snow seasons along the Gruvefjellet slope section.

In total 26 cornice fall avalanches were recorded in 2008/2009. The second observed snow season 2009/2010 indicated a significant increase in recorded cornice fall avalanches to 44 failures. This displayed a distinct increase in avalanche activity of nearly 60% (Diagram 14).

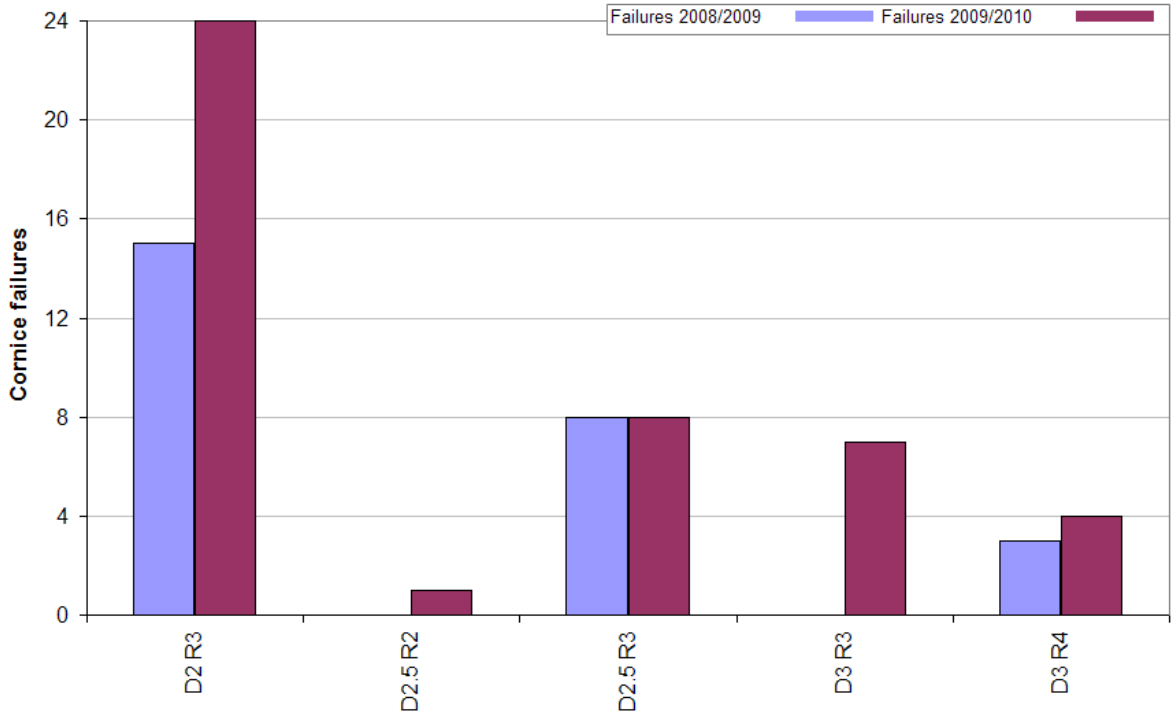

Diagram 14 Size distribution of 70 cornice fall avalanches comparing the two investigated snow seasons 2008/2009 and 2009/2010

5.4.4. Time distribution in relation to avalanche class

The time distribution in relation to avalanche classes affirmed the meteorological pattern described above. Within the two observed snow seasons, 57 cornice fall avalanches were recorded in June, whereof 37 were classified as "D2 R3" failures. Notably only two further "D2 R3" failures were recorded which occurred in March and April (Diagram 15). Those were most likely just failures of the leading edge and accretion face independent of the large magnitude failures.

The early part of the snow season was dominated by large magnitude failures. In December 2009 three large cornice fall avalanches occurred presumably as a response to temperatures up to 1.9°C on 10/11 December 2009 followed by a temperature drop.

The same pattern reoccurred in February 2010 when three large cornice fall avalanches were categorized as “D3 R3” and “D3 R4”, which occurred as a direct response to the pronounced mid-winter warm spell in January 2010. Thus, six of 14 high magnitude events occurred in the early part of the snow seasons. These entire cornice fall avalanches in the early part of the snow season displayed the brittle behaviour of cornices. Furthermore one “D3 R4” failure was recorded in April, which still represented an entire cornice failure and only the lateral remnants stayed intact.

In May, with rising temperatures above freezing, four avalanches were recorded as “D2.5 R3” and “D3 R3” which mostly constituted central parts of cracked cornices, which eventually failed. Hereby the upper layers may already have been softened and therefore weakened due to melting conditions.

In June the high numbers of comparable low magnitude failures can be subdivided into having several origins. Many of these failures are due to the collapse of cornice scarps and pillows. Furthermore the unsupported lateral remnants of cracked cornices progressively avalanched in a number of rather small events (Figure 31). Additionally the leading edge and accretion face of cracked and tilted cornices failed, which led to a rounding of the remaining cornice mass. In the end large magnitude failures also occurred in June. Towards the end of the snow season five “D3 R3” and “D3 R4” failures were recorded (Diagram 15). These represent cornices that had cracked, progressively tilted for a period of time and eventually reached the breakover point.

Towards the end of the snow season the snow conditions on the Gruvefjellet slope beneath the cornices has to be taken into account. The snow cover gets progressively uncontinuous and avalanches may run out on bare ground (Figure 27). Thereby hardly further snow can be entrained and run out distances are somewhat shortened.

These results indicate that even though cornice fall avalanches occur throughout the main part of the snow season, their particular classes vary considerably with respect to the time distribution.

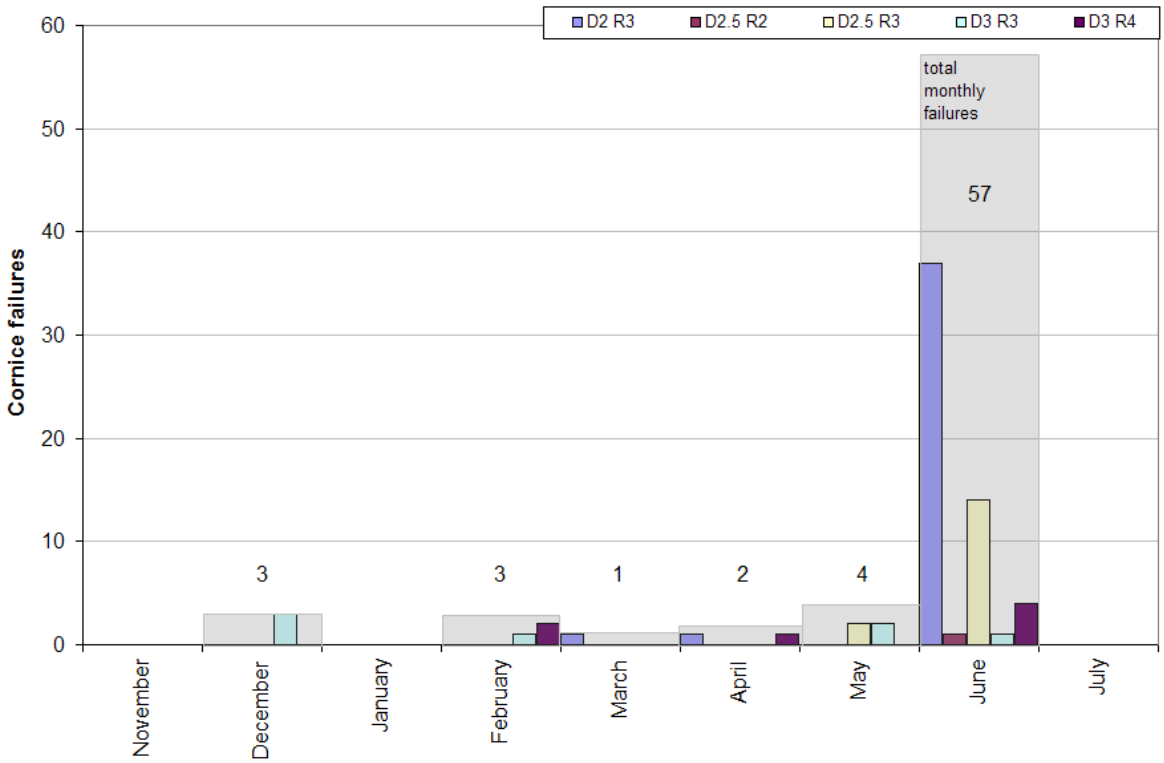

Diagram 15 Time distribution of 70 cornice fall avalanches and total monthly failures of the two investigated snow seasons 2008/2009 and 2009/2010 in relation to avalanche classes

5.4.5. Size distribution in relation to their runout

The 70 recorded cornice fall avalanches indicate a clear trend to fan-out wider, with increasing magnitude. The low magnitude classes are still dominated by a tongue shaped run-out or are split up into several minor tongues. This is generally due to the limited amount of snow involved in these failures. Additionally the runout of this avalanche class still displays the influence of the canalisation of the Gruvefjellet slope by intermediated rock noses (Figure 20, Figure 27). The high magnitude failures involve larger amounts of snow and essentially reach low inclined terrain. This, in combination with the particular shape of the talus cones, leads to the fan-out of the large magnitude failures.

5.4.6. Size distribution in relation to their starting zone

Generally all five distinguished gullies were found to produce various avalanches classes (Figure 2). The geomorphological characteristics of the gullies and its starting zones highly influence the magnitude of failures. “Einbahnstraße”, “Triple Y” and “S” constituted a predominance of the observed “D2 R3” and “D2.5 R3” failures (Diagram 16). The two latter gullies display a subdivided starting zone into three and four minor channels, respectively. Thereby the upper rock noses at the plateau edge delimit the horizontal extent of the cornices. This reflects the scarcity of very large failures. The gully “Einbahnstraße” constitutes the most confined gully with only one main starting zone. Therefore no failures were observed here categorized as destructive force “D3”.

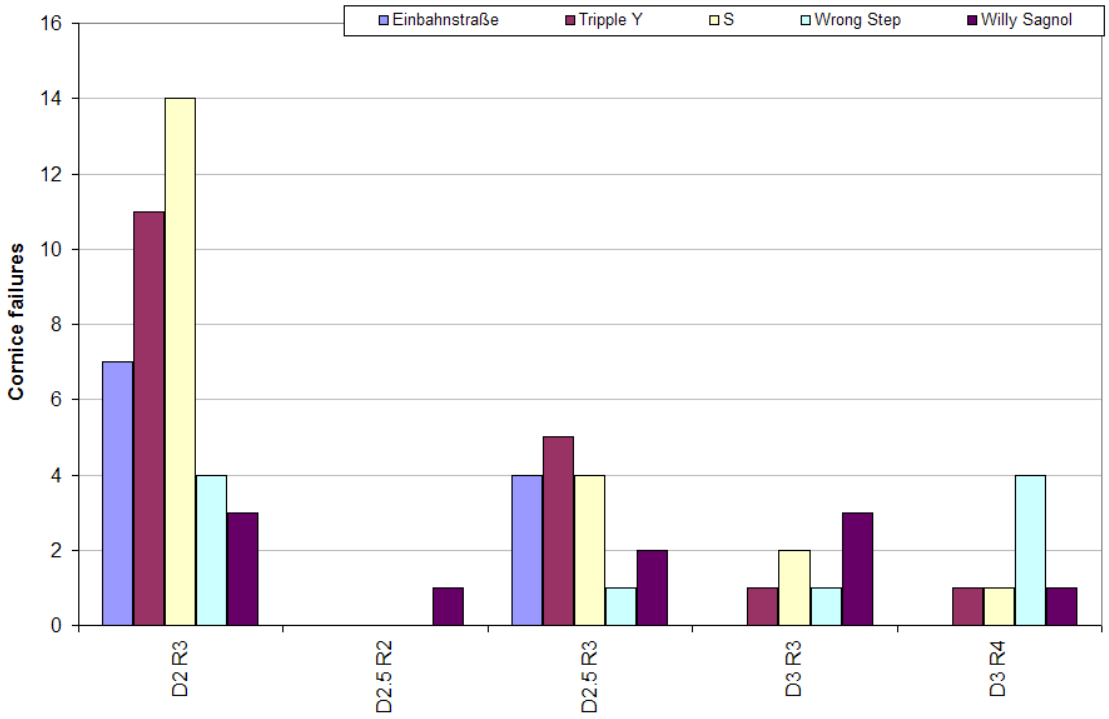

Diagram 16 Size distribution of 70 cornice fall avalanches of the two investigated snow seasons 2008/2009 and 2009/2010 in relation to their starting zone

In contrast to this, the gully “Wrong Step” constituted a clear dominance of the “D3 R4” class. However, only one failure of this gully was classified as “D3 R3” and “D2.5 R3”.

Along the plateau edge two main canals are divided where large cornices build up in addition to two minor sections.

In general, the rock noses beneath the plateau edge are less pronounced in the gullies "Wrong Step" and "Willy Sagnol". The latter one constituted all avalanche categories, with a slight predominance of "D3 R3" failures (Diagram 16). The starting zone is split up into two main canals and one minor. The main gully displays a minor central rock nose within the track and larger avalanches were found to flow around this nose and merge again beneath the obstacle (Figure 27).

Figure 27 Aerial mosaic of 112 images taken 680 m above the valley bottom on 20 June 2010. The Gruvefjellet plateau and ridgeline are in the lowermost part and the houses of Nybyen in the upper part of the picture. The snow cover in the Gruvefjellet slope section is uncontinuous and talus cones are visible at the terminus of the five gullies. © KOLIBRI GEO SERVICES

These findings reflect the geomorphological setting of the lower Gruvefjellet slope. The talus below the gullies “Triple Y” and particularly “Einbahnstraße” are very weakly developed. “S” and “Wrong Step” display the largest talus cones developed within the investigated Gruvefjellet slope section. Both reach low inclined terrain with a smooth transition zone. This is in contrast to the talus formed below “Willy Sagnol”, which terminates rather abrupt in the distinct inclined basal footslope (Figure 27).

5.4.7. Documented cornice fall avalanches of previous years and comparison

Between 2006 and 2008 12 cornice fall avalanches were documented in the observed Gruvefjellet slope section as part of the CRYOSLOPE project (*www.skred-svalbard.no*). Thereby no automatic cameras were used and avalanche observations were during regular fieldwork. Clearly only comparable large cornice fall avalanches were documented.

In 2005/2006 one “D3 R4” failure was noted, while 2006/2007 and 2007/2008 each displayed four failures of that class. Furthermore three failures rated as “D2 R3” and “D2.5 R3” were documented in 2007/2008.

These numbers presumably reflect a complete record of the high magnitude events of these snow seasons. Assuming this might enable a comparison of five snow seasons with respect to their high magnitude events categorized as “D3 R3” and “D3 R4”. In turn this comparison enables a better comprehension of the two investigated snow seasons 2008/2009 and 2009/2010 (Diagram 14). While the snow season 2008/2009 displayed three “D3 R4” cornice fall avalanches, 11 failures categorized as “D3 R3” and “D3 R4” were observed during the second observed snow season 2009/2010. This indicates that the latter snow season was rather exceptional with respect to their high magnitude events. The one “D3 R4” failure that occurred in 2005/2006 may reveal the only large magnitude failure of that snow season or just the beginning of more frequent observation. Therefore the comparison in relation to cornice fall avalanche frequency is hereby not reliable.

It is striking that between 2005/2006 and 2009/2010 the largest annual cornice fall avalanches in the studied slope section were equal in magnitude. This suggests that failures categorized as “D3 R4” represent an annual return period. Therefore the observed variations between the snow seasons 2008/2009 and 2009/2010 in relation to their avalanche classes are remarkable (Diagram 14). Furthermore a “D3 R4” cornice fall avalanche might display a kind of natural limit under average snow conditions due to the particular setting of the Gruvefjellet slope section.

The nine high magnitude events of previous snow seasons between 2005/2006 and 2007/2008 also affirm the observations on the coherency of avalanche classes and the particular starting zones (Diagram 16, Figure 27). The gully ‘Wrong Step’ showed a distinct predominance of the “D3 R4” class with five documented failures. Thus, between 2005/2006 and 2009/2010 10 “D3” cornice fall avalanches occurred in ‘Wrong Step’ which constitutes nearly 45% of all 23 high magnitude events documented. Nine of those ‘Wrong Step’ failures were categorized as “D3 R4” failures. Six “D3” failures occurred in ‘Willy Sagnol’ and therefore account for about 25% of all high magnitude events. Between 2005/2006 and 2009/2010 the gullies ‘S’ and ‘Triple Y’ showed fewer “D3” cornice fall avalanches with four and three failures recorded, respectively. Notably, within the five snow seasons no high magnitude event occurred in the most confined gully ‘Einbahnstraße’ (Figure 27).

5.5. Geomorphological impact of cornice fall avalanches

5.5.1. Overview

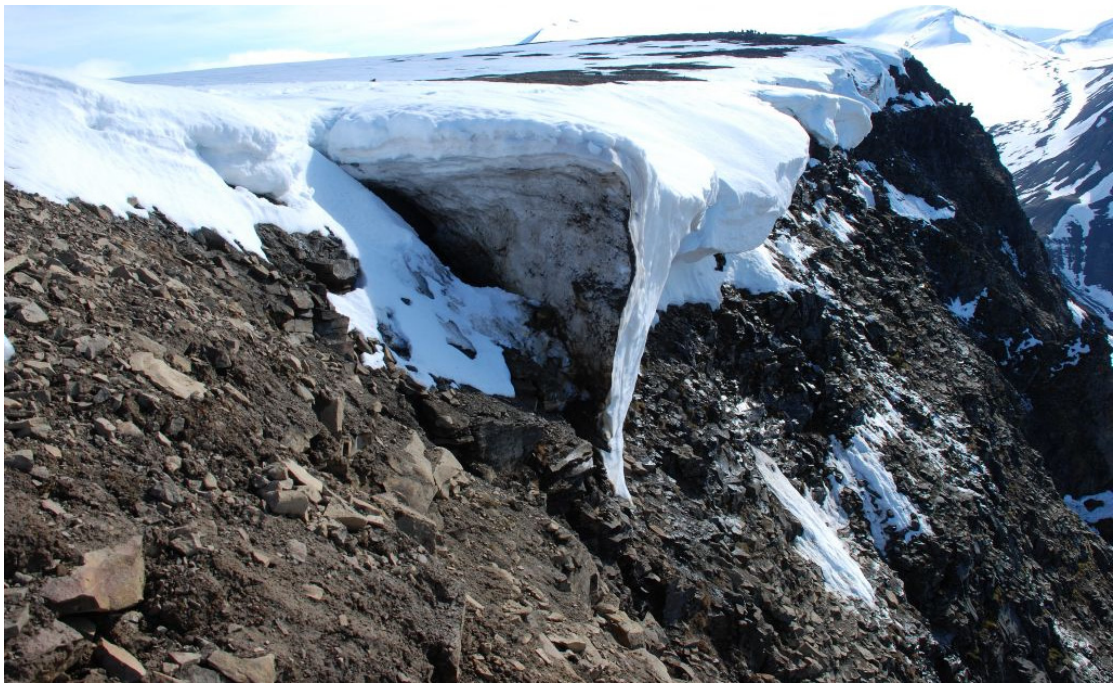

Figure 28 Cornice remnants along the Gruvefjellet plateau edge on 24 June 2010. The main cornice mass is sitting on the second sedimentary step. Cornice scarp and pillow have already collapsed. Photograph towards S

The geomorphological impact of cornice fall avalanches has been investigated within the Gruvefjellet slope section and the adjacent areas. Two sedimentary steps were observed just below the Gruvefjellet plateau edge due to erosion (Figure 29). The upper one represents the position of the cornice root onset. The second step is situated several meters below the plateau edge and presumably displays the pivotal point during cornice crack opening. The main mass of the cornice is resting on this step. This observation is confirmed by the last cornice remnants found here at the very end of the snow season (Figure 28). The sedimentary bedrock above these steps is physically weathered and significantly loosened-up.

Figure 29 Last cornice remnants along the Gruvefjellet plateau edge 13 July 2009. The transition from the plateau area to the main slope displays two sedimentary steps. Note the horizontal cornice bedding and vertical cornice face. Photograph towards S

5.5.2. Embedment of debris into the cornice mass

I found distinctive amounts of sediment frozen into the lower cornice mass when enhanced cornice cracking enabled the investigation of the cracks (Figure 30). The actual process of how these sediments were frozen and embedded into the cornice snow remained unclear. Though the topography of the mountain crest, the sedimentary conditions and the underlying continuous permafrost presumably interact in this process. The debris was ripped off from the headwall during cornice cracking. The majority of the debris visible was several centimetres in diameter, though small blocks up to 0.5 m in diameter were also observed. A wooden stake drilled into the plateau edge the previous summer was observed ripped off and frozen into the cornice mass when the cornice cracked. Furthermore the process of cornice cracking led to the loosening-up of the plateau headwall bedrock and therefore the development of the two distinct sedimentary steps observed (Figure 29).

Figure 30 Debris embedded into the cornice mass becomes visible once cornice cracks open. The debris is mostly several cm in diameter but vary up to small blocks of 0.5 m in diameter. Photograph taken 18 May 2010

With the successional opening of the cornice crack debris accumulated in its lower part (Figure 31). Besides the ripped off debris further sediments were transported to the cornice crack from the freshly exposed plateau headwall by miniature rock falls. The latter one was seen to be more pronounced towards the end of the snow season with rising temperatures.

Figure 31 Debris accumulation in the lower part of a cracked cornice on 10 June 2010. The central cornice mass already failed. The two unsupported lateral wings will avalanche in a number of rather small events and eventually release the remaining debris. Photograph towards NE

5.5.3. Release of accumulated debris and redistribution

The accumulated debris got eventually released by cornice fall avalanches (Figure 21). The majority of the involved snow and therefore also the debris was deposited in the runout. Most of the cracked cornices eventually failed in a rather distinct avalanche and reached low inclined terrain. In addition to this, further debris was picked up during the release along the avalanche path especially around rock noses. Several large avalanches displayed pronounced dirty stripes indicating high debris contents along their track. This was seen most distinctly later in the snow season when the cornice fall avalanches ran out partly on bare ground. Though I assume that the ripped off debris from the plateau edge constitutes the major part of the overall entrained sediments (Figure 32).

Figure 32 Debris embedded into a large cornice block observed in the runout of the adjacent site on the glacier Larsbreen on 27 May 2010. Ski for scale

In the Gruvefjellet slope section and the adjacent areas cracked cornices have been observed not to fail in a complete cornice fall avalanche. Large cornice parts remained sitting at the plateau edge with the centre of gravity on the second sedimentary step. Thereby the cornice face was essentially vertical. Large amounts of debris were visible exposed on the upper cornice part (Figure 33). These progressively melted out and consequently slid downslope in a number of small events. Naturally the runout distances hereby were rather limited. This unconsolidated debris was presumably transported further downslope by a number of different slope processes including cornice fall avalanches in the subsequent snow season.

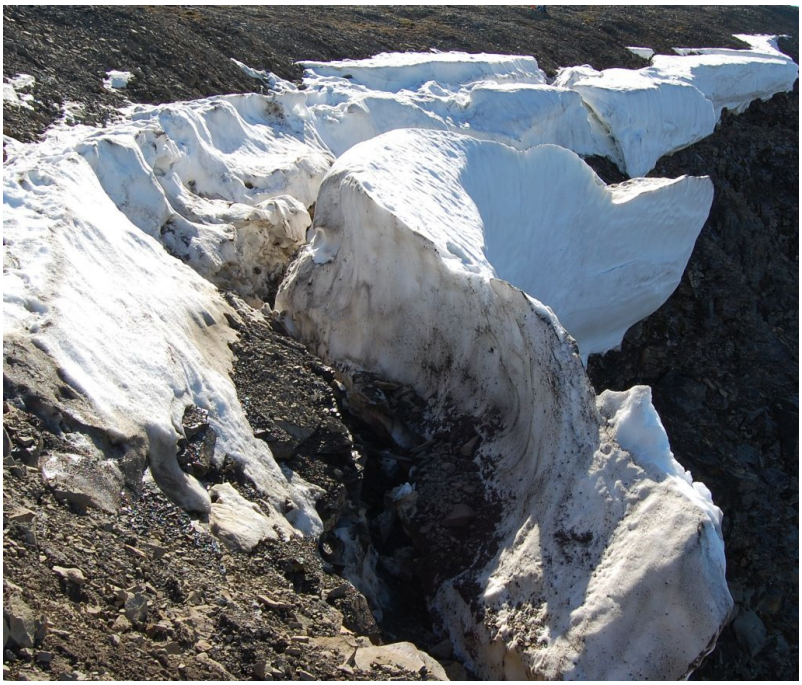

Figure 33 Last remnants of cracked cornices along the Gruvefjellet ridgeline which did not avalanche as entire cornice falls. Accumulated debris is visible in the wide cornice crack. Note no cornice remnants survived the summer time of the two investigated snow seasons. Photograph taken on 23 July 2008 towards S by Markus Eckerstorfer

5.5.4. Debris content of cornice fall avalanches in relation to time

The recorded 180 cornice failures showed rising debris contents towards the end of the snow season (Diagram 17). In June a predominance of failures with visible debris content at the surface ("DC2") displayed the eventual failure of cracked cornices and subsequently their remnants. Thereby the accumulated debris got released. Furthermore towards the end of the snow season the scarp and pillow below the cornices were mostly collapsed (Figure 28) and failures impacted directly onto exposed bedrock and also entrained loose sediments. Additional debris was dragged along with cornice avalanches in the track when the snow cover became uncontinuous within the Gruvefjellet slope. At the very beginning of the snow season all failures were rated as "DC1" even though complete cornice fall avalanches have been observed (Diagram 17). These ripped off large amounts of debris and transported it downslope, though this was not observed by the automatic camera 'Sverdrupbyen' due to the polar night.

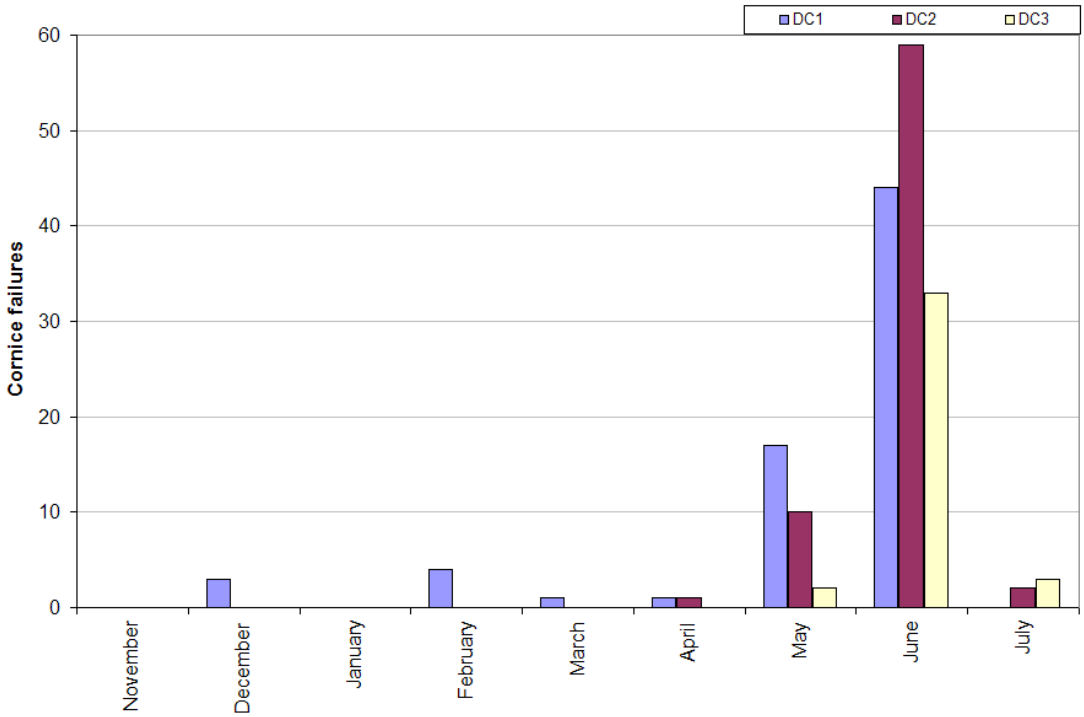

Diagram 17 Visual observed debris content of 170 cornice failures throughout the two investigated snow seasons 2008/2009 and 2009/2010

5.5.5. Debris content of cornice fall avalanches in relation to avalanche class

The class distribution of avalanches in relation to their debris content categories revealed that all failure classes transport debris in some way (Diagram 18). The overall picture did not indicate any predominance of particular avalanche sizes with respect to their debris content. Though, as described in the previous section, the debris content in particular of the high magnitude failures was presumably underestimated. Irrespective of their timing these failure classes transport the highest quantity of debris (Figure 32) and display longest run outs. The small failures with high debris contents are rather accounted for as redistribution of unconsolidated sediments within the avalanche track or the pick up of debris when impacting bedrock. In general, the rather small failures showed increasing debris contents towards the very end of the snow season.

In spite of the limitations determining the visible debris content of cornice fall avalanches by automatic camera, the photographs gave valuable information on the relative amount of debris entrained in relation to time and avalanche size. Thereby the latter one is of special interest as it determines how far downslope the amount of debris is actually transported.

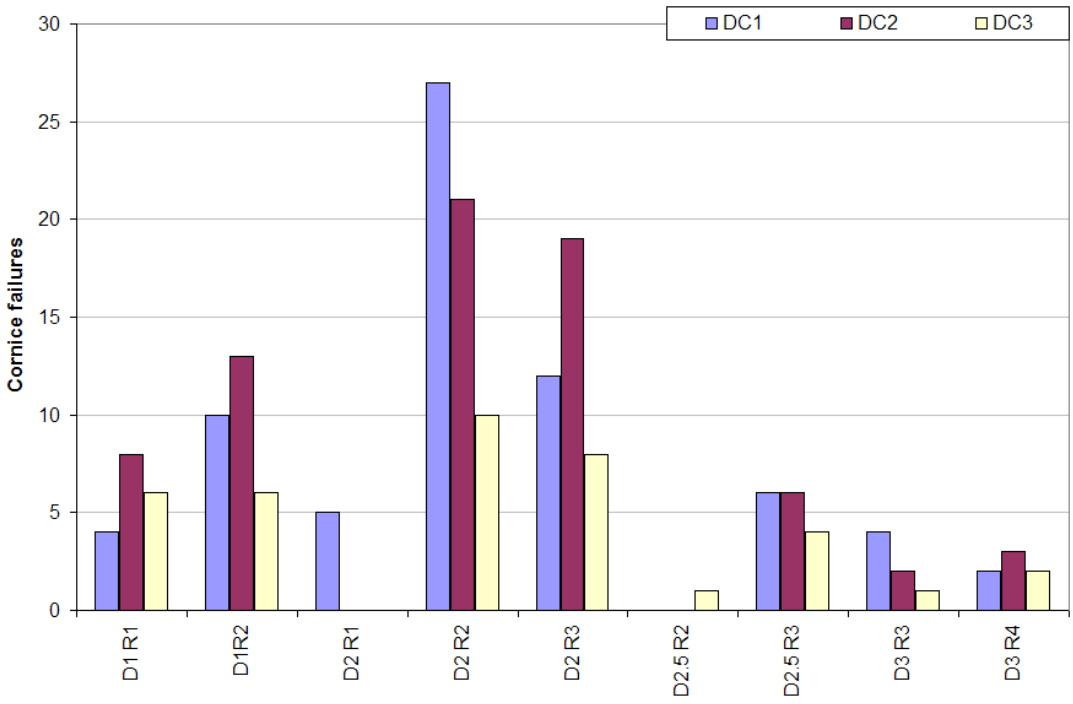

Diagram 18 Visually observed debris content of 170 cornice failures of the two investigated snow seasons 2008/2009 and 2009/2010 with regards to avalanche classes

6. DISCUSSION

The objective of this study was to investigate the development, accretion, cracking and eventual failure of cornices along the ridgeline of the Gruvefjellet plateau mountain and their controlling meteorological factors in the two consecutive snow seasons 2008/2009 and 2009/2010. My motivation results from the scarcity of knowledge on cornices in general and in connection with their ability to trigger avalanches when breaking off. Cornice fall avalanches represent a natural recurrent threat to the inhabitants of Nybyen. This is the first study of its kind in the High Arctic and one of the few long lasting investigations on cornices in general. In the following section I will discuss the four significant processes of cornice development - cornice accretion, scouring, cracking and eventually cornice failure as well as the geomorphological impact of cornice fall avalanches.

6.1. Cornice accretion

Cornice accretion occurred as a direct response to the first snowfalls and proceeded throughout the entire snow season under a wide range of temperatures (Diagram 7, Diagram 8). Even towards the end of both snow seasons under air temperature conditions close to 0°C cornice accretion occurred. Wind speed thresholds for drifting snow increases with increasing temperature (McClung and Schaerer 2006). Though the drifting snow in these events resulted from ongoing snow fall and mainly did not include the surface layer of the isothermal snow pack. Therefore an actual temperature threshold with respect to wind drifting and consequent cornice accretion was not observed.

The observed average hourly wind speed for accretion was about 8 m/s in both snow seasons. The storms average hourly maximum wind speed was 10.9 m/s for the snow season 2008/2009 and 12.1 m/s in 2009/2010. These average values are close to the threshold wind speeds of the snow transport modes saltation and turbulent suspension. Saltation is the transport of snow particles in wind speeds of 5 to 10 m/s close to the surface of cold, loose snow (McClung and Schaerer 2006). If the wind speed exceeds about 15 m/s, snow particles are lifted up to tens of meters above the snow surface and form a turbulent suspension (McClung and Schaerer 2006).

Hourly maximum wind speeds reached the suspension threshold wind speed temporarily in the majority of the observed storm events. Though these thresholds are rated for cold, loose snow. After snow deposition the formation of bonds between the surface grains hardens the surface and thus increases the threshold wind speed (McClung and Schaerer 2006).

Sokratov and Sato (2001) investigated the effect of wind on the snow cover in a four day long wind tunnel experiment with a cold-room temperature of -15°C. Thereby wind speeds of 5 m/s and 10 m/s have been simulated intermittently with no-wind conditions. The authors found that mechanical wind pressure both on the snow surface as well as in the near-surface snow layer leads to a densification of the snowpack, with an effect only to a certain depth. Thereby the near-surface wind turbulence is responsible for the fluctuation pressure over the snow surface and the turbulence inside this snow layer. In their experimental study the densification of the snowpack under the influence of wind was found to a depth of about 7 cm (Sokratov and Sato 2001).

Kosugi et al. (2004) compared saltation length of drifted snow over loose and hard snow surfaces with increasing wind velocities in a cold wind tunnel at a constant temperature of -15°C. For the same wind speed, mean saltation length over hard snow surfaces was several times larger then over loose snow surfaces. The authors attributed this to the difference in the splash processes, because on loose snow surfaces saltating particles not only rebound but also eject some additional particles off the snow surface. Therefore essentially more particles existed in snow drifting over a loose surface, which indicates shorter saltation length than under hard snow surface conditions. With increasing wind speed the most frequent saltation length increased in drifting snow over a hard snow surface, which is in contrast to saltation length distribution over loose snow surfaces (Kosugi et al. 2004).

This reflects a natural limitation for the cornice accretion process on the Gruvefjellet ridgeline as hard snow surface conditions on the exposed plateau are common. The increased saltation length during snow drifting in turn reduces the effective contacts of the snow particles on the plateau surface. Therefore the probability of adhesion on the cornice mass is reduced.

In contrast it may reveal the effectiveness of cornice accretion under comparable calm conditions and the supply of stellar flakes. Hereby the snow cover is soft, thus - following Kosugi et al. (2004) - saltation lengths are shorter and more snow particles are involved in the snow drift due to the ejection of additional particles by collision with the snow surface. Montagne et al. (1968) accounted these conditions for the sheet accretion type due to the clinging of stellar snow and effective grain to grain adhesion. The author furthermore described the vertical accretion type and the wedge accretion type (Figure 5). On Gruvefjellet these three accretion types could not be distinguished and therefore attributed to particular meteorological conditions.

Seligman (1936) called lighter layers incorporated in the cornice "hooked-on" layers, which presumably result from the clinging of stellar flakes. The two observed storms on 8 March 2009 and 14 March 2009 led to cornice accretion and showed maximum wind speeds slightly above the seasonal average. Contemporaneous with the first storm a significant increase in snow depth of 15 cm was recorded (Diagram 5). Hence, these two events might have occurred under conditions favourable for the formation of "hooked-on" layers (Seligman 1936) and sheet accretion (Montagne et al. 1968).

Though a cornice trenching in Fardalen 12 May 2009 did not depict distinct low density internal cornice layers, which may have resulted from these particular accretion conditions (Figure 8). Different accretion types might have been observed here during the experimental observation period in the snow season 2009/2010, but none of them were persistently developed.

McClung and Schaerer (2006) stated that the threshold wind speed for cornice formation is similar to that of snow transport over loose, cold snow. Despite events like these in March 2009 with the supply of recently fallen snow, the threshold wind speed for drifting snow on the Gruvefjellet plateau and consequently cornice formation might be at the upper limit of the stated 5 to 10 m/s range. Montagne et al. (1968) described somewhat higher threshold wind speeds of 7 to 15 m/s for granular cornice growth.

Following Sokratov and Sato (2001) and McClung and Schaerer (2006), the average hourly maximum wind speed in excess of 6 m/s throughout the snow season may lead to a densification of the snow pack surface and furthermore the destruction of snow particles into smaller fragments which in turn pack to higher densities on the Gruvefjellet plateau. This restricts the cornice accretion to storm events with significantly higher wind speeds than the overall snow season average or the coincidence with recent snow fall.

The cornice accretion experimental side in Fardalen is located at lower elevation (about 100 m a.s.l.) and not as exposed as the high plateau area of Gruvefjellet (Figure 3). Thus, the average wind speeds might be somewhat lower at this site. It remains elusive if the resulting less compacted snow surface enabled a higher quantity of snow drift events. Though 12 cornice accretion events have been observed in Fardalen during the automatic camera coverage between 19 March and 20 May 2010. Certainly the particular cornice and the corresponding accretion events were of lower magnitude as the majority of those observed along the Gruvefjellet plateau ridge (Figure 16). This might imply a lower average threshold wind speed for drifting snow and thus cornice accretion at this particular site.

On Gruvefjellet periods without daily automatic camera photographs were not investigated with respect to cornice accretion. The observations during fieldwork did not exhibit the applied accuracy in particular with respect to time resolution. Thus, the fieldwork observations could not be coupled to the meteorological data and snow depth measurements which were also dependent on camera observation. Variations observed on the storms that led to cornice accretion revealed the dependency and in turn effectiveness of automatic camera observations. The actual amount of cornice accretion periods was presumably higher in both snow seasons. 10 additional storm events have been observed in both snow season which included the polar night and periods without daily automatic camera photographs.

A slight difference was observed between the overall snow seasons wind direction from SE and the average storm wind direction from ESE. Only one storm which led to cornice accretion differed from these findings. On 19 December 2009 a storm lasted for 30 hours and indicated an ENE direction which displays a rather acute angle towards the plateau ridgeline. In spite of this, considerable cornice growth was observed (Diagram 8).
Winther et al. (2003) described studies in the lower Bayelva catchment near Ny Ålesund and compared these to a study site in De Geerdalen, a valley about 11 km ENE of Longyearbyen. Similar to the Longyeardalen conditions prevailing easterly winds lead to accumulation on westerly mountain sides due to their leeward position. Though, the authors stated a dominant WNW wind direction during precipitation events which also led to snow accumulation found on ESE facing slopes (Winther et al. 2003).
On Gruvefjellet the observed storm events that led to cornice accretion did not indicate a pronounced variation from the overall snow season's prevailing winter wind direction from SE. Merely the two cornice scouring events observed in March 2010 showed a significant difference in the recorded wind direction.

6.2. Cornice scouring

Distinct scouring events indicated particularly high winds speeds for 3 hours on 7 March and 7 hours on 8/9 March 2010, respectively (Diagram 9). A lower time limit for cornice scouring could not be observed. Data for cornice scouring threshold wind speeds are sparse. Montagne et al. (1968) found wind speeds in excess of 27 m/s for cornice scouring which was reached by the 7 March 2010 storm with gusts up to 32 m/s. The hourly maximum wind speeds of the second event were significant lower and varied between 15–19 m/s.
Similar hourly maximum wind speeds were observed several times in both snow seasons during storm events that also led to cornice growth. Giving the low time resolution of the Gruvefjellet automatic camera photographs prohibited the investigation of possible temporary cornice scouring. McClung and Schaerer (2006) stated that surface conditions, temperature, humidity and other factors may cause variations in the cornice scouring threshold.

Notably, the recorded wind direction of the two observed scouring events was in contrast to the prevailing winter wind direction from SE and varied between S-SW (7 March 2010) to WNW-NW (8/9 March 2010). These wind directions display a distinct angle against the plateau ridgeline. Therefore scouring occurred not only along the cornice root and roof but also on the rather frail cornice face and scarp below which was observed on 8 March 2010. Scouring threshold wind speeds might be somewhat higher across the smooth Gruvefjellet plateau area due to the limited contact surface.

A snow depth reduction of 4 cm was recorded at the crossover of the Gruvefjellet plateau and the cornice root after both cornice scouring events (Diagram 6). Taking into account the short duration of the two events nevertheless shows the considerable impact on the cornice development. But as only two cornice scouring events were visually observed in the investigated snow seasons by the Gruvefjellet automatic camera their general impact on the cornice development throughout the snow season cannot be depicted more quantitatively.

6.3. Cornice cracking

Significant temperature fluctuations have been recorded prior to the development of six cornice cracks observed during the two investigated snow seasons 2008/2009 (Diagram 7) and 2009/2010 (Diagram 8). Certainly the amount of investigated cornice cracks was rather limited. Though, a very close relationship between the opening of cornice tension cracks in connection with initial tilting of the cornice mass and very pronounced temperature variations appeared.

Schweizer and Jamieson (2010) investigated the effect of surface warming on snow pack stability. The authors suggested that increased deformation within the near-surface layer of a slab accounted for the instability in the case of dry-snow slab avalanches. Surface layer stiffness can be effectively reduced by surface penetrating solar radiation, which in turn directly affects the snow instability (Schweizer and Jamieson 2010).

The effects of rain-on-snow events on dry snow slabs have been investigated by Conway (1998). The author found an immediate increase in the surface layer creep rate, which led to a decrease in slab stability.

These observations on slab fracture mechanics may also be accounted for in cornice stability due to their particular cantilevered slab structure (Burrows and McClung 2006). Notably, both Schweizer and Jamieson (2010) as well as Conway (1998) described effects restricted to the upper surface layers and not the entire snowpack.

Extensive cornice cracks have been observed along the Gruvefjellet ridgeline in the early part of the snow season on 23 January 2010 as a direct response to a distinct mid-winter warm spell with large amounts of rain between 14 and 19 January 2010 (Figure 25). Though, the majority of the investigated cornice cracks developed later in the snow season following significant warm spells. Fieldwork observations on the adjacent areas affirmed this additionally. Mosimann (2009) attributed the development of cornice cracks between the ridgeline and the cornice mass to the process of snow settlement and Montagne et al. (1968) referred to ongoing creep and glide processes.

In both snow seasons steady cornice crack opening rates were measured due to constant snow creep under the influence of gravity, metamorphism and temperature (Diagram 10, Diagram 11). The cornice mass tilts around a fixed pivotal point which may be the second sedimentary step observed. After a period of time at the beginning of the snow season the temperature conditions here presumably remain steady despite the large air temperature variations measured throughout the crack development. This insulating characteristic of the snow cover became apparent on 23 April 2010 when wide spread surface hoar was observed in the surroundings of the most recently opened cornice cracks being exposed to the cold air.

I excluded the very end of both snow seasons of the two long lasting series of cornice crack measurements, since the upper cornice layers were water saturated due to melting conditions. In the snow season 2008/2009 an investigated cornice crack opened a relative distance of 105 cm within 38 days (28 April and 6 June 2009), which resulted in an opening rate of 2.76 cm/d. Between 16 April and 6 June 2010 (51 days) a relative distance of 22 cm was measured, which resulted in an opening rate of 0.43 cm/d.

I excluded surface perturbations from this time series which caused false measurements and may indicate the limitation of this measuring technique (Figure 19).

The highest cornice crack opening rate of 8.6 cm/d was measured in the short series between 5 and 10 February 2010. Variations in the snow cover thickness may be of minor importance. The significant differences in the obtained opening rates are accounted for in the particular cornice size, the micro topography of the plateau edge and the delimiting rock noses giving varying support to the cornices.

The impact of these factors becomes evident in comparison with the adjacent site above the glacier Larsbreen. Here the delimiting rock noses on the plateau level are only weakly developed. Furthermore the slope's crest is more pronounced and hardly any sedimentary steps are developed (Figure 34). Therefore the support on the cornice foot is significantly less then on the studied slope section. The cracked cornices reach their particular breakover point earlier and thus, cornice crack widths are less prior to failure.

Figure 34 Large cornice triggered slab avalanche on the adjacent site near the glacier Larsbreen. A large cornice block stayed intact and reached 0° of slope inclination. Photograph taken 18 May 2009 towards SE. Note the close to vertical slope's crest and the person for scale standing on the cornice block

Even though no measurements were carried out on the Larsbreen site, the time period from initial tilting and cracking to eventual failure was observed to be significantly shorter. In the studied slope section the period of cracking to eventual failure varied between four to five weeks.

In three cases a stage of cornice tilting was observed prior to the crack appearance at the surface which varied between one to four weeks. The overall duration from initial cornice tilting and cracking to eventual failure was about six weeks.
This order of magnitude goes along with fieldwork observations in Juneau, Alaska (personal communication Bill Glude 2010). Though, no particular research was carried out here.

6.4. Cornice failure

Significant work has been done on cornice control using permanent structures (e.g. Montagne et al. 1968, Chaudhary and Singh 2006, Margreth 2007) and explosives (McCarty et al. 1986). But basically no work was carried out particularly on cornice failure and their fracture mechanics.
Burrows and McClung (2006) described meteorologically-related triggers, similar to those of slab avalanche release. McCarty et al. (1986) stated that cornices respond quickly to their meteorological environment. Their monitoring programme, using among other methods ram profiles , indicated in particular cornice strength variations of the overhanging lee side since it is subjected to warming or cooling from three sides (Figure 9). The authors summarized that the strength of cornices may often be unpredictable. Ward (1981) differentiated between old and new cornices and stated that cold weather might toughen old ones, however, this may not be accounted for in new cornices. Mosimann (2009) stated that cornices in high mountains might be more 'breaking resistant' during summer time when the snow is heavily compacted.
In the two investigated snow seasons entire cornice failures have not been observed immediately after temperature variations or snow loading due to storm events on Gruvefjellet. In turn, I found that distinct temperature variation mostly associated with storm events rather account for initial cracking of the cornices which in turn may lead to eventual failure after a period of time. Therefore the meteorological conditions concurrent to cornice failures are of less importance than the length of time since crack initiation and tilting. Thereby the duration between initial cracking and eventual failure is controlled by the particular breakover point of the cornice.

Notably, I did not observe the development of cornice tension cracks in all cases prior to larger failures. The cornice failure on 17 April 2010 displayed the only exception with respect to high magnitude events. No open cracks have been observed the day before failure during fieldwork. The failure occurred after a significant temperature drop of 11°C within two days to -16°C on 14 April 2010 and was categorised as "D3 R4" failure. The scar along the ridgeline where the entire cornice broke off was about four meters wide.

Even towards the end of the snow season spontaneous larger failures occurred within the Gruvefjellet slope section and the adjacent areas but these did not include entire cornice failures. The late spontaneous failures depict the brittle behaviour of the cornice mass even though the surface layer was already affected by melting conditions. These findings may imply that cornice fall avalanches are in particular difficult to forecast.

Spontaneous failures of cornices occur already at a premature cornice stage (Mosimann 2009) or during thaw conditions (Ward 1981, Mosimann 2009). Clearly failures of smaller cornice sections such as the leading edge, scarp or pillow may be directly attributed to distinct meteorological fluctuations. The majority of these smaller failures are caused by seasonal warming towards the end of the snow season in particular in June.

The two investigated snow seasons differed with respect to time distribution, quantity as well as magnitude of the cornice failures (Diagram 14). In the snow season 2008/2009 no failures were observed before 5 May 2009. The first high magnitude failure was recorded 3 June 2009. This is in contrast to observations of previous years, when first failures already occurred in January (18 January 2007) and February (24 February 2008) (*www.skred-svalbard.no*). In the second observed snow season the first failures were observed 22 December 2009 and 13 February 2010. All of these failures in the early part of the snow season were entire cornice failures rated as "D3 R3" and "D3 R4" avalanches.

The absence of any cornice failures in the early part of the season 2008/2009 is even more striking as on 30 March 2009 a major cornice fall avalanche occurred on the adjacent Gruvefjellet side towards NE which triggered a large slab below the free face (Eckerstorfer et al. 2009) (Figure 35).

Figure 35 Major cornice triggered slab avalanche on the adjacent site towards N. The old mine ('Nye Gruve II') is seen on the right side. The destroyed taubanebukkene is visible in the avalanche path and the street connecting Nybyen and Longyearbyen in the foreground. Photograph taken towards E on 30 March 2009 by Markus Eckerstorfer

This cornice triggered slab ran out to about 10° slope inclination, buried the street and indicated an averaged deposition depth of about 1.5 m. The total deposition volume was estimated to be about 19.000 m³ (*www.skred-svalbard.no*). This failure destroyed a taubanebukkene – a wooden transport structure used during past mining activity. According to the Cultural Heritage Advisor, this particular taubanebukke leading up to the mine 2b ('Nye Gruve II') was built about 1938 (personal communication Hilde Arna Tokle 2009).

These 71 years of existence depict the sparsity of such high magnitude failures which may be accounted for as a maximum cornice fall avalanche along the Gruvefjellet slope. Between the snow seasons 2005/2006 and 2009/2010 “D3 R4” avalanches displayed an annual return period in the studied Gruvefjellet slope section.

In comparison to the previous snow season, the snow season of 2009/2010 was exceptional both in quantity as well as the magnitude of the failures. 26 cornice fall avalanches were recorded in 2008/2009, while in the second snow season 44 cornice fall avalanches occurred, which is an increase of nearly 60 %. Furthermore only three high magnitude events occurred in 2008/2009, while the second snow season showed 11 events categorized as “D3” avalanches (Diagram 14).

Mild temperatures up to 1.9°C on 10-12 December 2009 followed by a significant cooling to about -13°C on 20 December 2009 and the very pronounced mid-winter warm spell between 14 and 19 January 2010 with large amounts of precipitation mainly accounts for these differences, respectively (Diagram 3). Three “D3 R3” cornice fall avalanches occurred on 22 December 2009 in the Gruvefjellet slope section. The latter event led to the release of 10 slush avalanches followed by 31 large slab avalanches in the area surrounding Longyearbyen between 14 and 31 January 2010. Three “D3 R4” cornice fall avalanches occurred in the studied slope section, which were directly related to this mid-winter warm spell. Eckerstorfer and Christiansen (2010) investigated the meteorological as well as snow pack conditions and suggested that this event was extreme both in magnitude and frequency.

Furthermore the Gruvefjellet gullies that produced the high magnitude avalanches in the early part of the snow season – ‘S’(22 December 2009), ‘Wrong Step’ (22 December 2009, 13 February 20010) and ‘Willy Sagnol’ (22 December 2009, 13/15 February 20010) – showed very large failures again later in the snow season in April (‘Wrong Step’), May (‘Willy Sagnol’) and June (‘Wrong Step’ and ‘S’) after the rebuilding of the cornices. The same was documented in the snow season 2006/2007 when a high magnitude failure occurred in January in ‘Wrong Step’. After the rebuilding of the cornice, two very large failures occurred again in April 2007 (*www.skred-svalbard.no*).

All failures in the studied slope section are related to cornice failures other than minor loose snow avalanches, which are in particular released after snow storms and towards the end of the snow season. It is notable that in the two investigated snow seasons only three minor slabs were triggered by cornice failures which did not entrain big amounts of snow.

The same applies for the four cornice triggered slabs documented between 2005/2006 and 2007/2008 which displayed only minor crowns (*www.skred-svalbard.no*). This is very much in contrast to the adjacent site above Larsbreen (Figure 34). Observations during fieldwork revealed that the frequency of cornice triggered slabs is significantly higher at this site. The ridgeline topography in combination with the less pronounced channel development within the slope constitutes presumably a major influence here. Furthermore the generally larger cornice collapses lead to larger exerted stresses on the slope when impacting. This reveals that the particular slope morphology constitutes a huge impact on the resulting avalanches, both in type as well as in magnitude.

6.5. Geomorphological impact of cornice fall avalanches

This study shows that the geomorphological impact of cornice fall avalanches in a High Arctic setting is significant. I observed debris of mostly several centimetres in diameter frozen and embedded into the cornice mass (Figure 30). This was also briefly noted by Montagne et al. (1968) for a cornice in south western Montana. The topography of the Gruvefjellet mountain crest exposed to freezing from two sides, the sedimentary conditions and the underlying continuous permafrost presumably interact in this process. Also the snow densification along the ridgeline during ongoing cornice formation may be of particular importance. The weathered rock debris at the plateau edge is covered by snow at the beginning of the snow season. Snow density increases considerably to about 500 kg/m³ (McClung and Schaerer 2006) due to ongoing snow accumulation and the mechanical impact of wind on the snow surface according to Sokratov and Sato (2001). Thereby the debris is presumably enclosed and embedded into the cornice mass. The snow densification and contemporaneous settlement in the snowpack cause further sediments to get in direct contact with the dense cornice snow and the associated debris is eventually frozen to it.

Certainly this process needs deeper investigation in particular in the early part of the snow season. Temperature profiles will clarify the thermal regime of cornices and their sedimentary bedrock interface.

The development of two sedimentary steps was observed (Figure 29), of which the first one just below the plateau edge indicates the position of the cornice root. The second step developed several meters below the plateau edge and presumably displays the pivotal point during the cornice crack development. Furthermore the main mass of the cornice is resting on this lower step which is confirmed by the last cornice remnants found here at the very end of the snow season (Figure 28). Here snow is present for about 10 months a year. The sedimentary bedrock above these steps is physically weathered and significantly loosened-up.

Sediments are ripped off the headwall during cornice cracking and consequently accumulate in the opening cornice crack (Figure 31). These amounts of debris are eventually released by cornice fall avalanches and redeposited on to the talus cones in the runout zone with the main mass of the cornice. Further debris is picked up along the avalanche track in particular towards the end of the snow season when the remaining snow cover is thin or even absent. These 'dirty avalanches' were described among others by André (1990b) from Northwest Spitsbergen and more recently by Decaulne and Saemundsson (2006) from western Island which depicts a somewhat comparable setting. But the ripped off sediments from the Gruvefjellet plateau edge presumably represent the major part of the overall entrained debris (Figure 32).

André (1990b) used persistent snow cover as debris traps to study the accumulation of debris transported by snow avalanches. The author related the geomorphological efficiency of avalanches to the channelization of debris. Furthermore the author found strong variations in the amount of transported debris depending on the type of underlying bedrock. Episodic slush avalanches create substantial long-lasting boulder tongues and modify slope profiles, which is also accounted for by debris flow episodes (André 1990b).

Though, the frequency of more effective debris flows is rather limited. Most of the debris flows found in the valley Longyeardalen occurred as a result of heavy rain in July 1972 (Larsson 1984). The entire westfacing slopes of the valley indicate variable amounts of debris flow tracks from 0 to more then three tracks observed within 1 km long talus slope sections (Åkerman 1984).

In contrast to episodic slush avalanches and debris flows, André (1990b) summarized that annual snow avalanches only scrape and slightly reshape scree slopes by rearranging debris and therefore display only minor geomorphological impact.

Decaulne and Saemundsson (2006) found full-depth slab avalanches triggered by cornice falls may lead to boulder transport. These form a diffuse accumulation at the base of the slope. Unconsolidated debris is redistributed by wet slabs triggered by cornice failures when the remaining snow cover is thin or even snow free areas are present in the avalanche path. Slush avalanches have the same geomorphological effect, leaving both erosional and depositional features on the slope. Though, the authors stressed that the redistribution of material on the slope is not exclusively due to high magnitude events. During early winter with unfrozen surface and only thin snow pack conditions, snow avalanches are a scouring agent transferring coarse material downslope. This is in contrast to mid-winter conditions when a thick snow cover prevents the redistribution of coarse material and in addition to this limits the impact of transported boulders on the slope (Decaulne and Saemundsson 2006).

The same accounts for the 10 mid-winter slush avalanches investigated by Eckerstorfer and Christiansen (2010). These slush avalanches occurred between 14 January and 29 January 2010 and slid on an ice layer which prevented a direct geomorphological impact of this extreme event.

Notably, both André (1990b) and Decaulne and Saemundsson (2006) noted cornice fall avalanches in their studies but did not describe a direct geomorphological impact of these. Åkerman (1984) investigated talus formation processes in the Kapp Linné area in central Spitsbergen. He found tracks of slush avalanches but did not generally describe the geomorphological impact of snow avalanches with respect to talus formation.

In contrast to these studies, I found that cornice fall avalanches represent an active debris transport agent from the plateau edge to the basal slope and thus display an important geomorphological process in relation to talus formation. Furthermore, Humlum et al. (2007) investigated the rock glacier development adjacent to the cornice side near the glacier Larsbreen (Figure 3). The authors found that these rock glaciers are fed by cornice triggered slab avalanches. Those lead to the yearly build up of 1-5 m thick avalanche deposits in the runout which contain distinctive amounts of rock debris.

Over time the snow accumulations form annually layers of the remaining avalanche deposits with incorporated rock fragments and a layer of concentrated debris above which display a protective surface (Humlum et al. 2007). Observations at this site during fieldwork confirmed that all but minor loose snow avalanches are accounted for as cornice falls or cornice triggered slab avalanches (Figure 34). Therefore the geomorphological impact of cornice fall avalanches can also be linked to rock glacier development in the High Arctic.

7. CONCLUSION AND FUTURE PROSPECTS

Cornices are found to form annually along the ridgeline of Gruvefjellet due to the combination of a prevailing winter wind direction from the SE, the large plateau source area and the distinct slope inflection. Cornice accretion occurs as a direct response to the first snow falls and proceeds throughout the entire snow season due to significant storm events. Particular high wind speeds lead to cornice scouring. Pronounced temperature fluctuations cause cornice cracking and progressive tilting around a fixed pivotal point which is presumably around the observed second sedimentary step. Despite temperature fluctuations, the measured cornice crack openings display a linear development.

Cornice failure occurs once the particular breakover point is reached as a consequence of constant snow creep. The duration from initial cracking to eventual failure is variable, though averages between four to five weeks. Cornice fall avalanches occur throughout the entire snow season with the vast majority being released towards the end of the snow season in June.

The geomorphological impact of cornice fall avalanches is significant in this High Arctic setting. Large amounts of debris are embedded into the cornice mass and ripped out during the process of cracking. The debris is successively accumulated in the opening cornice crack and eventually released by cornice fall avalanches. Cornice fall avalanches are therefore active sediment transport agents that accumulate sediment from the plateau ridgeline on the talus slope.

The continuous observation of cornice development using automatic time lapse photography has proven to be a valuable method. The particular setup with the 'Sverdrupbyen' camera, covering the entire Gruvefjellet slope from below, in combination with the 'Gruvefjellet' camera, placed parallel to the plateau ridgeline, enabled very detailed observations. Analysing the obtained automatic camera photographs gave insight into the cornice formation, initial cracking and eventual failure. A complete database of 180 cornice failures in the Gruvefjellet slope section could be established enabling comparisons of particular meteorological conditions and generally of previous seasons.

Furthermore a measuring stake with coloured height indications installed close to the camera at the crossover of the main plateau to the cornice root enabled daily snow depth measurements in a simple manner. In addition to this, periods of cornice accretion and scouring could be depicted more quantitatively. Therefore the continuous observations using these two cameras should be maintained. After the return of sunlight an increased time resolution of several pictures a day was reasonable. Certainly the use of automatic time lapse photography is restricted by the polar night in general as well as drifting snow causing low visibility. Furthermore recurrent malfunction of the 'Gruvefjellet' automatic camera indicated the partly unreliability of these setups in High Arctic conditions. Therefore future studies should not only be dependent on this technique.
The field area Gruvefjellet also displays some limitations. The area beneath the cornices is not accessible due to the morphological setting of the Gruvefjellet slope which excludes some fieldwork aspects. Furthermore the area regulations prohibit the use of snow machines and confine the fieldwork and equipment transportation to ski and foot. Though, cornice observations should be carried on along the Gruvefjellet ridgeline in particular with respect to the safety point of view of Nybyen. The automatic weather station 'Gruvefjellet' situated about 500 m towards the plateau centre records hourly meteorological data and thus enables a beneficial correlation of observation and concurrent meteorological conditions.

In this study the opening of cornice tension cracks was measured for the first time. These results gave valuable insight into the cornice development form initial cracking to eventual failure and the driving factors. Clearly these manual measurements indicate a comparable low time resolution and accuracy, but capture the main trend. More cornice crack measurements will increase our understanding of factors influencing the continuous opening rate and the determination of the particular cornice breakover point. The destruction of the measuring setup on 14 February 2010 caused by a large cornice failure indicate that some sophisticated apparatus such as that used for ice wedge monitoring (Christiansen 2005) are not applicable along the ridgeline. Burrows and McClung (2006) suggested to use a glide shoe-type instrument package installed in the cornice to achieve linear displacement, tilt and snow temperature data.

Such instruments have been applied by Conway (1998) in relation to snow creep and the effects of rain-on-snow events in dry snow slabs. Several feasible approaches were carried out with respect to glide avalanches. Carrera-Gómez et al. (2010) used a combination of 'UTL-1' temperature loggers installed at the substrate-snow interface and a 'Onset Hobo UA-004-64' inclination data logger to monitor basal activity attributed to snow glide. Thereby the authors identified periods of basal movement and correlated these with the thermal regime. Hendrikx et al. (2010) used a series of stakes, reflectors and a 'LaserTech TruPulse360B' laser rangefinder which was linked to a 'Trimble Geo XH' GPS to monitor glide crack activity. But similar to my cornice crack measuring set-up, any stakes installed in the cornice will inevitably be affected by temperatures above freezing towards the end of the snow season.

Recent approaches are validating the incorporation of infrasound arrays (Ripepe et al. 2010) and seismic sensor arrays (Van Herwijnen et al. 2010) to detect occurring avalanches more accurately in order to compare these with predictions. Applying the methods over the course of three winters in the eastern Swiss Alps, Van Herwijnen et al. (2010) were able to distinguish loose snow avalanches from slab avalanches despite considerable background noise originating from the nearby town and ski slopes. Lawrence and Williams (1976) carried out a broad-band acoustic study between 1974 and 1975 in the Bridger Range of south-western Montana to detect instabilities associated with avalanche release. The authors used a seismometer placed in the starting zone of a major slide path to monitor any ground and snow movement. Thereby the seismic signals generated by snow movement were clearly distinguishable from extraneous sources. Furthermore signals associated with slab avalanches, loose snow avalanches, cornice falls and internal fracture of the snowpack could be identified. The signal associated to a cornice fall was subdivided into the initial cornice fracture, the impact of the cornice on a slope and the downslope rolling of the cornice. Lawrence and Williams (1976) summarized that the seismic monitoring of major slide paths provides a valuable tool for avalanche forecasting, in particular since the starting zones may occasionally not be accessible.

The investigation of the geomorphological impact of cornice failures is challenging. Using persistent snow cover as debris traps, following André (1990b), was difficult at the Gruvefjellet site due to the interference of single rock falls. The author used the open Randkluft to isolate snow avalanche transported debris from deposits of rock falls and scree slides. Humlum et al. (2007) used 18 m² large sheets of durable plastic placed in the avalanche runout zone of the adjacent site near the glacier Larsbreen to quantify the sediment input. After two snow seasons the average sediment input was 13 kg/m²/yr, but the particular results varied considerably between 0 – 50.4 kg/m²/yr (Humlum et al. 2007). Observations during fieldwork suggest that towards the end of the snow season and with temperatures above freezing, single rock falls and small scree slides also reach the avalanche runout zones and thus contribute to the measured sediment input. Data from sampled snow cover sites and plastic sediment traps coupled with the cornice failure database will give more quantitative insight into the sediment transfer by cornice fall avalanches. Eckerstorfer (personal communication 2010) placed coloured debris along the plateau edge which should confirm the observations of debris transport from the plateau edge to the talus cones by cornice fall avalanches in the coming snow season.

The safety aspect of the Gruvefjellet slope forms a crucial factor since high magnitude failures cover the talus cones and annually reach the low inclined terrain in the vicinity of Nybyen. Therefore cornice fall avalanches represent a recurrent natural hazard for residents and the infrastructure of Nybyen.

The problem is enhanced since cornice cracks are not visible from the valley bottom unless the cornices reach a distinct tilted position. Thus, no stability evaluation is performable from below, which would be beneficial in particular for skiing and snow machining recreationist. In May 2008 an array of breaking mounds of compacted snow was pushed up in front of three houses in Nybyen supervised by UNIS professor Jan Otto Larsen (personal communication Larsen 2009). This protective measure was established as a consequence of a cracked cornice which reached a close to vertical position in the starting zone of the gully ‘Wrong Step’. However, forming breaking mounts does not represent a routine annual measure. No structural protective measures exist along the ridgeline or the Gruvefjellet slope.

The area around Patreksfjorður in western Iceland shows a very comparable setting with a prevailing winter wind direction and plateau shaped mountains (Margreth 2006, Hákonardóttir et al. 2008). As a consequence large cornices form along the ridgeline of the plateau Brellur-mountain which rises 200 to 340 m directly above the town Patreksfjorður and the Urđir area. A combination of several lines of snow fences on the plateau area as well as the installation of 25-30 wind baffles along the ridgeline was suggested by Margreth (2006) to limit the snow transport over the plateau area and to break up cornice formation.
The temporary closure the entire Gruvefjellet slope by the local authorities for example at the end of May 2009 has proven to be an unsatisfactory measure since people still used the slope as a recreation area without precaution. Furthermore general announcements of increased avalanche danger in the areas around Longyearbyen do not always address peoples understanding of the situation. Education and improved protective measures are crucial factors for the safety of Nybyen.

This might be of special importance when predicted downscaled climate models indicate more winter precipitation in the Longyearbyen region (Benestad et al. 2002). Larger amounts of precipitation may not only increase the effective snow depth on the slopes, but may also lead to an increase in cornice fall avalanche magnitude. Rogers et al. (2005) linked local cyclone activity with both, Spitsbergen winter temperatures and ice export from the Fram Strait. Analysing meteorological data of about 90 years (1912-1976 from Isfjord Radio and 1977-2003 from Longyearbyen Lufthavn) the authors found a higher cyclone frequency in warm Spitsbergen winters compared to cold ones. Zahn and von Storch (2008) derived a long-term climatology of polar lows using dynamical downscaled data from 1948-2006 by NCEP/NCAR. A strong year to year variability of polar low activity appeared with negligible overall and regional scale trends. The highest frequency of polar lows was found in the winter season in December and January, while hardly any polar lows occurred during the summer time (Zahn and von Storch 2008).

Most recent analysis of projections for the end of the twenty-first century by Zahn and von Storch (2010) indicated that the polar low frequency will decline considerably. Concurrent with a future warmer climate, the mean genesis region of polar lows is shifted towards the North as a consequence of elevated atmospheric greenhouse gas concentration. The authors attribute these changes to rising temperatures of the North Atlantic sea surface and in particular the mid-troposphere. The resulting enhanced stability will impede the formation and intensification of polar lows (Zahn and von Storch 2010). These predictions are to some extent in contrast to the analysis by Rogers et al. (2005) who found a higher cyclone frequency in warm Spitsbergen winters.
The future prediction of less polar low activity may in turn imply a lower frequency of storms that lead to cornice accretion. The observations of the snow seasons 2008/2009 and 2009/2010 showed that cornice accretion is driven by distinct storm events with maximum wind speeds significantly above the snow season's average. Despite increasing predicted precipitation, the reduction of future cyclonic events may confine the cornice formation and in turn the avalanche activity.

Nevertheless a better understanding of these natural processes that endanger life and the infrastructure of Nybyen is vital. Thereby the findings of spontaneous cornice failures without previous cracking display a particular challenge. A better understanding of the processes and meteorological conditions that cause cornice cracking and in turn may lead to cornice fall avalanches is crucial to allow improved stability analysis. This will ultimately improve the effectiveness of safety measures and may enable forecasting methods in the future.

ACKNOWLEDGEMENT

First of all I'd like to express my thanks to my supervisor Hanne H. Christianson, for enabling me to write my master thesis as part of the CRYOSLOPE Svalbard project. Allowing me to develop and adapt my thesis to the fieldwork carried out in the course of two snow seasons was eminent. In the very beginning the final outcome was still hidden in clouds. I'm also thankful to Ole Humlum and the other CRYOSLOPE project members for giving all these educated guesses in times when question marks and exclamation marks played hide-and-seek in my head.

Markus Eckerstorfer I am particularly thankful for sharing uncountable 'Chicken Curry' and freezing fingers in the field. His input in the field as well as indoors was more than valuable. His help became permanent when unintentionally naming the gully 'Wrong Step'.

Thank goes out to Ulli Neumann for being a brilliant arctic crash pilot and for the achievement of aerial pictures of the Gruvefjellet slope. In the end I learned not to bring a fork when eating drytec food out of the bag…

I owe Berit Jakobsen more than just a few 'tusen takk' for the support in finding some of the infrequent used literature – even if it was written it was in Chinese.

I am also grateful to all those people who joined my on fieldwork and enjoyed the ride home. Takk for turen!

This master study was supported by the Svalbard Science Forum Arctic Field Grant 2010.

First automatic photograph of the 'Gruvefjellet' time lapse camera.

Three guys on Gruvefjellet – freezing but happy!

LIST OF DIAGRAMS

LIST OF FIGURES

REFERENCE LIST

Åkerman, J. 1984. Notes on talus morphology and processes in Spitsbergen. *Geografiska Annaler* 66 A.

André, M.-F. 1990a. Frequency of debris flows and slush avalanches in Spitsbergen: a tentative evaluation from lichenometry *Polish PolarResearch* 11, 345-363.

André, M.-F. 1990b. Geomorphic impact of spring avalanches in Northwest Spitsbergen (79N). *Permafrost and Periglacial Processes* 1, 97-110.

Benestad, R.E., Hanssen-Bauer, I., Skaugen, T.E. and Førland, E.J. 2002. Associations between sea-ice and the local climate on Svalbard. *Klima* 7(2):13.

Burrows, R. and McClung, D.M. 2006. Snow Cornice Development and Failure Monitoring. Paper read at International Snow Science Workshop, at Telluride Colorado.

Carrera-Gómez, P., Valcárcel-Díaz, M. and Blanco-Chao, R. 2010. Snow-Push Activity at a Seasonal Snowpatch Site, Sierra de Ancares, Northwestern Spain. Paper read at EUCOP III, at Longyearbyen.

Chaudhary, V. and Singh, G. 2006. Structural Measures for Controlling Avalanches in Formation Zone. *Defence Science Journal* 56.

Christiansen, H. 2001. Snow-cover depth, distribution and duration data from northeast Greenland obtained by continuous automatic digital camera. *Annals of Glaciology* 32, 102-108.

Christiansen, H. 2005. Thermal regime of ice-wedge cracking in Adventdalen, Svalbard. *Permafrost and Periglacial Processes* 16, 87-98.

Conway, H. 1998. The impact of surface perturbations on snow-slope stability. *Annals of Glaciology* 26, 307-312.

Decaulne, A. and Saemundsson, T. 2006. Geomorphic evidence from present-day sow-avalanche and debris-flow impact in the Icelandic Westfjords. *Geomorphology* 80, 80-93.

Eckerstorfer, M. 2010. personal communication. Longyearbyen.

Eckerstorfer, M. and Christiansen, H. 2010. An Extreme Slush and Slab Avalanche Event in High Arctic Maritime Svalbard. Paper read at International Snow Science Workshop, at Squaw Valley.

Eckerstorfer, M. and Christiansen, H. accepted. The “High Arctic maritime snow climate” in central Svalbard. *Arctic, Antarctic, and Alpine Research*.

Eckerstorfer, M., Christiansen, H.H. and Neumann, U. 2009. Avalanches and snow mobile traffic around Longyearbyen, Svalbard. Paper read at International Snow Science Workshop, at Davos.

Eckerstorfer, M., Neumann, U. and Christiansen, H. 2008. High arctic avalanche monitoring in maritime Svalbard. Paper read at International Snow Science Workshop, at Whistler.

Ellehauge, J. 2003. *Influence of meteorological and topographic conditions on snow avalanches in central Spitsbergen, Svalbard*, UNIS. 65.

Førland, E.J., Hanssen-Bauer, I. and Nordli, P.Ø. 1997. Climate statistics and longterm series of temperature and precipitation at Svalbard and Jan Mayen. *Klima* 21/97.

French, M.H. 2007. *The Periglacial Environment*: Third Edition: Wiley & Sons. 458 pp.

Glude, B. 2010. personal communication. ISSW Squaw Valley.

Greene, E.M., Birkeland, K.W., Elder, K., Johnson, G., Landry, C., McCammon, I., Moore, M., Sharaf, D., Sterbenz, C., Tremper, B. and Willimas, K. 2004. *Snow, Weather, and Avalanches: Observational Guidelines for Avalanche Programs in the United States*. *American Avalanche Association*. Pagosa Springs, Colorado.

Hákonardóttir, K.M., Margreth, S., Tómasson, G.G., Indriđason, H.D. and þórđarson, S. 2008. Snow drift measures as protection against snow avalanches in Iceland. Paper read at International Symposium on Mitigative Measures against Snow Avalanches, at Egilsstađir, Iceland.

Hanssen-Bauer, I., Kristensen Solås, M. and Steffensen, E.L. 1990. The climate of Spitsbergen. *Klima* 39, 40.

Hendrikx, J., Peitzsch, E.H. and Fagre, D.B. 2010. A practitioners's tool for assessing glite crack activity. Paper read at International Snow Science Workshop, at Squaw Valley.

Heskestad, G. 1965. *Remarks on Snow Cornice Theory and Related Experiments with Sink Flows*. New York. American Society of Mechanical Engineers. 9 pp.

Hestnes, E. 1996a. *Barnehage, Longeyarbyen. Vurdering av skredfaren mot aktuelle tomter for ny barnehage ved kirka*. Oslo.

Hestnes, E. 1996b. *Det gamle sykehuset, Longeyarbyen. Skredfarevurdering*. Oslo.

Hestnes, E. 1999. *Permafrost response to environmental and industrial loads. Snø og snøskred på Svalbard. Registrering av snøforhold, snøskred og utløpslengder.* Longyearbyen.

Hestnes, E. 2000. Impact of rapid mass movement and drifting snow on the infrastructure and development of Longyearbyen, Svalbard Paper read at *International Workshop on Permafrost Engineering* at Longyearbyen.

Humlum, O. 2002. Modelling 20th-century precipitation in Nordenskiold Land, Svalbard, by geomorphic means. *Norsk Geografisk Tidsskrift* 56, 96-103.

Humlum, O., Christiansen, H. and Juliussen, H. 2007. Avalanche-derived Rock Glaciers in Svalbard. *Permafrost and Periglacial Processes* 18, 75-88.

Humlum, O., Instanes, A. and Sollid, J.L. 2003. Permafrost in Svalbard: a review of research history, climatic background and engeneering challanges. *Polar Research* 22.

Jaedicke, C. and Gauer, P. 2005. The influence of drifting snow on the location of glaciers on western Spitsbergen, Svalbard. *Annals of Glaciology* 42, 237-242.

Kobayashi, D., Ishikawa, N. and Nishio, F. 1988. Formation process and direction distribution of snow cornices. *Cold Regions Science and Technology* 15, 131-136.

Kosugi, K., Sato, T. and Sato, A. 2004. Dependence of drifting snow saltation length on snow surface hardness. *Cold Regions Science and Technology* 39, 133-139.

Kottek, M., Grieser, J., Beck, C., Rudolf, B. and Rubel, F. 2006. World Map of the Koeppen-Geiger climate classification updated. *Meteorologische Zeitschrift* 15, 5.

Larsen, J.O. 2009. personal communication. Longyearbyen.

Larsson, S. 1984. Geomorphological Effects on the Slopes of Longyear Valley, Spitsbergen, after a Heavy Rainstorm in July 1972. *Geografiska Annaler* 64, 105-125.

Latham, J. and Montagne, J. 1970. The possible importance of electrical forces in the development of snow cornices. *Journal of Glaciology* 9.

Lawrence, W.S. and Williams, T.R. 1976. Seismic signals associated with avalanches. *Journal of Glaciology* 17, 521-526.

Major, H., Haremo, P., Dallmann, W. and Andresen, A. 2001. *Geological map of Svalbard. 1:100 000*. Norsk Polarinst Temakart 31/32.

Margreth, S. 2006. *Memo concerning the application of snow supporting structures and snow drift measures in Patreksfjördur/IS*. Davos. SLF.

Margreth, S. 2007. *Basics for the design of snow drift measures*. *Modul Schneemechanik und Lawinenverbau*. Davos: Eidg. Institut für Schnee- und Lawinenforschung SLF.

McCarty, D., Brown, R.L. and Montagne, J. 1986. Cornices: Their Growth, Properties, and Control. Paper read at International Snow Science Workshop, at Lake Tahoe.

McClung, D.M. and Schaerer, P. 2006. *The Avalanche Handbook, 3rd edition*: The Mountaineers.

Montagne, J., McPartland, J.T., Super, A.B. and Townes, H.W. 1968. *The Nature and control of snow cornices on the Bridger Range, southwestern Montana*: Alta Avalanche Study Center, Miscellaneous Report No. 14.

Mosimann, U. 2009. Wechten, faszinierend und gefährlich. *bergundsteigen*.

Naruse, R., Nishimaru, H. and Maeno, N. 1985. Structural Characteristics of Snow Drifts and Cornices. *Annals of Glaciology* 6, 287-288.

Paulcke, W. and Welzenbach, W. 1928. Schnee, Wächten, Lawinen. *Zeitschrift für Gletscherkunde, Eiszeitforschung und Geschichte* 16, 49-69.

Ripepe, M., Ulivieri, G., Marchetti, E., Segor, V., Chiambretti, I., Pitet, L. and Dellavedova, P. 2010. Infrasound monitoring of snow avalanches activity in the Italian Alps. Paper read at International Snow Science Workshop, at Squaw Valley.

Rogers, J.C., Yang, L. and Li, L. 2005. The role of Fram Strait winter cyclones on sea ice flux and on Spitsbergen air temperature. *Geophysical Research Letters* L06709.

Schweizer, J. and Jamieson, B. 2010. On surface warming and snow instability. Paper read at International Snow Science Workshop, at Squaw Valley.

Seligman, G. 1936. *Snow structures and ski fields* London: Macmillian.

Sokratov, S.A. and Sato, A. 2001. The effect of wind on the snow cover. *Annals of Glaciology* 32.

Stratham, G., Haegli, P., Birkeland, K.W., Greene, E.M., Israelson, C., Tremper, B., Stethem, C., McMahon, B., White, B. and Kelly, J. 2010. The North American public avalanche danger scale. Paper read at International Snow Science Workshop, at Squaw Valley.

Tokle, H.A. 2009. personal communication.

Tremper, B. 2008. *Staying Alive in Avalanche Terrain, 2nd edition*: The Mountaineers.

Van Herwijnen, A., Turner, J. and Schweizer, J. 2010. Listening to snow - Avalanche detection using a seismic sensor array. Paper read at International Snow Science Workshop, at Squaw Valley.

Ward, R.G.W. 1981. Snow variability and Avalanche release. *Scottish Mountaineering Club Journal* 32, 146-149.

Winther, J.-G., Bruland, O., Sand, K., Gerland, S., Marechal, D., Ivanov, B., Glowacki, P. and König, M. 2003. Snow research in Svalbard - an overview. *Polar Research* 22, 125-144.

www.eklima.no. Norwegian Meteorological Institute Accsessed: October 2010.

www.skred-svalbard.no. CRYOSLOPE Svalbard Accsessed: October 2010.

Zahn, M. and von Storch, H. 2008. A long-term climatology of North Atlantic polar lows. *Geophysical Research Letters* 35.

Zahn, M. and von Storch, H. 2010. Decreased frequency of North Atlantic polar lows associated with future climate warming. *Nature* 467, 309-312.